

# **Development of Racemization Catalysts for Dynamic Kinetic Resolution**

**Denys Mavrynsky**



Laboratory of Organic Chemistry  
Department of Natural Sciences and Technology  
Åbo Akademi University  
Åbo, Finland  
2012



Denys Mavrynsky

b. 1981 in Kerch, Ukraine, USSR

M. Sc. Chemistry, 2002

Moscow State University, Russia

Cover picture:

Formation of benzophenone ketyl over Na wire in THF

Photo by Denys Mavrynsky

# **Development of Racemization Catalysts for Dynamic Kinetic Resolution**

Denys Mavrynsky

Laboratory of Organic Chemistry  
Department of Natural Sciences and Technology  
Åbo Akademi University  
Åbo, Finland  
2012

## **SUPERVISOR AND CUSTOS**

### **Professor Reko Leino**

Laboratory of Organic Chemistry

Department of Natural Sciences and Technology

Åbo Akademi University

Åbo, Finland

## **OPPONENT**

### **Professor Belén Martín-Matute**

Department of Organic Chemistry

The Arrhenius Laboratory

Stockholm University

Stockholm, Sweden

## **REVIEWERS**

### **Professor Serafino Gladiali**

Department of Chemistry

University of Sassari

Sassary, Italy

*and*

### **Kevin H. Shaughnessy**

Department of Chemistry

The University of Alabama

Tuscaloosa, AL, USA

ISBN 978-952-12-2813-1

Painosalama Oy – Turku/Åbo, Finland 2012

*Neverending, forever searching  
Chasing dreams, the dreams of my heart  
Always seeking, always asking  
Questions right from the start*

*B. Dickinson, N. McBrain*



## PREFACE

The present work was carried out at the Laboratory of Organic Chemistry, Department of Natural Sciences, Åbo Akademi University between the years 2007 and 2012. Financial support from the Finnish Funding Agency for Technology and Innovation (TEKES), Magnus Ehrnrooth Foundation, the National Doctoral Program of Organic Chemistry and Chemical Biology and the Rector of Åbo Akademi University is gratefully acknowledged.

I wish to express my deep gratitude to my supervisor, Professor Reko Leino for giving me the opportunity to join his research group, for his endless patience and for supporting and trusting me during these years.

I am very thankful to Professor Serafino Gladiali (University of Sassari) and Professor Kevin H. Shaughnessy (The University of Alabama) for reviewing my thesis. Furthermore, I wish to thank my opponent Professor Belén Martín-Matute (Stockholm University).

Special appreciation is addressed to Jan-Erling Bäckvall (Stockholm University) and his group who accepted me as a trainee and kindly shared their experience and expertise in the field of DKR. My sincerest thanks go to Krisztián Bogár for his exceptional helpfulness, guidance and answers to my countless questions.

I wish to thank Päivi Pennanen for everyday valuable help with the routine lab issues, my fellow Yury Brusentsev for the debates helping the thoughts to thrive, our students Magnus Perander, Jani Rahkila and Petra Nordman for their significant contributions to the experiments, Professor Dmitry Yu. Murzin for fruitful discussions on chemical kinetics and Professor Reijo Sillanpää (University of Jyväskylä) for solving the X-ray structures. Professors Rainer Sjöholm and Leif Kronberg and Dr. Patrick Eklund, Dr. Ari Lehtonen and Dr. Jari Sinkkonen are thanked for their kind help, Markku Reunanen for mass spectra measurements, Peter Holmlund, Dr. Wojciech Zawartka and Otto Långvik for their help with maintenance of the lab equipment, Dr. Anton Tokarev and Dr. Zhanna Boeva for scientific discussions and experimental help, Dr. Filip Ekholm and Dr. Mattias Roslund for introducing me into NMR techniques, Risto Savela for his jokes creating a great working atmosphere. My office mates Dr. Jonas Forsman, Jesper Svanfelt, Lucas Lagerquist and Sabine Rendon are thanked for sharing the workspace with me and for the nice communication. Dr. Igor Busigyn and Kseniya Marushkevich are thanked for their help in my moving and adaptation to the new country. My collaborators Professor Liisa T. Kanerva and

Mari Päiviö (University of Turku) are thanked for helping me to acquire team work skills. I would also like to thank all my colleagues at the Laboratory of Organic Chemistry whom I have met during these years for their help.

Many thanks to all the great people who participated in sports and leisure activities after workdays in the lab: Cesar Araujo, Zhanna Boeva, Vitaly Boguslavsky, Yury Brusentsev, Sergey Chernov, Milver Colmenares, Yulia Demidova, Dr. Gordon Driver, Alexey Kirilin, Ekaterina Korotkova, Anastasia Krivova, Dr. Bright Kusema, Dr. Alexander Lobur, Viktor Lukashov, Ida Mattson, Axel Meierjohann, Konstantin Mikhaylov, Irina Mostovaya, Magnus Perander, Juan Pinoargote, Maria Platova, Elena Privalova, Janne Raitanen, Dr. Elizaveta Rastorgueva-Foi, Dr. Tiina Saloranta, Dr. Olga Simakova, Nadine Stumpf, Nadezda Vlasova, Sandra Uitto, Peter Uppstu and Marco Zanella. Also thanks to Pictura vid Åbo Akademi, Turun Akateemiset Soutajat and Turun Jyryn Nyrkkeilyjaosto.

Finally, I thank my mother Valentina for her endless love and support.

Åbo, October 2012

*Denys MAVRYNSKY*





## ABSTRACT

Preparation of optically active compounds is of high importance in modern medicinal chemistry. Despite recent advances in the field of asymmetric synthesis, resolution of racemates still remains the most utilized way for preparation of single enantiomers in industrial scale due to its cost-efficiency and simplicity. Enzymatic kinetic resolution (KR) of racemates is a classical method for separation of enantiomers. One of its drawbacks is the limitation of target enantiomer yield to 50%. Dynamic Kinetic Resolution (DKR) allows to reach yields up to 100% by *in situ* racemization of the less reactive enantiomer.

In the first part of this thesis, a number of half-sandwich ruthenium complexes were prepared and evaluated as catalysts for racemization of optically active secondary alcohols. A leading catalyst,  $\text{Bn}_5\text{CpRu}(\text{CO})_2\text{Cl}$ , was identified. The catalyst discovered was extensively characterized by its application for DKR of a broad range of secondary alcohols in a wide range of reaction loadings (1 mmol – 1 mol). Cost-efficient chromatography-free procedure for preparation of this catalyst was developed.

Further, detailed kinetic and mechanistic studies of the racemization reactions were performed. Comparison of racemization rates in the presence of  $\text{Bn}_5\text{CpRu}(\text{CO})_2\text{Cl}$  and  $\text{Ph}_5\text{CpRu}(\text{CO})_2\text{Cl}$  catalysts reveals that the performance of the catalytic system can be adjusted by matching of the electronic properties of the catalysts and the substrates. Moreover, dependence of the rate-limiting step from the electronic properties of the reagents was observed. Important conclusions about reaction mechanism were made.

Finally, an alternative approach to DKR of amines based on space separated vessels was addressed. This procedure allows the combination of thermolabile enzyme with racemization catalysts active only at high temperatures.

## ABSTRAKT

Framställning av optiskt aktiva föreningar är högaktuellt för den moderna läkemedelskemin. Trots framsteg inom asymmetrisk syntes är resolvering av racemater den mest använda metoden vid framställning av optiskt rena enantiomerer i industriella processer, tack vare dess kostnadseffektivitet och enkelhet. Enzymatisk kinetisk resolvering (KR) är en klassisk resolveringsmetod av racemater. En av metodens nackdelar är att utbytet av målprodukten endast uppnår maximalt 50 %. Dynamisk kinetisk resolvering (DKR) möjliggör utbyten upp till 100 %, genom *in situ* racemisering av den mindre reaktiva enantiomeren.

I avhandlingens första del framställdes och evaluerades en mängd olika monocyklopentadienylruteniumkomplex som katalysatorer för racemisering av optiskt aktiva sekundära alkoholer. En ledande katalysator,  $\text{Bn}_5\text{CpRu}(\text{CO})_2\text{Cl}$  identifierades. Den upptäckta katalysatorns DKR egenskaper karakteriserades omfattande för en stor mängd sekundära alkoholer i varierande mängder från 1 mmol till 1 mol. En kostnadseffektiv procedur utan kromatografiska reningar för framställning av katalysatorn utvecklades.

Vidare har detaljerade kinetiska och mekanistiska studier av racemiseringsreaktionerna utförts. Genom att jämföra racemiseringshastigheterna för katalysatorerna  $\text{Bn}_5\text{CpRu}(\text{CO})_2\text{Cl}$  och  $\text{Ph}_5\text{CpRu}(\text{CO})_2\text{Cl}$  kunde det visas att resultaten av det katalytiska systemet kan justeras genom att anpassa de elektroniska egenskaperna hos katalysatorn och substraten. Dessutom observerades det att det hastighetsbestämmande steget var beroende av de elektroniska egenskaperna hos reagensen. Viktiga slutsatser om reaktionmekanismen kunde göras.

Slutligen, en alternativ metod för DKR av aminer baserad på separerade reaktionskärl evaluerades. Denna procedur tillät en kombination av värmeinstabila enzymer med katalysatorer som endast är aktiva vid höga temperaturer.

## LIST OF ORIGINAL PUBLICATIONS AND MANUSCRIPTS

1. Mavrynsky, D.; Sillanpää, R.; Leino, R. **Cyclopenta[*l*]phenanthrenyl and Cyclopenta[*a*]acenaphthylenyl Half-Sandwich Complexes of Ruthenium as Racemization Catalysts for Secondary Alcohols**, *Organometallics* **2009**, 28, 598–605.
2. Mavrynsky, D.; Päiviö, M.; Lundell, K.; Sillanpää, R.; Kanerva, L. T.; Leino, R. **Dicarbonylchloro(pentabenzylcyclopentadienyl)ruthenium as Racemization Catalyst in the Dynamic Kinetic Resolution of Secondary Alcohols**, *Eur. J. Org. Chem.* **2009**, 1317-1320.
3. Mavrynsky, D.; Kanerva, L. T.; Sillanpää, R.; Leino, R. **Improved synthesis of  $\text{Bn}_5\text{CpRu}(\text{CO})_2\text{Cl}$  and its application as racemization catalyst in preparative-scale metalloenzymatic dynamic kinetic resolution of 1-phenylethanol**, *Pure Appl. Chem.* **2011**, 83, 479-487.
4. Päiviö, M.; Mavrynsky, D.; Leino, R.; Kanerva, L. T. **Dynamic Kinetic Resolution of a Wide Range of Secondary Alcohols: Cooperation of Dicarbonylchlorido(pentabenzylcyclopentadienyl)ruthenium and CAL-B**, *Eur. J. Org. Chem.* **2011**, 1452–1457.
5. Mavrynsky, D.; Murzin, D. Yu.; Leino, R. **Kinetic Studies on *sec*-Alcohol Racemization with Dicarbonylchloro(pentabenzylcyclopentadienyl) and Dicarbonylchloro(pentaphenylcyclopentadienyl) Ruthenium Catalysts**, submitted for publication.
6. Mavrynsky, D.; Leino, R. **An Approach to Chemoenzymatic DKR of Amines in Soxhlet Apparatus**, manuscript.

## LIST OF ABBREVIATIONS

Ac	acetyl
Bn	benzyl
Bz	benzoyl
bp	boiling point
CAL-B	<i>Candida antarctica</i> lipase B
Cp	cyclopentadienyl
DKR	dynamic kinetic resolution
ee	enantiomeric excess
equiv	equivalent
GC	gas chromatography
Hal	halogen
HPLC	high performance liquid chromatography
HSQC	heteronuclear single-quantum coherence
KR	kinetic resolution
Me	methyl
mp	melting point
NMR	nuclear magnetic resonance
Np	naphthyl
Ph	phenyl
<i>rac</i>	racemic
RT	room temperature
THF	tetrahydrofuran
Ts	tosyl
vol	volume

## TABLE OF CONTENTS

1 Introduction	1
1.1 Chirality and biological properties	1
1.2 Preparation of enantiopure compounds	3
1.2.1 Kinetic resolution (KR)	5
1.2.2 Dynamic kinetic resolution (DKR)	7
1.2.3 Catalysts for DKR of <i>sec</i> -alcohols	10
1.2.4 Standard requirements for DKR	13
1.2.5 DKR of amines	16
1.3 Aims and outline of this thesis	17
2 Synthesis and characterization of potential candidates for racemization catalysis	19
2.1 Introduction	19
2.2 Preparation and characterization of complexes with different ligands	19
2.2.1 Complexes with polycyclic fused aromatic ligands	19
2.2.2 Complexes with pentasubstituted cyclopentadienyl ligands	24
2.2.3 Complexes with indenyl-based ligands	26
2.3 Molecular structures of the metal complexes	26
2.4 Summary and conclusions	34
3 Characterization and application of $\text{Bn}_5\text{CpRu}(\text{CO})_2\text{Cl}$ as racemization catalyst	35
3.1 Large scale preparation of $\text{Bn}_5\text{CpRu}(\text{CO})_2\text{Cl}$	35
3.2 Utilization of the new catalyst for DKR of a broad range of substrates	37
3.2.1 General issues	37
3.2.2 Methodological aspects	38
3.2.3 Substrate scope	42
3.3 Utilization of the new catalyst for large scale DKR	47
3.4 Epimerization of terpenoids	50
3.5 Summary and conclusions	51
4 Kinetic and mechanistic studies	53
4.1 Introduction	53
4.2 Comparison of the electronic properties of $\text{Bn}_5\text{CpRu}(\text{CO})_2\text{Cl}$ and $\text{Ph}_5\text{CpRu}(\text{CO})_2\text{Cl}$ catalysts	54
4.3 Experimental set-up for the racemization studies	56
4.4 Kinetic experiments	57
4.5 NMR studies on the $\text{Bn}_5\text{CpRu}(\text{CO})_2\text{Cl}$ catalyst activation	64

4.6 Transfer hydrogenation experiments	66
4.7 Summary and conclusions	68
5 DKR of amines	69
5.1 Introduction	69
5.2 Approach to the DKR of amines utilizing a Soxhlet apparatus	69
5.3 Utilization of the Soxhlet apparatus for a model DKR	71
5.4 Suppression of side product formation	72
5.5 Summary and conclusions	75
6 Concluding discussion	77
6.1 Summary	77
6.2 Conclusions	77
6.3 Future perspectives	78

## 1 Introduction

### 1.1 Chirality and biological properties

An  $sp^3$ -hybridized carbon atom forms four bonds pointed to the corners of a regular tetrahedron. If all four substituents at the carbon atom are different, then two non-superimposable mirror image molecules, or so called enantiomers, exist (Figure 1). Enantiomers demonstrate identical physical (melting and boiling points, density), chemical and spectral (NMR, IR, UV) properties in an achiral environment. Introduction of a chiral reagent or plane polarized light can lead to distinguishing of enantiomers. Enantiomers often possess different biological properties due to the fact that biochemical processes in all living beings involve chiral molecules.



**Figure 1.** Two enantiomeric molecules.

The first evidence of difference in biological properties of enantiomers was presented by L. Pasteur in 1858. He observed that the (+)-enantiomer was consumed faster upon fermentation of a solution of racemic ammonium tartrate while the (-)-enantiomer remained in the solution.<sup>1</sup> Later in 1886 it was reported that D-asparagin possesses a sweet taste while L-asparagine is tasteless.<sup>2</sup> In 1933, Easson and Steadman proposed the “three-point” contact model explaining the differences in the physiological properties of enantiomers (Figure 2).<sup>3</sup>

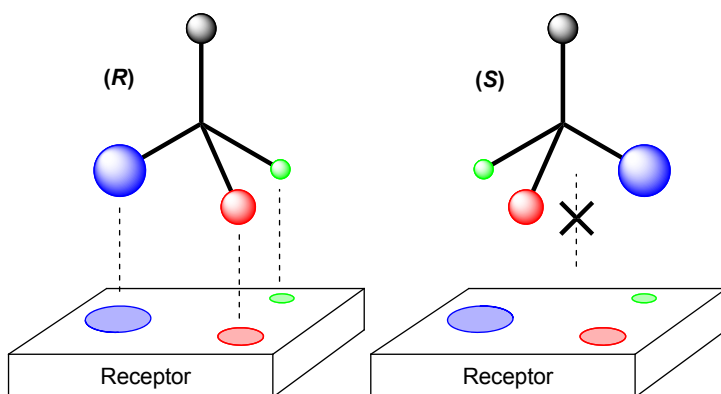


**Figure 2.** Chiral recognition of a substrate by a biomolecule.

Later a large number of observations revealing the different biological properties of enantiomers have been made. (*S*)-(-)-Dihydroxyphenylalanine (L-DOPA) (**1**) is used for the treatment of Parkinson's disease, while the (*R*)-(+)-enantiomer (D-DOPA) is biologically inactive. Among others, W. S. Knowles was awarded the Nobel Prize in Chemistry in 2001 for his contributions to the development of asymmetric hydrogenation, which has become widely utilized, particularly for industrial L-DOPA preparation.<sup>4</sup> Naturally occurring (*R*)-(+)-1-*p*-menthene-8-thiol (**2**) (grapefruit mercaptane) demonstrates the characteristic smell of grapefruit. The opposite enantiomer is nearly odorless. Another classical example is the difference between the enantiomers of limonene. The (*R*)-(+)-limonene (**3**) possesses an orange odor while the opposite enantiomer smells of lemon.<sup>5</sup> Fluoxetine (**4**) (commercial name Prozac) is utilized as a racemate, despite the enantiomers of its metabolite norfluoxetine possess different physiological properties.<sup>6</sup> A similar drug duloxetine (**5**) is produced in unichiral form.<sup>7</sup> Dextromethamphetamine (**6**) is a strictly controlled powerful psychostimulant, while the (*S*)-enantiomer demonstrates low effect on the central nervous system and is utilized as a component for nasal decongestion sprays.<sup>8</sup> In 1992, U.S. Food and Drug Administration (FDA) issued new guidelines prescribing separate characterization of each enantiomer of a potential drug for its physiological action.<sup>9</sup> These examples manifestate the importance of development of methods for production of enantiopure compounds.



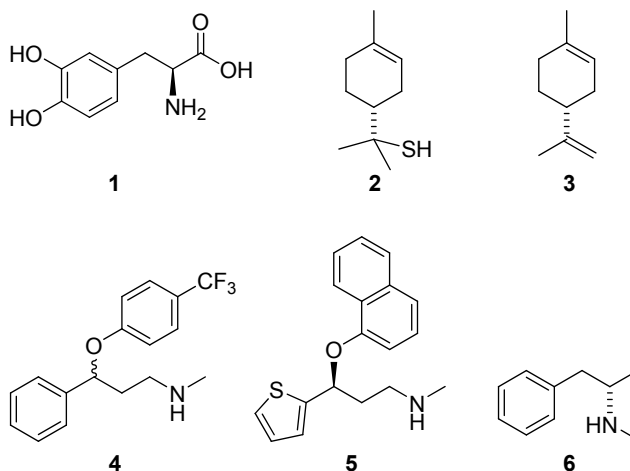


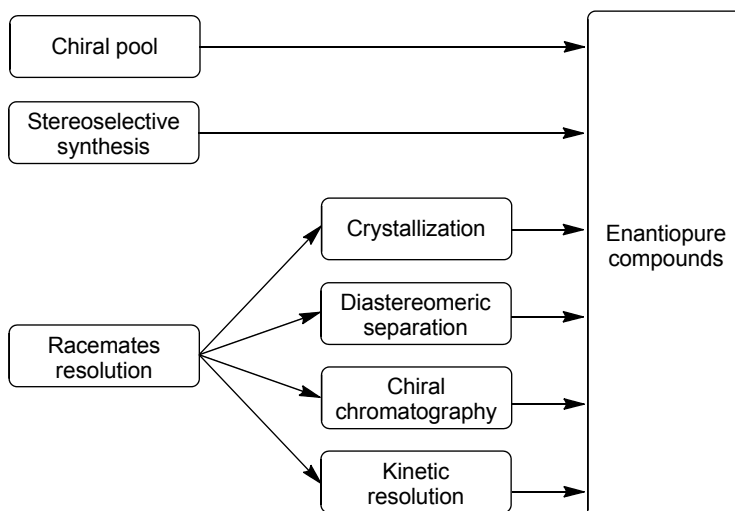
**Figure 3.** Structures of the physiologically active chiral molecules 1-6.

## 1.2 Preparation of enantiopure compounds

In general, enantiopure compounds can be prepared by three different routes (Scheme 1):

- Chiral pool strategy based on either direct utilization of naturally occurring homochiral compounds or their further chemical modifications<sup>10</sup>
- Stereoselective synthesis from prochiral substrates utilizing chiral auxiliaries or asymmetric catalysis<sup>11</sup>
- Resolution of readily available racemates into single enantiomers<sup>12</sup>

**Scheme 1.** Routes to enantiopure compounds

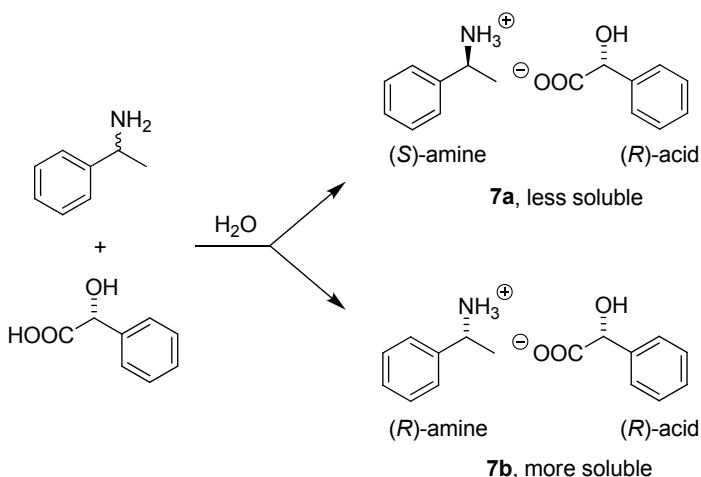


Resolution of racemates can be performed by different methods. The most significant of these are:

a) Preferential crystallization can be usually initiated by adding a seeding crystal consisting of one enantiomer to a supersaturated solution of a racemic mixture.<sup>12a</sup> The process for preparation of L-DOPA involving a preferential crystallization step was patented by Merck.<sup>13</sup> Generally, this approach is limited by the physical properties of the compound undergoing resolution. It is estimated that only about 10% of chiral compounds demonstrate a suitable crystallization pattern allowing preferential crystallization<sup>1a</sup>

b) Diastereomeric separation is the industrially most used method due to its simplicity and cost efficiency.<sup>12b</sup> In this method, a racemic compound is treated with an appropriate unichiral reagent providing a mixture of diastereomers. Diastereomers possess different properties and, therefore, can be separated by physical methods. For example, treatment of racemic 1-phenylethylamine with (*R*)-mandelic acid leads to the formation of two diastereomeric salts, **7a** and **b** (Scheme 2). Due to their different solubilities in water, these salts can be separated by crystallization<sup>14</sup>

**Scheme 2.** Diastereomeric separation of 1-phenylethylamine



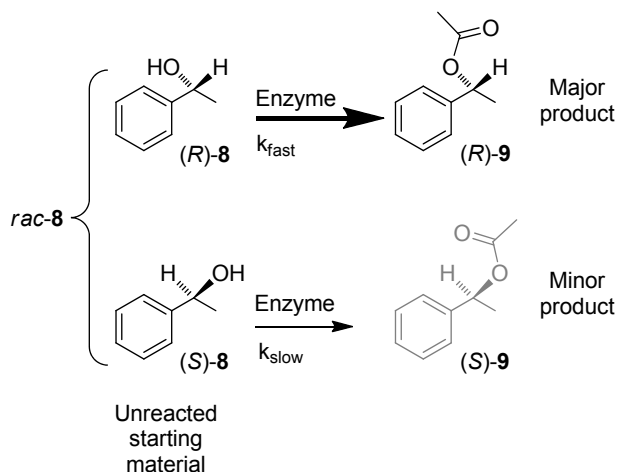
c) Chiral chromatography is a powerful analysis method for determination of the enantiopurity of chiral compounds. Preparative application of this approach is limited due to high cost and low productivity<sup>15</sup>

d) Kinetic resolution is based on the different reaction rates of enantiomers towards a chiral reagent or catalyst

### 1.2.1 Kinetic resolution (KR)

To exemplify, treatment of the racemic secondary alcohol *rac*-**8** with an appropriate enzyme in the presence of an acyl donor ideally leads to a mixture of the ester (*R*)-**9** and unreacted alcohol (*S*)-**8** (Scheme 3). Resulting mixture can be separated by physical or chemical methods.

**Scheme 3.** Kinetic resolution of racemic 1-phenylethanol



The efficiency of kinetic resolution of two enantiomers can be characterized by the ratio of the specificity constants. This parameter, called *E* (Equation 1) was introduced by Sih et al. in 1982.<sup>16</sup> *E*-values over 100 in kinetic resolutions are generally considered as excellent.

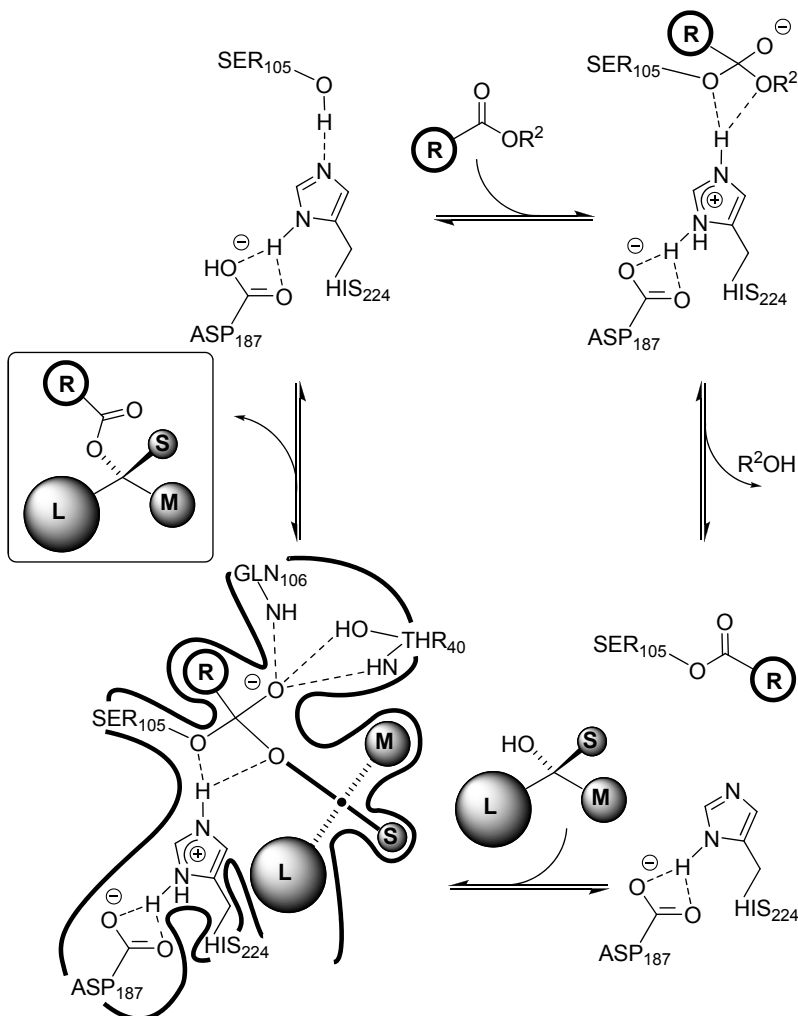
**Equation 1.** Sih's equation

$$E = \frac{\ln[1 - c(1 + ee_p)]}{\ln[1 - c(1 - ee_p)]}$$

KR method, affording in the best case both enantiomers of a racemic mixture at 50% conversion, is beneficial when both enantiomers are important. In such a case, one enantiomer remains unreacted while the other becomes the new reaction product. The lipase-catalyzed enantioselective acylation of racemic secondary alcohols with achiral esters in organic solvents has afforded a large number of alcohol enantiomers to be used as such or as intermediates for further transformations into pharmaceutically active compounds and fine chemicals.<sup>17</sup> Lipases (EC 3.1.1.3) are the most commonly used enantioselective biocatalysts in kinetic resolutions of racemic alcohols. This is a natural consequence of their good availability and excellent regio- and stereoselectivity in addition to their stability in a variety of reaction media, including organic

solvents and ionic liquids, which dissolve organic substrates better than aqueous environments do. Lipases also accept a broad range of structurally different alcohols (or more generally nucleophiles) and carboxylic acids or their derivatives as substrates in addition to the natural substrates, triglycerides. A serine hydrolase CAL-B (Candida Antarctica lipase, type B) is one of the most utilized lipases for transesterification of secondary alcohols.<sup>18</sup> It is often produced and utilized in immobilized form on polyacrylic support (commercial name Novozym 435).

The absolute configuration of the acylated product depends on the enantioselectivity of the enzyme. Kazlauskas' rule predicts that the acylation is (*R*)-selective when the large group at the asymmetric center has priority over the medium size group, for example, in the case of (*R*)-**8**.<sup>19</sup> Transesterification mechanism involves the following steps: (1) Acylation of the serine hydroxyl accompanied with release of the alcohol residue from the acyl donor; (2) Stereoselective addition of the substrate to the active center, followed by acylation of the free hydroxyl group and the subsequent release of the transesterification product.<sup>20</sup> CAL-B is compatible with different types of acyl donors, such as esters and acids. In the case of regular esters, e.g. ethylacetate, the reaction is reversible and requires the utilization of excess of acyl donor or removal of the produced alcohol in order to shift the equilibrium towards the product. Esters of less nucleophilic alcohols, such as trifluoroethanol or *p*-chlorophenol, can be utilized to suppress the reverse reaction. Another widely used option is the utilization of enol esters, e.g. vinyl or isopropenylacetate. The alcohols released upon transesterification undergo immediate tautomerization to the corresponding carbonyl compounds rendering the reaction irreversible.

**Scheme 4.** Enantioselective acylation of *sec*-alcohols in the active site of CAL-B

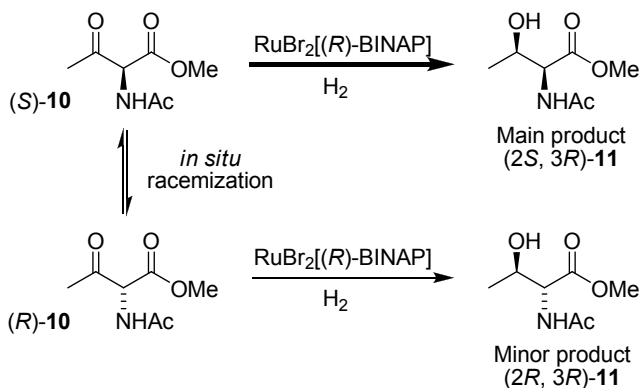
### 1.2.2 Dynamic kinetic resolution (DKR)

KR is limited by the maximum 50% yield of the desired enantiomer. The opposite enantiomer can be isolated and recycled. For example, the KR reaction mixture can be subjected to Mitsunobu esterification proceeding with inversion of the unreacted (*S*)-enantiomer to (*R*)-acetate providing conversions up to 90%.<sup>21</sup> Alternatively, the less reactive (*S*)-enantiomer can be isolated and racemized via oxidation-reduction sequence.

Dynamic kinetic resolution (DKR), in turn, utilizes *in situ* racemization of the less reactive enantiomer allowing the transformation of a racemic mixture into an enantiopure product with conversions up to 100%.

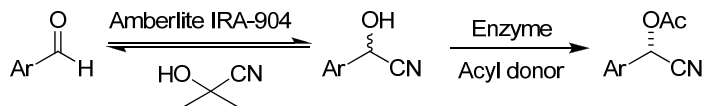
The first application of the dynamic kinetic resolution concept was described in 1989 by Noyori (Scheme 5).<sup>22</sup> The chiral ketone **10** is able to undergo fast racemization via keto-enol tautomerism. Upon transfer hydrogenation reaction it provided only one of the four possible diastereomers (2*S*, 3*R*)-**11** in 98% ee and de and 100% conversion. The substrate scope of this approach is, however, limited to configurationally labile compounds.

**Scheme 5.** The first application of DKR concept



The first enzymatic DKR was reported two years later.<sup>23</sup> The enzymatic acylation of cyanohydrins led to (*S*)-acetates, while the less reactive enantiomer was racemized *in situ* due to reversible transhydrocyanation (Scheme 6).

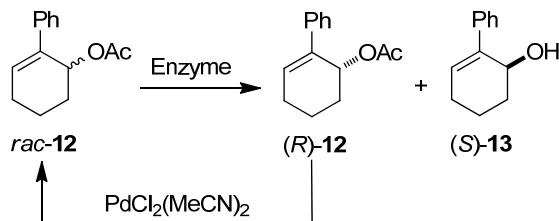
**Scheme 6.** The first enzymatic DKR



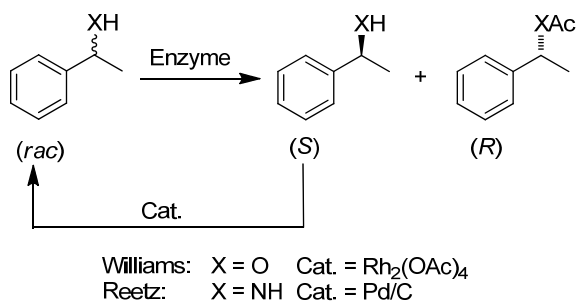
In 1996, Williams et al.<sup>24</sup> reported the first example of chemoenzymatic DKR where racemization was catalyzed by a transition metal complex. The allylic acetate (*R*)-**12** was enzymatically hydrolyzed to alcohol (*R*)-**13**. The unreacted starting material was racemized via allylic palladium  $\pi$ -complex (Scheme 7). Half a year later, the same group reported an enzymatic DKR of secondary alcohols utilizing rhodium and iridium complexes (Scheme 8).<sup>25</sup> The best result was achieved with rhodium (II) acetate. The same year, Reetz et al. reported the DKR of 1-phenylethylamine catalyzed by Pd/C.<sup>26</sup> All of the approaches discussed above suffered,

however, from long reaction times, nonoptimal yields or mediocre enantiopurities of the products.

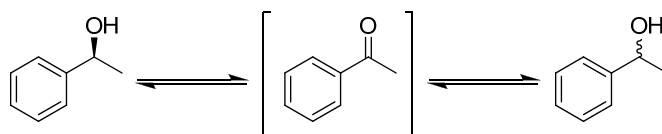
**Scheme 7.** The first DKR utilizing a transition metal racemization catalyst



**Scheme 8.** The first transition metal catalyzed chemoenzymatic DKRs of free alcohol and amine



**Scheme 9.** Racemization of *sec*-alcohol via oxidation-reduction sequence



Remarkable results were reported by Bäckvall and co-workers in 1997,<sup>27</sup> when the well-known transfer hydrogenation Shvo's catalyst<sup>28</sup> **14** was utilized for *in situ* racemization of *rac*-**8** (see Scheme 3) in a manner similar to Scheme 8. The dimeric catalyst employed required elevated temperature for generation of the active monoruthenium species. The reaction was performed in the presence of 1 equiv. of acetophenone promoting the hydrogen transfer reaction (Scheme 9).<sup>29</sup> Excellent conversion, yield and enantiopurity were achieved. After this breakthrough, a number of catalysts suitable for racemization of secondary alcohols have been reported.<sup>30</sup>

### 1.2.3 Catalysts for DKR of *sec*-alcohols

Park and co-workers have described the isopropylamino substituted catalyst **15** which is active at ambient temperature.<sup>31</sup> Applicability of the catalyst for DKR of a wide range of secondary alcohols was demonstrated. Bäckvall and co-workers, in turn, performed extensive studies on structures with common formula **16**. It was shown that pentarylsubstituted complexes with carbonyl ligands possessed the highest racemization activities. Significant influence of the nature of the halogen to the racemization rate was not observed. Complex **17a** was selected for further detailed studies due to its high activity and its more straightforward synthesis. Applicability of this complex for DKR of a broad range of secondary alcohols was then demonstrated.<sup>32</sup>

Benzyloxy- and benzoyloxy substituted complexes **18a** and **18b** were likewise tested for applicability in DKR.<sup>33</sup> A polymer-supported analogue of **18b** was reported and demonstrated activity similar to the parent compound.<sup>33a</sup>

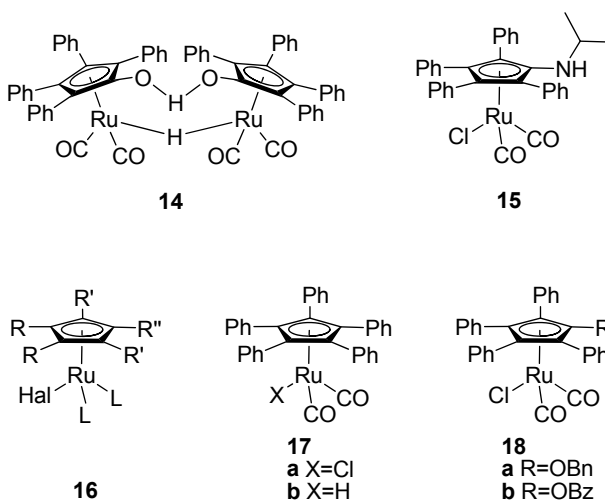


**Figure 4.** Leading racemization catalysts for DKR of *sec*-alcohols.

The results of DKR of *rac*-**8** utilizing the leading catalysts **14**, **15**, **17a** and **18a** are shown in Table 1. All reactions were performed in 1 mmol scale. Enantiomeric excesses of the products were excellent in all cases due to high enantioselectivity of the enzyme (CAL-B). The pentaphenylcyclopentadienyl catalyst **17a** appeared to be the leading candidate due to its high activity, ease of preparation and compatibility with a broad range of substrates.

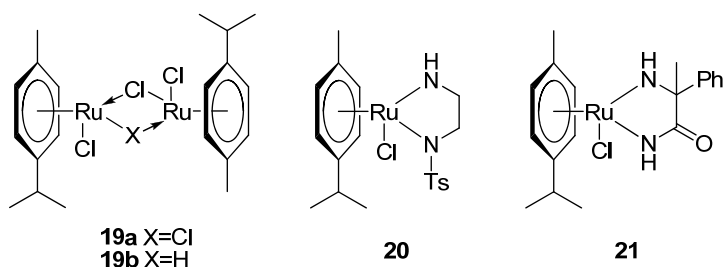


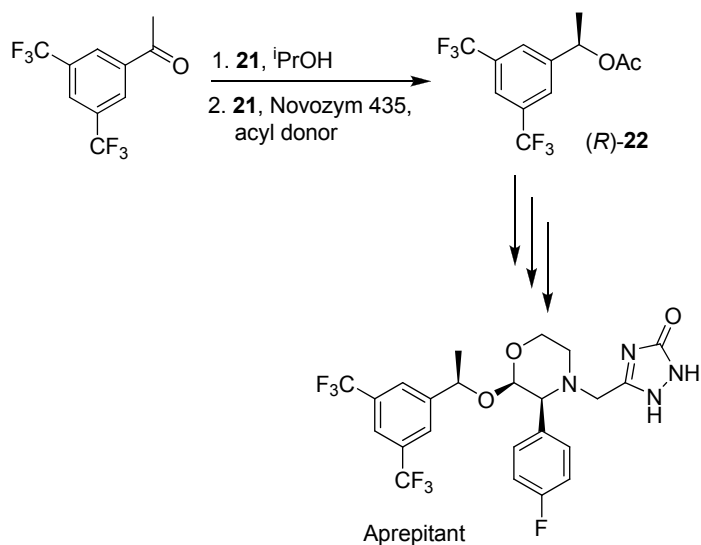
**Table 1.** Comparison of the leading catalysts for DKR of 1-phenylethanol<sup>a</sup>

Cat.	Cat. loading (mol%)	Conditions	Isol. yield (%)	Ref.
<b>14</b>	2	70 °C, 87 h	92	27, 29
<b>15</b>	4	RT, 1.5 d	95	31
<b>17a</b>	5	RT, 3 h	92	32
<b>18a</b>	4	RT, 20 h	98	33

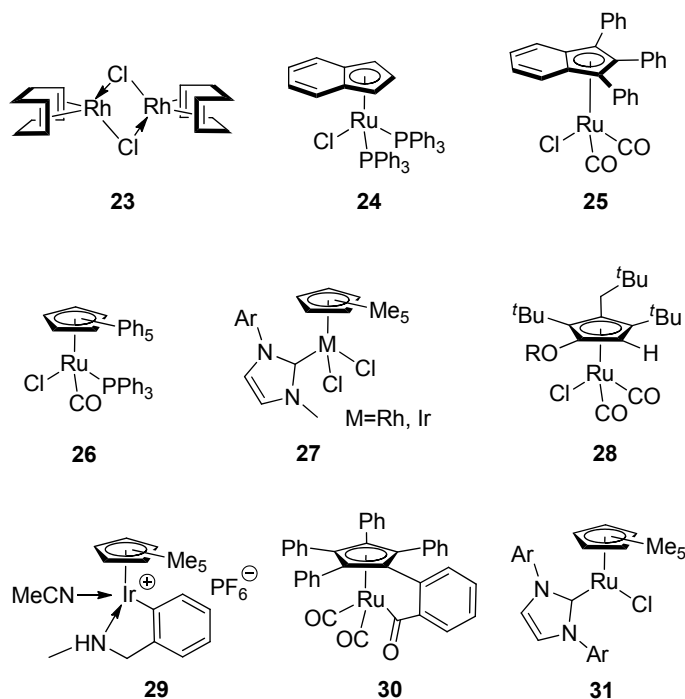
a) Substrate loading: 1 mmol; product ee >99%.

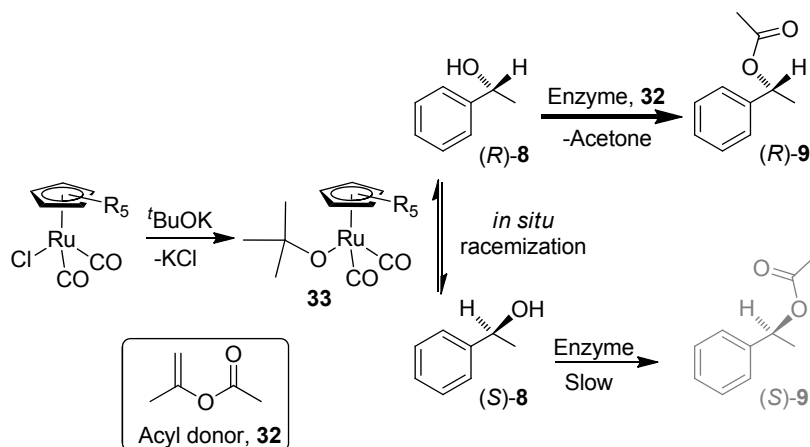
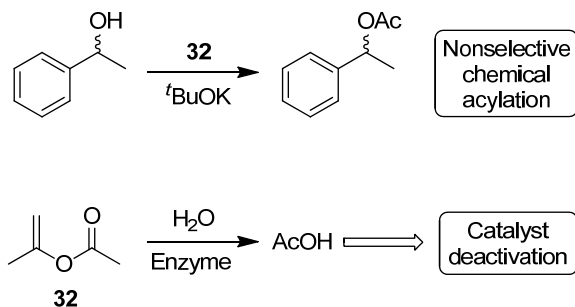
A number of examples on the utilization of ruthenium-cymene complexes for DKR of alcohols have been reported (Figure 5). Complexes **19a,b** were utilized for DKR of various allylic alcohols.<sup>34</sup> Complexes obtained by reaction of chelating diamines with **19a** were likewise utilized for DKR of various substrates. Complex **20** has been employed for DKR of 1-phenylethanol.<sup>35</sup> The racemic complex **21** was utilized for an iterative DKR producing chiral polyesters.<sup>36</sup> Chemical company DSM developed and patented a procedure for DKR of fluorinated alcohol (*R*)-**22** utilizing **21** both as a transfer hydrogenation and racemization catalyst.<sup>37</sup> The optically active alcohol produced is a precursor for the synthesis of the antiemetic drug Aprepitant (Emend) (Scheme 10).

**Figure 5.** Cumene-based ruthenium racemization catalysts.

**Scheme 10.** Utilization of **21** in DKR of fluorinated alcohol **22**

A number of other complexes have been tested in DKR and racemization applications:  
**23**,<sup>38</sup> **24**,<sup>39</sup> **25**,<sup>40</sup> **26**,<sup>41</sup> **27**,<sup>42</sup> **28**,<sup>43</sup> **29**,<sup>44</sup> **30**,<sup>45</sup> **31**<sup>46</sup> (Figure 6).

**Figure 6.** Other transition metal complexes utilized for DKR or racemization of *sec*-alcohols.

**Scheme 11.** The reaction network in the DKR of **8****Scheme 12.** Undesired side-reaction occurring during DKR of 1-phenylethanol **8**

### 1.2.4 Standard requirements for DKR<sup>47</sup>

The semi-reactions of racemization and enzymatic resolution should not interfere in an undesired fashion (Schemes 11, 12). For example, the strong base (usually *tert*-BuOK) required for catalyst activation should not be used in excess in order to avoid chemical acylation of the substrate which decreases the product enantiopurity. At the same time, residual water contained in the enzyme preparation or absorbed on a glassware surface can cause formation of acid due to hydrolysis of the acyl donor.<sup>48</sup> The acid released can deactivate the catalyst and decrease the racemization rate significantly. The racemization catalyst should be active at ambient temperatures since high temperatures can cause loss of enzyme activity and/or enantioselectivity. The enzymatic kinetic resolution should be irreversible. This condition is achieved by utilization of irreversible acyl donors, for example, iso-propenylacetate **32**. The reaction product should not undergo racemization under the reaction conditions employed. This requirement is achieved by formation of the alcohol ester making formation of the alkoxide complex with ruthenium impossible.

An appropriate ratio between the rates of racemization and enzymatic acylation is required. DKR is an example of a Curtin-Hammett system<sup>49</sup> (Figure 7). Several borderline cases should be discussed:

a) Both the enzyme and the catalyst show high performance:  $k_{\text{rac}} \gg k_R \gg k_S$ . The racemization rate is much higher compared to the rate of depletion of the more reactive enantiomer; the enzyme is highly enantioselective. According to the Curtin-Hammett rule, composition of the products is defined by Equation 2:

**Equation 2.** Application of the Curtin-Hammett rule to the DKR system

$$\frac{[(R)\text{-}\mathbf{9}]}{[(S)\text{-}\mathbf{9}]} = \frac{k_R}{k_S} K_{\text{eq}}$$

In case of racemization catalyzed by a non-chiral catalyst,  $K_{\text{eq}}=1$  and Equation 3 is obtained.

**Equation 3.** The simplified case of the Curtin-Hammett rule

$$\frac{[(R)\text{-}\mathbf{9}]}{[(S)\text{-}\mathbf{9}]} = \frac{k_R}{k_S}$$

Thus, enzymatic E-values (Chapter 1.2.1) equal to 50, 100 and 200 would provide the product with enantiomeric excesses 96%, 98% and 99%, respectively

b) The catalyst demonstrates high performance while the enzyme is moderately enantioselective:  $k_{\text{rac}} \gg k_R > k_S$ . A regular KR with low E-value, for example, 25 would produce the product in ~ 90% ee during the early stages of reaction. Further progress to 50% conversion would lead to decrease of ee to ~80%. By introduction of the racemization step, >90% ee would be maintained until the reaction is completed. Figure 8 obtained by numerical solution of Equation 1 demonstrates the dependence of product enantiopurity from conversion in case of KR and DKR utilizing an enzyme with a moderate enantioselectivity ( $E = 25$ )

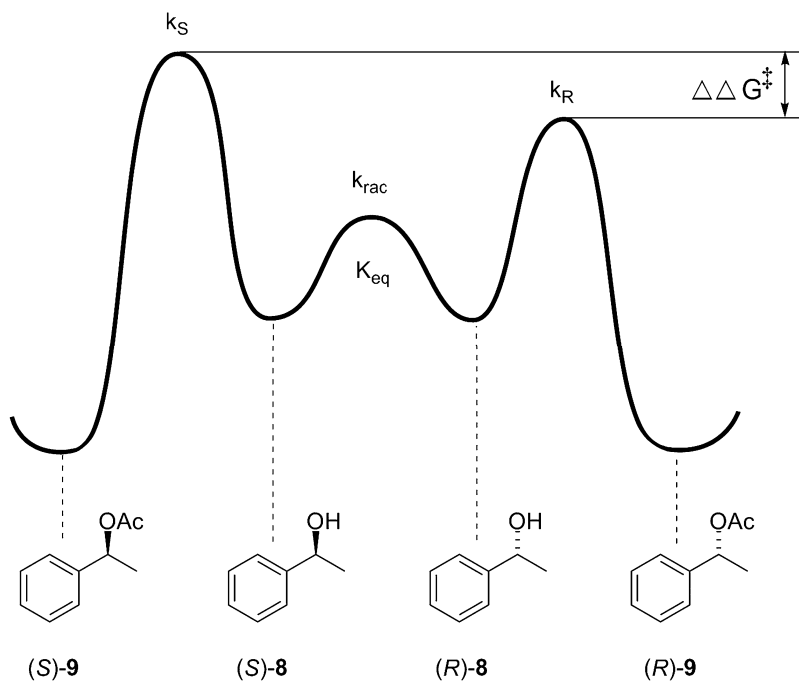


**Figure 7.** Application of the Curtin-Hammett rule to a DKR system.

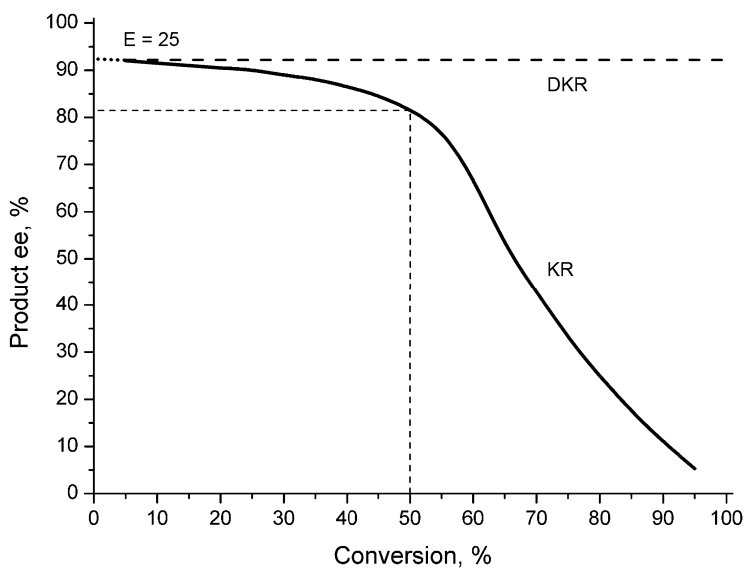


**Figure 8.** Benefits of DKR over a regular KR in case of moderate enzymatic enantioselectivity ( $E = 25$ ).

c) High enzymatic enantioselectivity and slower racemization rate:  $k_R > k_{rac} \gg k_S$ . Enantiopurity of the product would not be significantly affected albeit overall reaction rate would be extended due to depletion of the more reactive enantiomer. This limitation can be

overcome by increasing the reaction temperature leading to higher catalyst performance (Chapters 3.2.3 and 3.3).

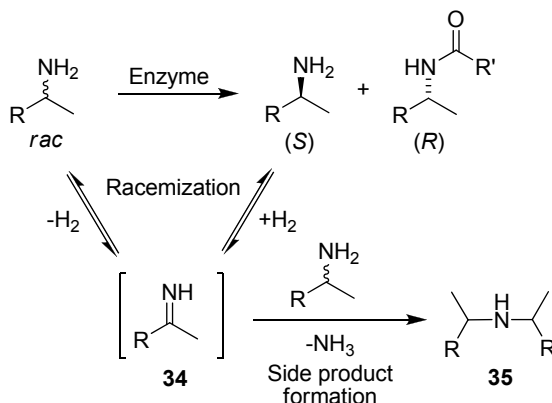
d) Both the enzymatic enantioselectivity and the racemization rate are mediocre:

$k_R > k_S \sim k_{\text{rac}}$ . The DKR system is not suitable for achieving good results.

### 1.2.5 DKR of amines

While the field of chemoenzymatic DKR of secondary alcohols has advanced remarkably in recent years, the analogous DKR of amines has remained challenging for various reasons. In general, racemization of amines is more difficult than the racemization of *sec*-alcohols, typically requiring much harsher conditions. Overall, the oxidation of an alcohol enantiomer to ketone and the subsequent reaction back to racemic alcohol is much more facile than the corresponding transformation from amine to imine **34**.<sup>30</sup> Furthermore, poisoning of metal-based racemization catalysts may take place in the presence of potentially ligating amines. Additional problems are encountered by the typically high temperatures required for racemization of amines being often detrimental for enzyme activity.

The first chemoenzymatic DKR of an amine utilizing Pd/C as the racemization catalyst in combination with CAL-B was described by Reetz.<sup>26</sup> The influence of the support material has been studied with Pd on modified silica providing the best results.<sup>50</sup> The reactions were carried out in autoclave under slight excess of H<sub>2</sub> pressure in order to facilitate racemization and suppress the formation of side products. A similar approach has been described for DKR of selenium-containing amines over Pd supported on BaSO<sub>4</sub>.<sup>51</sup> Pd nanoparticles precipitated on Al(OH)<sub>3</sub> have likewise been employed,<sup>52</sup> whereas attempts to use Raney Ni and Co have been less successful.<sup>53</sup> Bäckvall and co-workers investigated the homogeneous Shvo's catalyst<sup>54</sup> and its *para*-fluoro and *para*-methoxy substituted analogues for racemization of amines<sup>55</sup> with the last mentioned providing the best performance. The same *para*-methoxy substituted Shvo's catalyst has also been used by other investigators.<sup>56</sup> Other examples of homogeneous catalysts include half-sandwich iridium complexes investigated for DKR<sup>57</sup> and iridacycle based systems used for racemization only.<sup>58</sup> Photo-induced radical racemization in the DKR of amines has also been demonstrated.<sup>59</sup> An indirect way utilizing DKR of alcohols followed by Mitsunobu substitution of alcohol group with phthalimide with subsequent deprotection to amine has been also reported.<sup>60</sup> The DKR of amines is often complicated by formation of side products. Racemization of secondary amines commonly proceeds via the imine intermediate **34**, which upon reaction with a second amine molecule irreversibly results in the formation of dimer **35** (Scheme 13).<sup>30b,51,57b</sup>

**Scheme 13.** Side product formation during DKR of amines

### 1.3 Aims and outline of this thesis

The main aim of the present study was to prepare new ruthenium half-sandwich complexes and to screen their catalytic activities in racemization and DKR reactions in order to elucidate the underlying structure-activity relationships, reaction mechanisms and reaction kinetics. DKR catalysts described in the literature suffer from cost-inefficient preparation and not always satisfactory activity. Therefore, further development of the racemization catalysts is required. Moreover, DKR and especially racemization protocols reported recently are not optimal from the point of view of reproducibility and ease of monitoring. A significant part of this thesis is dedicated to development of reliable and reproducible procedures for DKR and racemization processes.

A paradigm of the racemization mechanism of secondary alcohols in the presence of half-sandwich ruthenium complexes underwent significant changes during last decade. Therefore, understanding of the reaction mechanism is very important for further developments in this field.

The thesis also describes the utilization of chemoenzymatic DKR procedure employing the developed catalyst(s) for preparation of a wide range of optically active secondary alcohols and esters. Scale-up of the DKR reactions up to hundreds gram loading has been reported in the literature earlier despite only optically active esters were obtained. Due to importance of free optically active alcohols for further synthetic utilization, possibility of large scale DKRs followed by alkaline hydrolysis of the products to the corresponding free alcohols is demonstrated.

In Chapter 2, screening of different racemization catalysts followed by identification of a leading catalyst candidate is described.

In Chapter 3, characterization of the new catalyst and its application in chemoenzymatic DKR is addressed.

In Chapter 4, detailed kinetic studies on the racemization process are described.

In Chapter 5, an alternative approach to chemoenzymatic DKR of amines is discussed.



## 2 Synthesis and characterization of potential candidates for racemization catalysts.

### 2.1 Introduction

Predominantly, in earlier studies pentasubstituted monocyclopentadienyl complexes of ruthenium have been utilized as racemization catalysts for alcohols.<sup>27,29-33,41-46</sup> Only a few examples based on indenyl<sup>39,40</sup> and aryl<sup>34-36</sup> ruthenium complexes have been described. For further structural tuning as well as for improvements in activities and stabilities of the racemization catalysts, the screening of new ligand modifications is desirable. Here, the indenyl ligand platform provides a number of opportunities for structural variation. Examples of transition metal complexes containing fused-ring, polycyclic indenyl-type ligands, such as cyclopenta[*l*]phenanthrenyl<sup>61</sup> and cyclopenta[*a*]acenaphthylenyl<sup>62</sup> are relatively scarce, but have been, in the context of catalytic  $\alpha$ -olefin polymerization (mainly  $M = \text{Zr}$ ),<sup>61b,c</sup> shown to result in enhanced catalyst properties. Prior to this work, ruthenium complexes containing cyclopenta[*l*]phenanthrenyl ligands have been reported in two cases only: Sato and co-workers obtained unsubstituted cyclopenta[*l*]phenanthrenyl complex of ruthenium by double arylation of ruthenocenyl-dioxaborolane with 2,2'-diiodobiphenyl;<sup>63</sup> Hagiwara and co-workers recently utilized the 1,2,3-triphenyl cyclopenta[*l*]phenanthrenyl moiety as a ligand in their catalyst design for Suzuki-Miyaura coupling.<sup>64</sup>

### 2.2 Preparation and characterization of complexes with different ligands

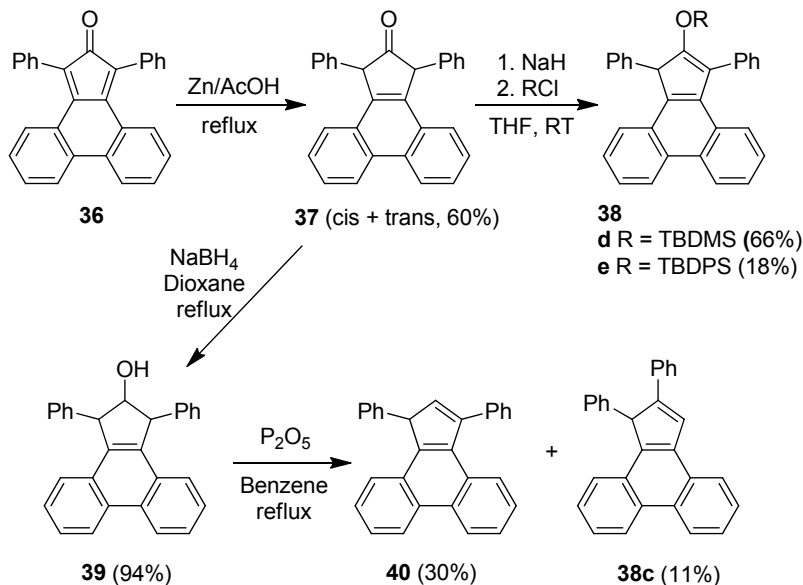
In the present chapter the initial results in the use of cyclopenta[*l*]phenanthrenyl, cyclopenta[*a*]acenaphthylenyl and indenyl ligands as structural motifs for alcohol racemization catalysts with potential applications in DKR in combination with enzymes are described. The resulting monocyclopentadienyl ruthenium complexes combine the elements of the previously reported metallocene racemization catalysts containing polysubstituted cyclopentadienyl ligands with a flat polycyclic part. Also a number of pentasubstituted cyclopentadienyl complexes of ruthenium and palladium were prepared and screened for their catalytic activities. The specific purpose of the work was to investigate the relationships between the structures and catalytic activities of these half-sandwich metallocene complexes.

#### 2.2.1 Complexes with polycyclic fused aromatic ligands

The substituted cyclopenta[*l*]phenanthrenyl ligand precursors **38a**, **b** and the triphenyl substituted cyclopenta[*a*]acenaphthylenyl ligand precursor **38f** were prepared according to previously reported procedures.<sup>61a, 65</sup> The siloxy substituted ligands **38d**, **e** were synthesized by silylation of the corresponding enolized ketone in a manner similar to that reported earlier for 1,3-dihydro-2-oxocyclopenta[*l*]phenanthrene,<sup>61d</sup> 2-indanone and its analogues (Scheme 14).<sup>66</sup>

The preparation of the diphenyl substituted ligand precursor **38c** is illustrated in Scheme 14. A similar transformation has been described earlier,<sup>67</sup> where the authors claimed the formation of the symmetrical 1,3-(diphenyl)cyclopenta[*l*]phenanthrene **40**. In this work, however, a rearrangement was observed to take place leading to a mixture of the 1,3- and 1,2-substituted products **40** and **38c** in 1:3 ratio. A similar rearrangement in the case of a trisubstituted analogue under acidic conditions has been described earlier.<sup>68</sup>

**Scheme 14.** Synthesis of the ligand precursors **38a, b, c**



Structures of the compounds isolated here were also confirmed by NMR analysis of the corresponding anions. Upon deprotonation with *n*-BuLi in THF-*d*<sub>8</sub>, compound **40** produced a highly symmetrical anion while compound **38c** gave an unsymmetrical structure (Figure 9). The position of the double bond in **38c** was likewise confirmed by NMR-spectroscopy. The two protons of the C<sub>5</sub>-ring give rise to two doublets (<sup>4</sup>*J* = 1.1 Hz) in the <sup>1</sup>H NMR spectrum at 5.42 and 7.81 ppm, respectively. In addition, a weak interaction (typical for allyl or W-coupling) between these protons was observed in the COSY-spectrum while a geminal coupling typical for CH<sub>2</sub>-group was absent.

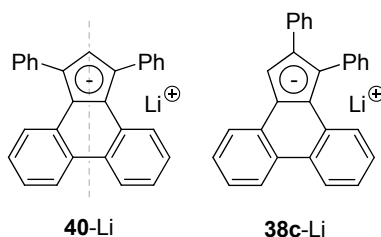
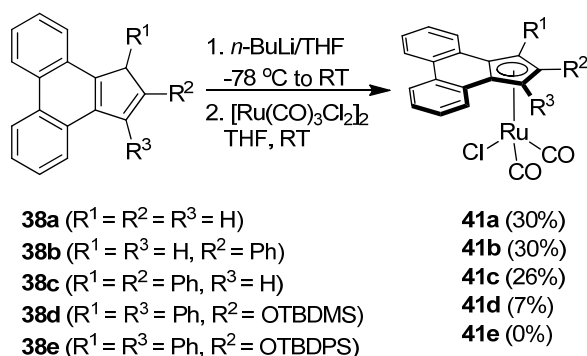


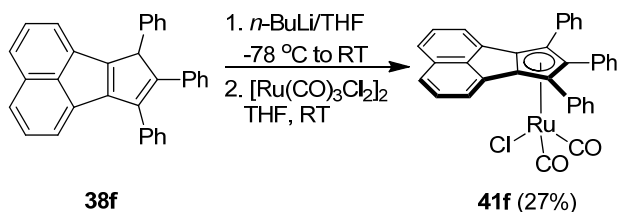
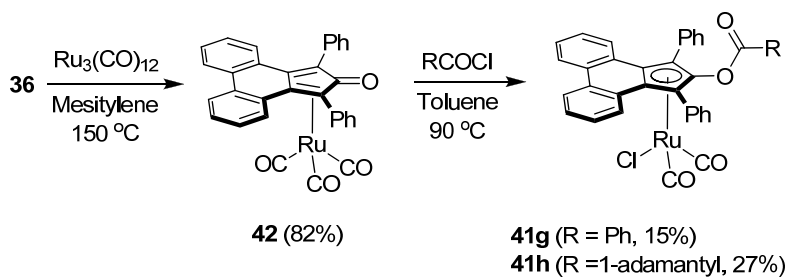
**Figure 9.** Lithium salts of the cyclopenta[7]phenanthrenyl ligand precursors **40** and **38c**.

Next, the new ruthenium complexes **41a-d, f** containing cyclopenta[7]phenanthrenyl and cyclopenta[*a*]acenaphthylenyl ligands were prepared by reactions of dichlorotricarbonylruthenium dimer with the corresponding ligand precursors deprotonated with butyllithium (Schemes 15 and 16). The fairly low yields obtained represent the non-optimized reaction conditions for metallation. In all cases significant amounts of starting ligand precursor were recovered during the reaction work-up. In case of **38e**, formation of the desired ruthenium complex was not observed, probably due to steric reasons. Complex **41a** is unstable, decomposing rapidly in solutions and slowly in the solid state during storage at ambient temperature. All other polysubstituted complexes are stable when stored in air.

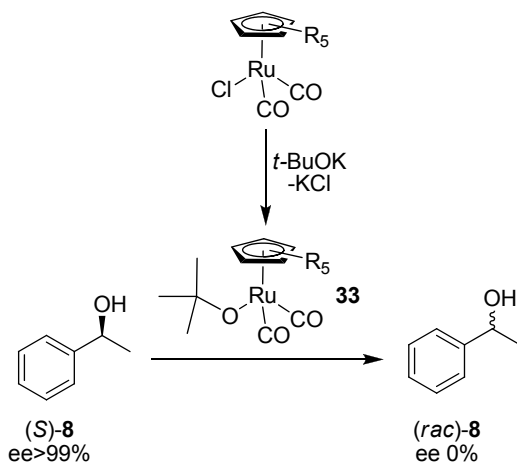
The synthesis of the trisubstituted cyclopenta[7]phenanthrenyl ruthenium complexes **41g** and **41h** containing an acyl substituent in position 2 of the C<sub>5</sub>-ring commenced, in turn, from the phencyclone precursor **36** followed by oxidative acylation of the Ru(0) diene complex **42** with the corresponding acyl chlorides (Scheme 17).

**Scheme 15.** Synthesis of the ruthenium complexes **41a-d**.



**Scheme 16.** Synthesis of the ruthenium complex **41f****Scheme 17.** Synthesis of the ruthenium complexes **41g** and **41h**

All ruthenium(II) complexes prepared **41a-d**, **f-h** were screened as catalysts for the racemization of (*S*)-**8**, a standard reference substrate utilized for initial investigation of catalytic activities in alcohol racemization and DKR (Scheme 18, Table 2). The catalysts were pre-activated with potassium tert-butoxide in order to form the active catalytic species **33**. The racemization reactions were carried out in toluene at ambient temperature by following the procedure described earlier by Bäckvall and co-workers.<sup>32c</sup>

**Scheme 18.** Racemization of (*S*)-**8**: Catalyst **41a-d**, **f-h** 1 mol-%, *t*-BuOK 3 mol-%, toluene, RT

**Table 2.** Time required to achieve 50% ee in racemization of (*S*)-**8** in presence of 1 mol-% of different catalysts

Catalyst	Time
<b>41a</b>	- <sup>a</sup>
<b>41b, c</b>	2-4 d
<b>41d, f, h</b>	~1 h
<b>41g</b>	~15 min
<b>17a, 43a, 46, 49a, b</b>	<5 min

(a) Reaction stops at 70% ee after 2 days.

The unsubstituted cyclopenta[*l*]phenanthrenyl complex **41a** was found to be inefficient as a catalyst for the racemization reaction. With this complex, the racemization stops at 70% ee after 2 days. Somewhat better activities were obtained with the mono- and disubstituted complexes **41b** and **41c**. The racemization rate remained, however, fairly low with 50% ee reached only after 4 and 2 days of reaction, respectively. Only in the case of the fully substituted complexes **41d, f, g, h** acceptable activities were obtained providing complete racemization in less than an hour. The complexes prepared can be arranged in a series according to their 1-phenylethanol racemization activities as follows: **41a** < **41b, c** << **41d, f, g, h**, clearly demonstrating increasing activities with increasing number of C<sub>5</sub>-ring substituents. Similar observations on dependence of activity from the substitution pattern were reported by Bäckvall and co-workers. The Ph<sub>5</sub>Cp complex **17a** demonstrated excellent performance while replacing one phenyl group in the Cp-ring with methyl resulted in decrease of racemization activity. Unsubstituted C<sub>5</sub>H<sub>5</sub> complex was not active in racemization (Figure 10).<sup>32a</sup>

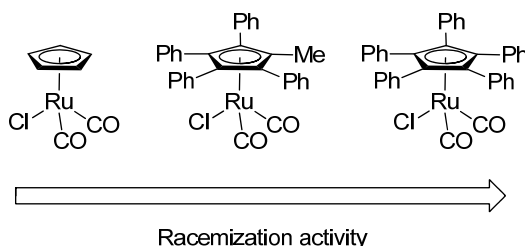


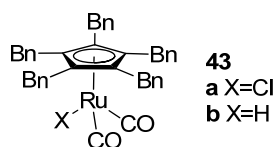
**Figure 10.** Dependence of racemization activity from the substitution pattern according to Bäckvall and co-workers.

The highest racemization rate was observed with benzoyloxysubstituted **41g**. It could be speculated that the pendant phenyl functionality of the 2-benzoyl substituent might have a

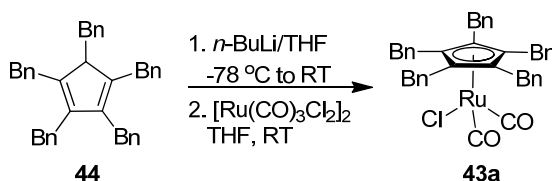
throughspace stabilizing, coordinative interaction with the ruthenium metal center. Similar intramolecular arene coordination is well known for Ti- and Zr-based mono(cyclopentadienyl) olefin polymerization catalysts<sup>69</sup> and has been described recently for Mo and W complexes.<sup>70</sup> The racemization rate obtained with **41g** is, however, slower than that observed for the (pentaphenyl)cyclopentadienyl-based complex **17a**. In case of **17a**, complete racemization under similar conditions was observed in 5 min. On the other hand, complex **18a**, structurally similar to **41g**, was reported by Park and co-workers to provide similar activities at 4 mol-% concentration<sup>33a</sup> than those observed here for **41g** at 1 mol-% loading.

### 2.2.2 Complexes with pentasubstituted cyclopentadienyl ligands

Preparation of a number of half-sandwich, indenyl-based Ru-complexes containing fused aromatic ring-substituents and initial screening of their efficiencies as racemization catalysts for (*S*)-**8** was described in chapter 2.2.1.<sup>71</sup> In this series of complexes, enhanced racemization performance (albeit clearly inferior to that of **17a**) was observed with the benzyloxy substituted catalyst **41g**, containing a pendant aromatic phenyl ring, when compared with its 1-adamantyl substituted analogue **41h**. This led us to further investigate the pendant aromatic substituent effects in DKR and preparation of the Bn<sub>5</sub>Cp analogue of **17a**, namely the chlorodicarbonyl ruthenium complex **43a** (Figure 11). The hydride analogue **43b** of **43a** has been described earlier in the patent literature in the context of diol dehydroxylation.<sup>72</sup> In comparison to Ph<sub>5</sub>CpH<sup>32c</sup> and other polyalkylated or arylated cyclopentadienyl ligands,<sup>73</sup> the high yield preparation of Bn<sub>5</sub>CpH is both seemingly simple and cost efficient, even in large scale, consisting of the reaction of cyclopentadiene with sodium benzyolate in BnOH.<sup>74</sup> Complex **43a** was characterized by <sup>1</sup>H and <sup>13</sup>C NMR and X-ray crystallography (Chapter 2.3). The first synthetic route towards **43a** was similar to those utilized for **41a-d, f** (Scheme 19) and suffered from low yield. Later an improved procedure for large scale preparation of **43a** was developed (Chapter 3.1).

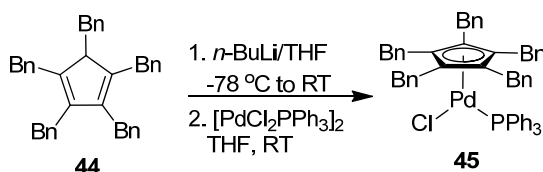


**Figure 11.** Pentabenzyl analogue of **17a**.

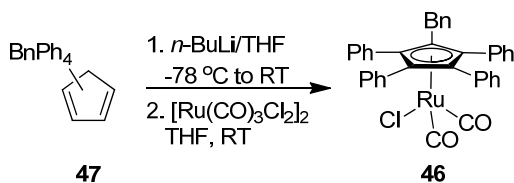
**Scheme 19.** Initial synthesis of **43a**

Preliminary racemization and DKR tests demonstrated that activity of the new catalyst **43a** is similar to that of the earlier reported lead candidate **17a**.<sup>75</sup> For further studies of applicability of **43a** see Chapter 3.

In previous reports by other investigators, the  $\text{Bn}_5\text{Cp}$  ligand has been complexed with other transition metals including Ti,<sup>76</sup> Co,<sup>74a</sup> Rh,<sup>74a</sup> Mn,<sup>77</sup> Re,<sup>77</sup> Fe,<sup>77,78</sup> Mo,<sup>79</sup> and W.<sup>79</sup> In order to further investigate the ligation properties of pentabenzylcyclopentadiene, the Pd-analogue  $\text{Bn}_5\text{CpPdCl}(\text{PPh}_3)$  **45** was prepared. The synthesis of **45** was performed by reaction of the pentabenzylcyclopentadienyl **44** anion lithium salt with dimeric chloro-phosphinocomplex  $[\text{PdCl}_2\text{PPh}_3]_2$  as the Pd source (Scheme 20). Complex **45** was characterized by  $^1\text{H}$ ,  $^{13}\text{C}$  and  $^{31}\text{P}$  NMR and X-ray crystallography being the first example of a  $\text{Bn}_5\text{Cp}$  ligated Pd-complex.<sup>80</sup> Simultaneously with this work, Janiak and co-workers prepared and reported a similar  $\text{Bn}_5\text{Cp}$  palladium complex, bearing triphenylarsine and perfluorophenyl ligands.<sup>81</sup> As expected, complex **45** is not active as a racemization catalyst for *sec*-alcohols under conditions employed for the ruthenium cyclopentadienyl systems.

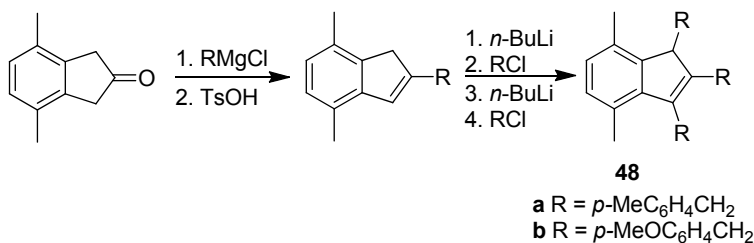
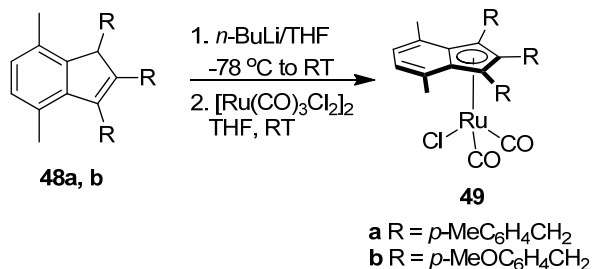
**Scheme 20.** Synthesis of **45**

For further investigating the effect of benzyl substituents in racemization catalysts, the mono-benzyl substituted analogue of **17a**, complex **46**, was prepared by reaction of deprotonated  $\text{Ph}_4\text{BnCpH}$  with  $[\text{Ru}(\text{CO})_3\text{Cl}_2]_2$  (Scheme 21). Later, an improved procedure for preparation of **46** was developed similar to the one utilized for **43a** (Chapter 3.1). The tetraphenylbenzylsubstituted ligand precursor **47** was prepared in a manner similar to that utilized earlier for the  $\text{Ph}_5\text{CpH}$  analogue.<sup>32c, 75</sup> The racemization activity of **46** towards (*S*)-**8** is similar to that of **17a** and **43a**.

**Scheme 21.** Synthesis of **46**

### 2.2.3 Complexes with indenyl-based ligands

Indene skeleton provides a versatile platform for further modifications. Relatively high acidity of the  $\alpha$ -protons allows easy deprotonation and the obtained anion can be quenched with a number of electrophiles providing, for example, alkylated products.<sup>82</sup> Two tri-benzyl substituted indenyl ligands **48a, b** precursors were prepared by this method (Scheme 22). The ligands were converted into the corresponding complexes **49a, b** (Scheme 23).<sup>83</sup> The complexes were characterized by  $^1\text{H}$  and  $^{13}\text{C}$  NMR and the structure of **48b** was also confirmed by X-ray analysis (chapter 2.3). Preliminary racemization tests demonstrated that the catalytic activities of the complexes **49a, b** are similar to those of **17a** and **43a**.

**Scheme 22.** Preparation of indenyl based ligands **48a, b****Scheme 23.** Preparation of indenyl complexes **49a, b**

### 2.3 Molecular structures of the metal complexes

In the  $^1\text{H}$  NMR spectra of **41d** and **41h** two kinds of  $o$ - and  $m$ -protons and carbons were observed indicating restricted rotation of the phenyl rings. This rotation remained blocked in VT



NMR experiments at 50 °C. The lithium salt of **38d** obtained by deprotonation with *n*-BuLi, however, showed in the  $^1\text{H}$  NMR spectrum time-averaged symmetry with only one type of *o*- and *m*-protons and carbons (Figures 12 and 13) consistent with rapid rotation of the phenyl rings in solution at ambient temperature resulting in coinciding resonances. Another explanation, however, is the potential lability of the ionically bound lithium cation. A rapid exchange of  $\text{Li}^+$  transitorily bound on one side of the ligand and the other (even being located in the solvent independently from the anion) may also result in time averaging of the NMR signals without rotation about the C-Ph bond. A similar effect was observed when NMR spectra of **38c** and **41c** were compared.

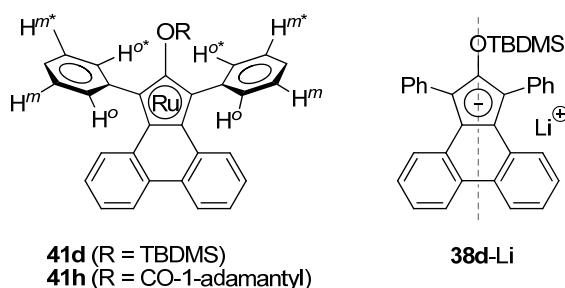


**Figure 12.** Top views of **41d**, **41h** and **38d-Li**. Carbonyls ligands and the chlorine atom are omitted for clarity.

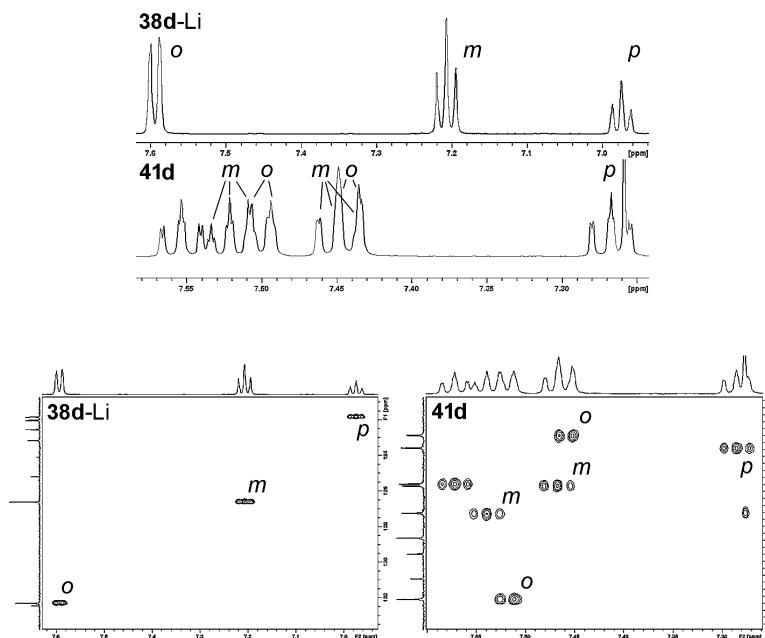


**Figure 13.**  $^1\text{H}$  and HSQC NMR of **38d-Li** and **41d**.

The molecular structures of the ruthenium and palladium complexes **41b**, **f**, **g**, **42**, **43a**, **45**, **46** and **49a** were determined by X-ray crystallography and are elucidated, together with selected bond lengths and angles, in Figures 14-21 and Table 3. The molecular structures of **41g**, **46** and **49a** show a disorder, in which the Cl ligand and one of the two CO ligands have two orientations in a 1:1 ratio. The ruthenium metal is  $\eta^5$ -coordinated in complexes **41b**, **f**, **g**, **43a**, **46** and **49a** (with similar Ru-C bond distances to all carbon atoms of the five-membered ring) and  $\eta^4$ -coordinated in complex **42** with the longest Ru-C distance to the carbonyl carbon of the C<sub>5</sub>-ring. The Ru-CO bond lengths are similar in all six  $\eta^5$ -coordinated complexes. In the  $\eta^5$ -coordinated complexes **41b**, **f**, **g** and **49a** containing fused ring ligands, the cyclopenta[*l*]phenanthrenyl, cyclopenta[*a*]acenaphthylenyl and indenyl moieties are nearly planar. A small distortion from planarity for the terminal C<sub>6</sub> ring of **41b** is observed, possibly due to repulsion of the partial negative charge on the ligand and the electronegative chlorine atom. Indenyl moiety of **49a** with substituents is planar, except for the 2-benzylic CH<sub>2</sub> group which is positioned slightly above the molecular plane. In the  $\eta^4$ -diene complex **42** the ligand plane is significantly distorted with one terminal C<sub>6</sub> ring tilted and the coordinated C<sub>5</sub> ring showing envelope geometry. Complex **41g** derived from **42** demonstrates a planar geometry of both the phenanthrene and cyclopentadienyl moieties. The formal oxidation states +2 for **41b**, **f**, **g**, **43a**, **46** and **49a** and 0 for **42** are in good accordance with the elongated Ru – carbonyl and Ru – C<sub>5</sub> centroid distances in the latter complex. The Ru – C<sub>5</sub>, Ru – carbonyl and Ru – Cl distances are similar to those in analogous complexes containing (pentaphenyl)cyclopentadienyl<sup>32c</sup> and (triphenyl)indenyl<sup>40</sup> ligands. The palladium complex **45**, however, displays a one-short, two-intermediate, two-long bonding pattern with the bond lengths between the metal atom and carbon atoms of the five-membered ring ranging from 2.203 to 2.449 Å being consistent with tendency towards  $\eta^3$  (or  $\eta^1$ ) bonding mode with three Pd-C bonds much shorter than the other two. Similar splitting of bond lengths has been observed earlier for other sterically encumbered cyclopentadienyl palladium complexes with Me<sub>5</sub>CpPdCl(*i*-Pr<sub>3</sub>P) displaying an one-short, two-intermediate, two-long bonding pattern (2.219-2.403 Å)<sup>84</sup> and Ph<sub>5</sub>CpPd( $\eta^3$ -CH<sub>2</sub>C(CH<sub>2</sub>OS(O)Ph)CH<sub>2</sub>) displaying a four-intermediate, one-long bonding pattern (2.294-2.443 Å).<sup>85</sup> The Bn<sub>5</sub>CpPd(AsPPh<sub>3</sub>)C<sub>6</sub>F<sub>5</sub> complex reported by Janiak and co-workers displays also one short, two-intermediate and two-long bonding pattern (2.240-2.405 Å).<sup>81</sup> In solution, the benzyl substituents of both Bn<sub>5</sub>Cp complexes **43a** and **45** rotate freely around the Cp-CH<sub>2</sub> bond at ambient temperature displaying only one sharp singlet for the benzylic CH<sub>2</sub> groups in the <sup>1</sup>H and <sup>13</sup>C NMR spectra. The structures of **43a** and **46** were by X-ray analysis confirmed to contain essentially features analogous to those of **17a**.<sup>32c</sup> The molecular structures of **43a** and **46** show the expected  $\eta^5$ -bonding of ruthenium also found in the closely analogous half-sandwich

pentabenzylcyclopentadienyl complexes  $\text{Bn}_5\text{CpM}(\text{CO})_3\text{OTf}$  ( $\text{M} = \text{Mo}, \text{W}$ )<sup>86</sup> and  $\text{Bn}_5\text{CpCo}(\text{CO})_2$ .<sup>74b</sup>

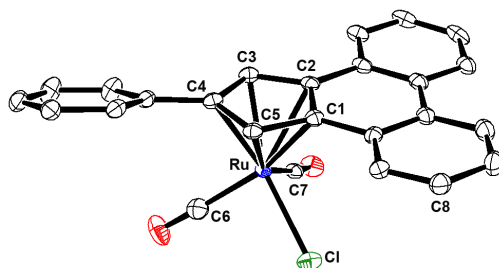


**Figure 14.** The molecular structure of **41b** (hydrogen atoms excluded for clarity, 50% probability ellipsoids).

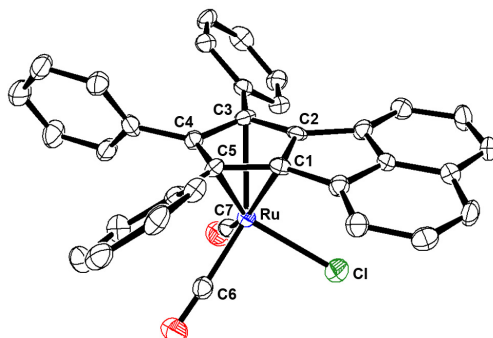


**Figure 15.** The molecular structure of **41f** (hydrogen atoms excluded for clarity, 50% probability ellipsoids).

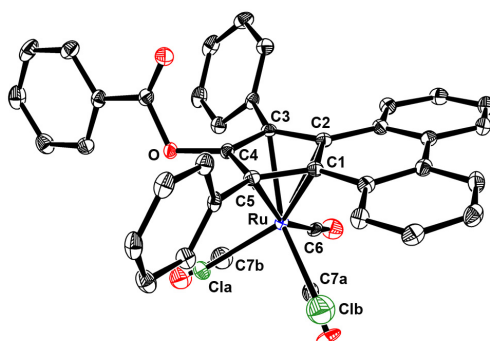


**Figure 16.** The molecular structure of **41g** (hydrogen atoms excluded for clarity, 50% probability ellipsoids).

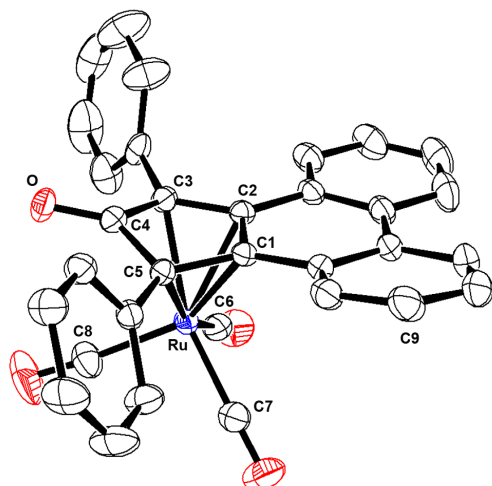


**Figure 17.** The molecular structure of **42** (hydrogen atoms excluded for clarity, 50% probability ellipsoids).

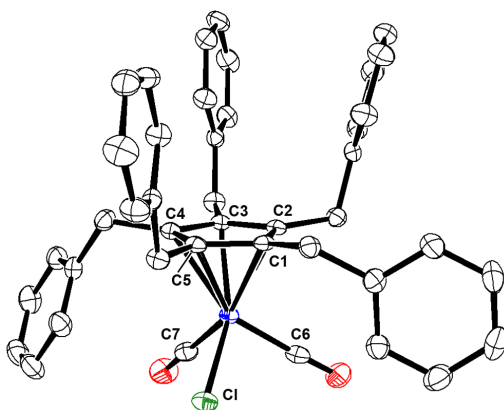


**Figure 18.** The molecular structure of **43a** (hydrogen atoms excluded for clarity, 50% probability ellipsoids).

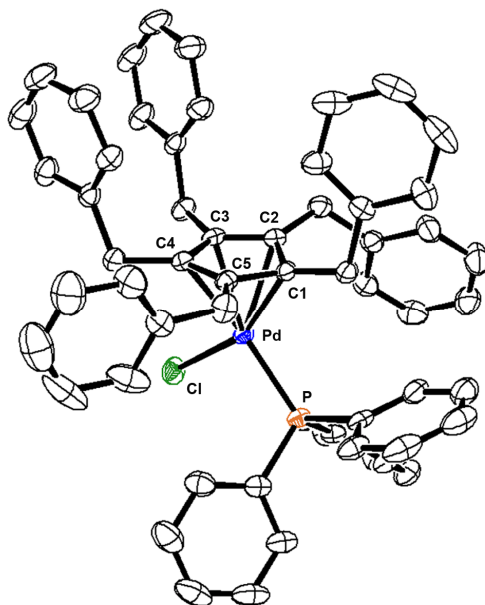


**Figure 19.** The molecular structure of **45** (hydrogen atoms excluded for clarity, 50% probability ellipsoids).

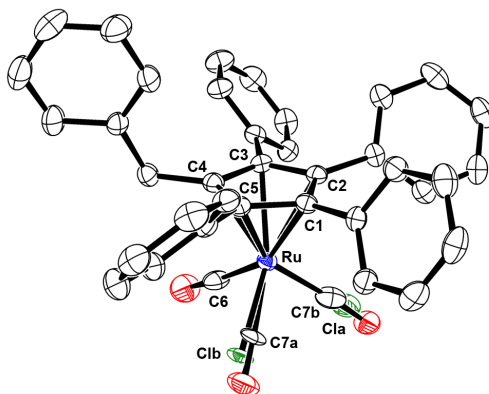


**Figure 20.** The molecular structure of **46** (hydrogen atoms excluded for clarity, 50% probability ellipsoids).

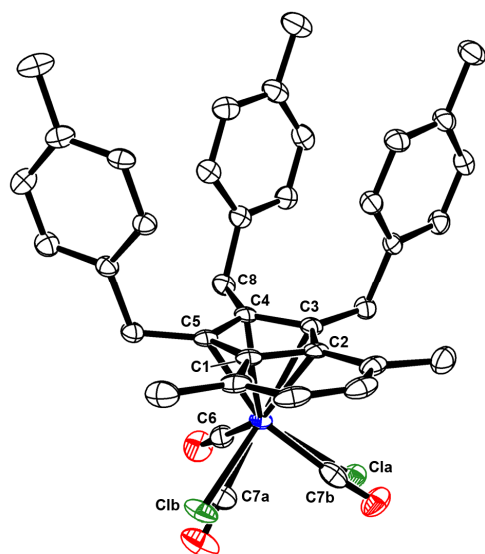


**Figure 21.** The molecular structure of **49a** (hydrogen atoms excluded for clarity, 50% probability ellipsoids).

**Table 3.** Selected bonding distances in the complexes **41b**, **f**, **g**, **42**, **43a**, **45**, **46** and **49a**

	M-Cp distances, Å					M-CO, Cl distances, Å				
	M-C1	M-C2	M-C3	M-C4	M-C5	M-Ct <sup>a</sup>	M-C6	M-C7	M-C1	
<b>41b</b> <sup>b</sup>	2.304(2)	2.281(3)	2.196(3)	2.253(3)	2.247(3)	1.899	1.889(3)	1.898(3)	2.3988(7)	
<b>41f</b>	2.285(4)	2.277(4)	2.269(4)	2.199(3)	2.286(4)	1.904	1.888(5)	1.876(5)	2.4030(10)	
	2.260(4) <sup>c</sup>	2.293(4) <sup>c</sup>	2.284(4) <sup>c</sup>	2.204(3) <sup>c</sup>	2.279(4) <sup>c</sup>	1.902 <sup>c</sup>	1.874(5) <sup>c</sup>	1.902(5) <sup>c</sup>	2.4043(10) <sup>c</sup>	
<b>41g</b> <sup>d</sup>	2.2444(18)	2.2384(19)	2.2407(18)	2.2405(18)	2.2383(18)	1.876	1.937(3)	1.871(4)	2.3910(10)	
<b>42</b> <sup>f</sup>	2.2673(17)	2.2139(17)	2.2186(18)	2.4896(18)	2.2207(18)	1.919	1.936(2)	1.932(2)	-	
<b>43a</b>	2.234(2)	2.210(2)	2.194(2)	2.275(2)	2.274(2)	1.875	1.890(2)	1.906(2)	2.4162(5)	
<b>45g</b>	2.203(2)	2.314(2)	2.323(2)	2.443(2)	2.418(2)	1.999	-	-	2.3552(6)	
	2.203(2) <sup>c</sup>	2.297(2) <sup>c</sup>	2.295(2) <sup>c</sup>	2.449(2) <sup>c</sup>	2.435(2) <sup>c</sup>	1.994	-	-	2.3594(6) <sup>c</sup>	
<b>46</b>	2.241(3)	2.280(3)	2.248(3)	2.224(3)	2.249(3)	1.884	1.910(4)	1.910(16)	2.392(4)	
<b>49a</b> <sup>h</sup>	2.3217(19)	2.3233(19)	2.218(2)	2.237(2)	2.202(2)	1.899	1.875(2)	1.877(13) <sup>e</sup>	2.380(4) <sup>e</sup>	
								1.888(11)	2.388(3)	
								1.962(13) <sup>e</sup>	2.400(2) <sup>e</sup>	

a) Ct is the C<sub>5</sub> ring centroid; b) C8-Pl 0.078, Pl – is the plane calculated for C<sub>5</sub> and two other C<sub>6</sub> rings; c) The corresponding bond lengths of the second molecule in the asymmetric unit; d) C4-O 1.369(2); e) The molecular structure shows a disorder in which the Cl ligand and one of the two CO ligands have two orientations in a 1:1 ratio; f) M-C8 1.928(2), C4-O 1.227(2), C9-Pl1 0.493, angle Pl2-Pl3 17.96, Pl1 is the plane calculated for two flat C<sub>6</sub> rings; Pl2 – for C1, C2, C3, C4; Pl3 – for C3, C4, C5, O; g) Pd-Pl1 2.2538(6)/2.2523(6), Pd-Cl 2.3552(6)/2.3594(6), see note c); h) C8-Pl 0.267, Pl is the plane calculated for the indenyl moiety.

## 2.4 Summary and conclusions

To summarize, a series of half-sandwich ruthenium complexes with substituted cyclopenta[*l*]phenanthrenyl, cyclopenta[*a*]acenaphthylenyl, indenyl and cyclopentadienyl ligands were prepared and characterized by NMR and in eight cases by X-ray crystallography. Restricted rotation of phenyl substituents in the ligand five-membered rings was observed in some cases when moving from the lithium salts to transition metal coordination.

The catalytic activities of the complexes in racemization of (*S*)-1-phenylethanol were investigated showing to depend strongly on the substitution pattern of the ligand framework. Acceptable racemization results were obtained with fully substituted complexes only (See table A1). The palladium based complex **45** was inactive. In the present work, the best performance was observed with complexes **43a**, **46** and **49a, b** containing a pendant aromatic moiety (benzyl). The pentabenzylsubstituted complex **43a** was selected for further detailed studies due to its ease of preparation and promising initial activity.

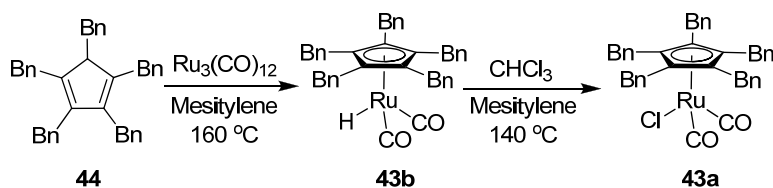


### 3 Characterization and application of $\text{Bn}_5\text{CpRu}(\text{CO})_2\text{Cl}$ as racemization catalyst

#### 3.1 Large scale preparation of $\text{Bn}_5\text{CpRu}(\text{CO})_2\text{Cl}$

In order to perform an extensive characterization and for studying the possible applications of the promising catalyst **43a**, large quantities of this compound were needed. Therefore, a reliable procedure for its preparative scale synthesis was required. In general, deprotonation of the corresponding cyclopentadienyl ligand followed by quenching with ruthenium chlorocarbonyl complex (Chapter 2.2.1) is a versatile method for research purposes when small amounts of a product are required. In case of gram-scale synthesis, this procedure becomes unfeasible due to low yield and high cost of the ruthenium precursor. Therefore, a procedure developed by Bäckvall and co-workers<sup>32c</sup> for preparation of **17a** was adapted also for **43a** (Scheme 24).

**Scheme 24.** An improved synthesis of **43a**



In this and earlier work, chlorodicarbonylcyclopentadienyl ruthenium complexes were prepared by one-pot chlorination of the corresponding hydrides obtained from the reaction of the ligand precursor with ruthenium carbonyl.<sup>32c,75</sup> Such metallation reactions are seldom quantitative and commonly require separation of the unreacted ligand from the metal complex by chromatography or crystallization. Due to the poor solubility of polyarylcyclopentadienyl ligands, isolation of the corresponding ruthenium complexes is often tedious. Purification by crystallization tends to result in contamination of the metal complex by small amounts of the ligand. Column chromatographic separation on silica in turn requires large amounts of eluent for removing the poorly soluble unreacted ligand having  $R_f$  value higher than the corresponding metal complex. Significant (up to 10 mass-%) inclusion of hexane from the eluent into the solid product purified by column chromatography was observed during preparation of **17**. Extended drying in vacuum did not remove the impurity. In case of **43a**, significant contamination with hexane was not observed. Beneficially, and in contrast to most polyarylated cyclopentadienyl ligand precursors,  $\text{Bn}_5\text{CpH}$  **44** is highly soluble in common organic solvents. In our earlier report, complex **43a** was initially purified by column chromatography providing the pure product in 53% yield.<sup>75</sup> Later, an improved chromatography-free purification method was developed which ideally provides pure metal complex in multigram scale either by washing of the

unreacted and highly soluble ligand precursor with a suitable solvent or, alternatively, by crystallization from a suitable solvent.<sup>80, 87</sup>

Heating of  $\text{Bn}_5\text{CpH}$  with  $\text{Ru}_3(\text{CO})_{12}$  in a tightly closed tube under argon atmosphere at 160 °C for 8 days in mesitylene was accompanied by purging of the CO formed under argon stream every 48 hours.  $^1\text{H}$  NMR was found to be a convenient method for monitoring the reaction progress by following the sharp and distinctive peak of the benzylic  $\text{CH}_2$  protons of the corresponding hydride. Subsequent addition of a small amount of chloroform and continued heating at 140 °C for one day provided, after filtration and removal of the solvents, the crude chlorodicarbonylruthenium complex. Subsequent washing of the crude material with a small amount of hot hexane gave pure metal complex **43a** as a microcrystalline solid in 88% yield. From this experiment nearly 8 grams of catalyst **43a** were obtained by use of a simple washing procedure. A minor mesitylene impurity (1 mass %) does not play a significant role for further utilization of the catalyst due to chemical stability of mesitylene and its similarity to toluene, a standard solvent for DKR reactions. Alternatively, complex **43a** can be purified by crystallization from dichloromethane-heptane mixture upon slow evaporation in a rotary evaporator. Washing of the crude product with an appropriate organic solvent appears, however, to be the method of choice.

The  $\text{Ph}_5\text{CpH}$  ligand can be considered far from optimal in terms of cost and ease of preparation.  $\text{Bn}_5\text{CpH}$ , in turn, can be easily prepared in large scale by base catalyzed alkylation of cyclopentadiene with benzyl alcohol facilitated by azeotropic water removal.<sup>74</sup>

An additional advantage of complex **43a** is its considerably higher solubility induced by the benzyl substituents when compared with the (polyphenyl)cyclopentadienyl ligated catalysts, which under some cases, in solvents commonly used for DKR reactions may operate at the limits of solubility.

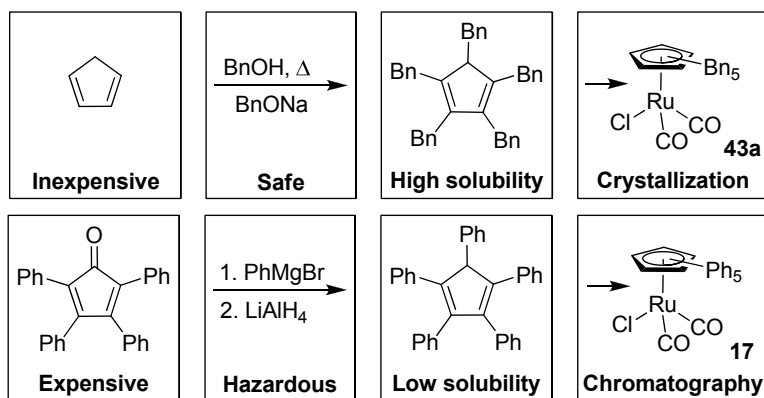


**Figure 22.** Advantages in preparation and purification of catalyst **43a** compared to **17a**.

## 3.2 Utilization of the new catalyst for DKR of a broad range of substrates

### 3.2.1 General issues

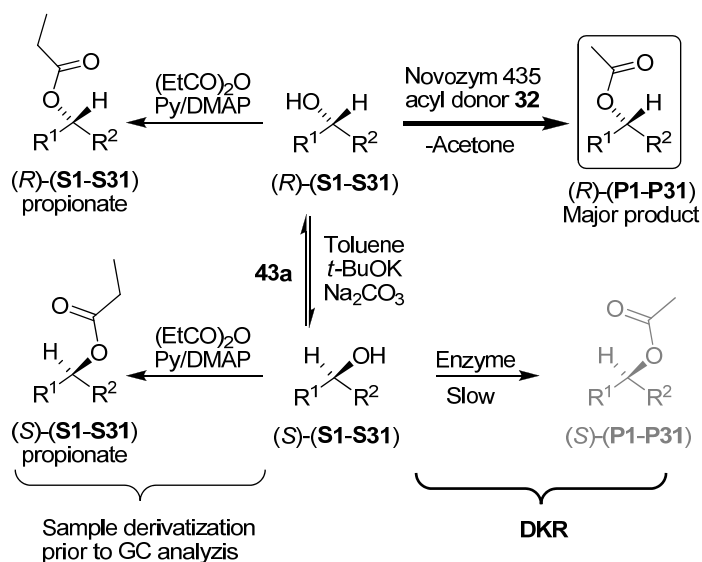
The aim of the present work was to study the general usability of **43a** as a racemization catalyst in the DKR of secondary alcohols. For this purpose, 31 alcohols (structures **S1-S31**, in accordance with the entries in Table 4) were subjected to acylation with isopropenyl acetate **32** in the presence of CAL-B and ruthenium catalyst **43a** in toluene (Scheme 25)<sup>88</sup>. The alcohols **S1**, **S3**, **S7-10**, **S18**, **S19**, **S22-28** and **S30** were selected due to their previously reported promising behaviour in the DKRs employing  $Ph_5Cp$  ruthenium complex **17a** and CAL-B.<sup>32c</sup> The remaining 14 secondary alcohols were selected for extending the structural diversity and due to their importance as enantiopure compounds for different purposes in synthetic and medicinal chemistry. To exemplify, alcohols **S5**, **S13** and **S16** are versatile building blocks for cross-coupling reactions.<sup>89</sup> The DKRs of polyfunctional substrates bearing conventional and easy to remove protective groups in turn, such as methoxymethyl ether (MOM) and *tert*-butyloxycarbonyl (Boc) in **S11** and **S12**, have not been described before. Also the DKRs of *ortho*-substituted alcohols **S14**, **S15** have not been disclosed earlier. Toluene was selected as the solvent being already proven to be well accepted by both the lipase and the ruthenium complexes **17a** and **43a**.<sup>32c, 75, 80</sup> Toluene also dissolves the aromatic secondary alcohols and ester products relatively well and is acceptable for industrial applications. One of the benefits of enzymatic synthesis is that enzymes allow efficient reactions at ambient temperatures, reducing the formation of side products. For example, formation of significant amounts of the corresponding ketone upon reversible oxidation-reduction sequence involved in racemization (Scheme 9) has been reported earlier.<sup>27</sup>

Formation of acetic acid caused by hydrolysis of the acyl donor with residual water can cause deactivation of the acid sensitive active intermediate **33** (Chapter 1.2.3). Therefore,  $Na_2CO_3$  must be added to neutralize the formed acetic acid *in situ*. It is well known that water absorbed on a glass surface is able to influence significantly organometallic reactions, especially in micro scale.<sup>90</sup> Another source of the residual water can be the seemingly dry enzyme preparation. This is particularly possible with CAL-B as the Novozym 435 preparation (CAL-B adsorbed on a divinylbenzene-crosslinked, hydrophobic macroporous polymer based on methyl and butyl methacrylic esters), because this lipophilic immobilization material will readily release any water contained into the dry reaction mixture.<sup>13</sup> With this in mind, the focus of the present work was the optimization of the reaction system in particular with respect to the catalyst loadings. Procedure similar to the one developed earlier by Bäckvall and co-workers<sup>32c</sup> was used as the starting point. After thorough drying of all components (Chapter 3.2.2) and transferring of the system under nitrogen atmosphere into a glovebox, a decrease in the Ru-catalyst loading by

one half (from 4 mol-% to 2 mol-%) in 1 mmol scale reaction without sacrificing the efficiency of the system was achieved.

The time required for reaching full conversion in DKR is one measure of its effectiveness. The comparison of literature results that are based on the use of lipase catalysis in KR and DKR is not always straightforward (although often performed in the literature),<sup>30</sup> as the activity of the enzyme is rarely given and may differ from one batch to another. Comparison of the DKR results of this work with catalyst **43a** and the published work<sup>32c</sup> with catalyst **17a** is not an exception in this respect. For the results collected in Table 4, the amount of CAL-B was set to 10 mg in order to match a reactivity profile where the DKR of 1-phenylethanol (1 mmol) reaches full conversion in 3 h as described in the published method utilizing complex **17a**.<sup>32c</sup>

**Scheme 25.** DKR of secondary alcohols with **43a**; the alcohols are shown in Table 4



### 3.2.2 Methodological aspects

Progress of the DKR was followed by chiral GC. This method allows to determine both the conversion and enantiopurity of the product and the remaining starting material. The response factor of an alcohol acetate in GC is higher compared to that of a free alcohol (Figure 23). This can lead to overestimation of the conversion value. Moreover, appearance of the free alcohols as broad peaks in the chromatograms makes the analysis less reliable. Quenching of the reaction mixture sample with propionic anhydride in the presence of DMAP stops the reaction and converts the unreacted alcohol to the corresponding propionate. Both the acetate and the propionate provide sharp peaks with similar response factors in GC (Figure 24).

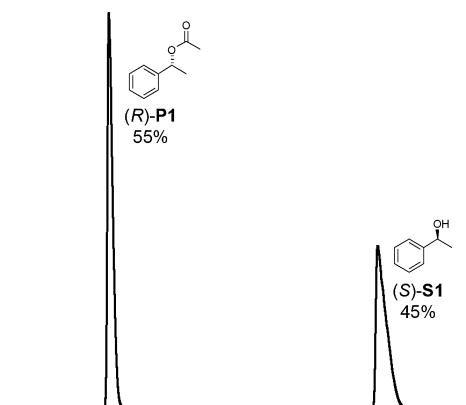


**Figure 23.** Chiral GC chromatogram of the *underivatized* mixture of (*R*)-acetate and the corresponding free (*S*)-alcohol (1:1 molar ratio). The numbers are relative integral intensities of the corresponding peaks.

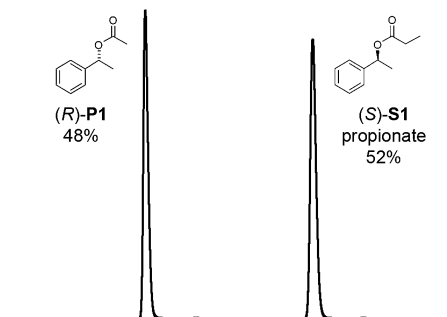


**Figure 24.** Chiral GC chromatogram of the *derivatized* mixture of (*R*)-acetate and the corresponding free (*S*)-alcohol (1:1 molar ratio). The numbers are relative integral intensities of the peaks.

The value of enantiomeric excess of a starting material allows to make conclusions about the rate-determining process in DKR (see also 1.2.4). High enantiopurity of the starting material induced by depletion of the more reactive enantiomer indicates that racemization is slower compared to kinetic resolution (Figure 25). Racemic starting material in turn, indicates that the enzymatic resolution is slower compared to racemization (Figure 26).

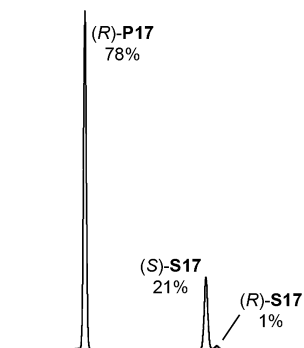


**Figure 25.** GC chromatogram of the derivatized sample from DKR of **S17**. Racemization is the rate-limiting step.

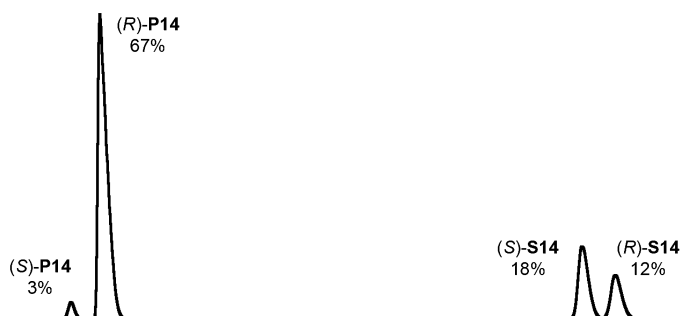
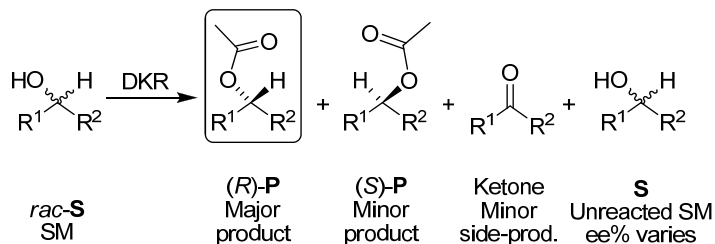


**Figure 26.** GC chromatogram of the derivatized sample from DKR of **S14**. Enzymatic resolution of this sterically hindered substrate is slow and less enantioselective compared to **S17**.

A typical composition of the DKR reaction mixture is shown in Scheme 26. The conversion values determined by chiral GC were calculated according to Equation 4.

**Scheme 26.** Content of the DKR reaction mixture



**Equation 4.** Determination of the DKR conversion

$$\text{Conversion} = (\text{R})\text{-P} + (\text{S})\text{-P} + \text{Ketone} = 100\% - (\text{R})\text{-S} - (\text{S})\text{-S}$$

In most cases formation of ketones was not detected, and, when observed (DKR of substrates **S7**, **S20**, **S21**, and **S25**), the levels were negligible ( $\leq 1\%$ ). Conversion  $>99\%$  is shown when remaining starting material was not observed by GC. Internal standards were not utilised. In the case of the non-volatile **P12**, the conversion was determined by  $^1H$  NMR. Complete transformation is denoted as  $>95\%$  as it can be considered that NMR integration accuracy usually does not exceed several %.<sup>91</sup>

Generally, in recent literature on synthetic organic chemistry, excellent yields, ee values and reaction times are commonly reported. The accuracy of such measurements and the error estimation are, however, questionable.<sup>92</sup> In this work, the following measures were taken in order to obtain reliable experimental values:

The products **P1-P31** were isolated by flash column chromatography utilizing hexane-DCM mixture for non-volatile compounds (**P5-P7**, **P9-P13**, **P16-P20**, **P29-P31**), pentane-DCM mixture for the volatile ones (**P1-P4**, **P8**, **P14**, **P15**, **P21-23**, **P25-P28**) and hexane-ethylacetate for the polar compound **P24**. The resulting solutions were concentrated using rotary evaporator and keeping the bath at ambient temperature in order to minimize the loss of the volatile acetates. Amounts of residual solvents in the obtained products were determined by  $^1H$  NMR spectroscopy and calculated values were subtracted from the weights measured. The obtained numbers were used to calculate isolated yields. Due to the small scale of the DKR experiments (1 mmol, approx 200 mg of the product) the error of these measurements can be high. Therefore, excellent and quantitative isolated yields observed are denoted as  $>95\%$  (see Table 4). The *tert*-butoxide present in the reaction mixture in slight excess with respect to the catalyst may undergo a reversible exchange with the substrate, allowing complete conversion of the substrate to the corresponding acetate. The reaction mixtures were stored for a few days in air before column chromatographic purification. This led to decomposition of the air-sensitive catalytic species facilitating the separation of ruthenium on silica.

Enantiomeric excess values  $>99\%$  were reported in cases where only one enantiomer was observed by chiral GC analysis. In two cases chiral GC was not applicable, namely, **P12** was non-volatile and sufficient resolution of the enantiomeric peaks was not achieved for **P19**. These products were subjected to alkaline hydrolysis followed by conversion to the corresponding Mosher's esters. Precise values of the enantiomeric excesses were defined by comparison of the integral intensities of the minor enantiomer peaks with the intensity of  $^{13}C$ -satellite peaks of the main enantiomer in the  $^1H$  NMR spectra.<sup>93</sup>

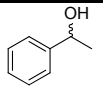
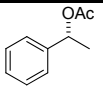
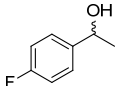
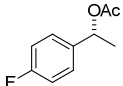
It was also observed that the reproducibility of the DKR reactions was extremely sensitive to traces of oxygen and moisture. In order to decrease the possible influence of these factors, the following precautions were taken:

- All liquid substrates and the solid at RT substrate **S24** were redistilled under reduced pressure over calcium hydride.
- The solid substrates **S12**, **S18**, **S19** were administered as stock solutions in THF (**S12**) or toluene (**S18**, **S19**). Prepared solutions were stored over molecular sieves for 18 h prior to use.
- The acyl donor (isopropenylacetate) was redistilled under inert atmosphere over calcium hydride.
- Toluene and THF were redistilled under inert atmosphere over sodium benzophenone ketyl.
- The commercially available potassium *tert*-butoxide was sublimated in vacuum.
- 4Å Molecular sieves and Na<sub>2</sub>CO<sub>3</sub> were subjected to prolonged drying in vacuum (<1 mbar) at 180 °C.
- All glassware was flame dried and cooled down in a dessicator over phosphorus oxide. Overnight drying at 150 °C was utilized for glassware not suitable for flame drying.
- All starting materials prepared were stored in a glovebox with water and oxygen content maintained below 1 ppm by means of a dry train.
- All DKR reactions were performed in a glovebox.

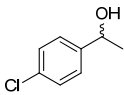
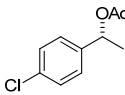
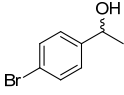
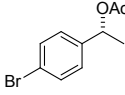
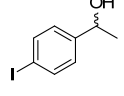
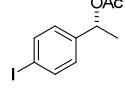
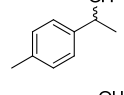
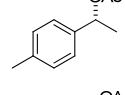
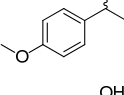
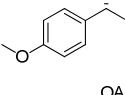
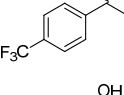
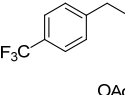
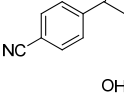
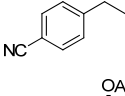
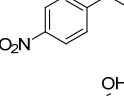
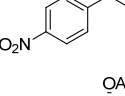
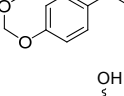
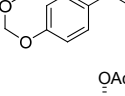
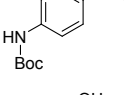
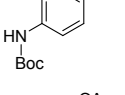
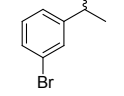
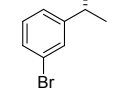
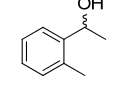
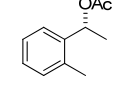
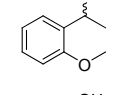
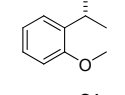
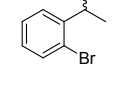
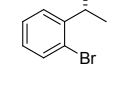
In order to eliminate the error associated with reproducibility of the experiments, DKRs of each substrate were performed at least in triplicate. Averaged conversion and enantiomeric excess values are reported. Isolations of the products and determinations of the isolated yields were performed only once for each substrate.

### 3.2.3 Substrate scope

**Table 4.** Dynamic kinetic resolution of secondary alcohols<sup>a</sup>

Entry	Substrate <b>S1-S31</b>	Product <b>P1-P31</b>	Time (h)	Conversion <sup>b</sup> (isolated yield) (%)	ee <sup>b</sup> (%)
1			3	>99 (95)	>99
2			3	>99 (>95)	>99



3			3	>99 (93)	>99
4			3	>99 (94)	>99
5			3	>99 (>95)	>99
6			3	>99 (>95)	>99
7			3	>99 (>95)	>99
8			6	>99 (95)	>99
9			30	99 (92)	>99
10			96	98 (95)	98
11			3	99 (95)	>99
12 <sup>c</sup>			24	>95 <sup>d</sup> (>95)	98 <sup>c</sup>
13			6	>99 (95)	>99
14			24	>99 (93)	96
15			9	>99 (>95)	>99
16			168	>99 (91)	>99

17			18	>99 (>95)	>99
18 <sup>f</sup>			6	99 (>95)	>99
19 <sup>f</sup>			120	>99 (94)	99 <sup>e</sup>
20			36	97 (>95)	>99
21			24	95 (92)	98
22			24	99 (90)	>99
23			9	98 (94)	>99
24 <sup>g</sup>			24	>99 (90)	>99
25			3	>99 (>95)	97
26			3	98 (94)	>99
27			9	>99 (>95)	>99
28			6	>99 (>95)	93
29			3	>99 (>95)	94
30			3	>99 (>95)	98
31 <sup>h</sup>			168	99 (>95)	95

(a) Conditions: substrate 1 mmol, isopropenyl acetate 1.2 mmol, **43a** 2 mol-%, Novozym 435 10 mg, *t*-BuOK 2.5 mol-% (as 0.25 M solution in THF), Na<sub>2</sub>CO<sub>3</sub> 0.5 mmol, toluene 2 mL, 23 °C, under nitrogen. Conversions and ee% values are averages of at least 3 reaction runs. (b) Determined by chiral GC, unless otherwise noted. (c) Toluene/THF mixture (4:1, 5 mL). (d) Determined by <sup>1</sup>H NMR. (e) Determined by

$^1H$  NMR for the corresponding Mosher's ester. (f) Toluene 4 mL. (g) Toluene/THF mixture (4:1, 2.5 mL), 60 °C. (h) CAL-B 40 mg.

Generally, all racemic *sec*-alcohols were smoothly transformed into the corresponding (*R*)-acetates under DKR conditions adopted.

It has been reported earlier that the DKR of the fluorinated alcohols **S2** and **S8** required prolonged reaction times (72 and 24 h respectively).<sup>32c</sup> Here, for these substrates, excellent results were obtained in 3 and 6 h respectively. Moreover, 95-98% conversions were detected for **S8** already after 3 h.

The brominated and iodinated substrates **S4** and **S5** underwent partial dehalogenation under the DKR conditions employed. The resulting isolated products **P4** and **P5** contained 3 and 2 mass% of the respective dehalogenated product **P1**. Cleavage of carbon-halogen bonds by ruthenium hydride species has been reported earlier.<sup>32a, 94</sup>

DKR of the electron-rich *para*-methoxy substituted compound **S7** proceeded smoothly. Direct comparison of the DKR systems using **17a** vs. **43a** was not attempted here. Nevertheless, in some cases relevant comparisons were made.<sup>95</sup> Detailed experimental analysis demonstrated that the conversion of **S7** in 3 h under identical reaction conditions varied from 61-70% (6 consecutive experiments) with **17a** and from 98-99+% (4 consecutive experiments) in the case of **43a**. The DKR of **S7** was performed under standard reaction conditions in the presence of 2 mol-% of **17a** or **43a**. The starting material remained racemic during the course of the reaction in the case of **43a** and slightly enantioenriched (ee ~50%) in the case of **17a**. This indicates that **43a** is more efficient for racemization of electron-rich substrates as compared to **17a** (Chapter 4.4).

DKR of the electron-deficient substrates **S9** and **S10** required an extended reaction time. Monitoring of the reaction progress revealed that the starting material remained almost enantiopure during the reaction. Control runs with 2 mol% of **17a** led to a complete conversion in 24 h for **S9** and 8 h for **S10**. Compound **S9** remained slightly enantiomerically enriched (ee~50%) and **S10** was racemic during the course of the reaction. This observation indicates that **43a** is less efficient for racemization of electron-deficient substrates as compared to **17a** (Chapter 4.4).

DKRs of *ortho*-substituted 1-arylethanol were generally less efficient. Enantioselectivity in the DKR of **S14** was slightly lower compared to the *para*-substituted analogue **S6** (96% vs >99% ee respectively). It has been reported earlier that the enantioselectivity of lipase towards this substrate is far from optimal.<sup>96</sup> At the same time, DKR of the *ortho*-methoxy substituted substrate **S15** proceeded faster and more enantioselectively, probably due to the higher conformational lability of this substrate. DKR of the *ortho*-bromo substituted **S16** was very slow,

despite that the starting material remained racemic during the reaction. This observation is consistent with enzymatic acylation being the rate limiting step. The bicyclic substrates **S19**, **S20** and **S21** containing an ortho-substituted moiety showed longer reaction times, especially in case of the bulky substrate **S19**.

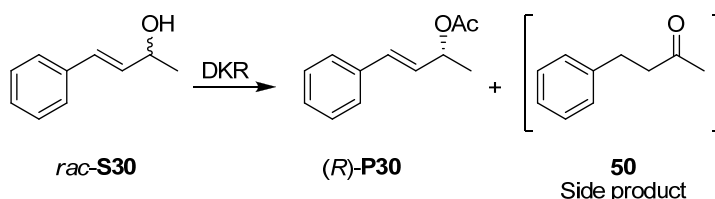
DKR of 1-thienylethanol **S22** required a longer reaction time due to low racemization rate. A 50% conversion was observed already after 3 h indicating that the rate of enzymatic acylation was not the rate determining step. Generally, sulfur containing compounds are known to be poisons for noble metal catalysts.

The pyridyl containing heterocyclic substrate **S24** underwent enzymatic acylation smoothly at RT while no racemization was observed. Performing the reaction at elevated temperature (60 °C) enabled a successful DKR. Inefficiency of the DKR at RT in this case can be explained by interaction of the pyridyl moiety as a ligand blocking the ruthenium center. Similar results have been reported by Bäckvall and co-workers.<sup>32c</sup>

The substrates containing longer aliphatic chains, namely **S28** and **S29** were converted to the corresponding (*R*)-acetates with slightly decreased enantioselectivity. Insertion of one or two methylene groups between the reaction center and the large group (Scheme 4) decreases the enantioselectivity of the enzyme.<sup>19</sup>

Bäckvall and co-workers have reported that significant amounts (11%) of ketone **50** are formed during the DKR of the  $\alpha,\beta$ -unsaturated substrate **S30** (Scheme 27).<sup>32c</sup> Later, by the same authors an efficient procedure for rearrangement of allylic alcohols to the corresponding ketones was developed. Chen *et al.* reported the DKR of this substrate under harsher reaction conditions (20 h, 50 °C) providing 92% isolated yield.<sup>45</sup> In the present work, reaction proceeded rapidly and smoothly (3 h, RT) providing the product in quantitative isolated yield. Formation of the side product **50** was not observed.

**Scheme 27.** Side product formation during the DKR of  $\alpha,\beta$ -unsaturated alcohol **S30**



DKR of the homoallylic alcohol **S31** required some optimizations to the standard procedure. In the first attempt a standard enzyme loading (10 mg) was utilized. The reaction rate was low and 82% conversion was achieved after 7 d (Table 5). While the starting material

remained enantioenriched during the reaction, the racemization catalyst performance was only satisfactory. For example, in the DKR of **S9** lasting for 30 h, the starting material remained almost enantiopure. Increase in the catalyst loading was not considered feasible due to risk of undesired side reaction between the unsaturated substrate and the ruthenium hydride species. An increased amount of enzyme (40 mg) was therefore utilized for the improved procedure providing excellent conversion and isolated yield. Enantioselectivity of the transformation was lower due to reasons similar to those described above for **S28** and **S29**.

**Table 5.** Monitoring of the reaction progress of the DKR of the substrate **S31** under the standard DKR conditions

Time (h)	Conversion (%)	SM ee (%)
3	10	10
24	48	63
48	63	68
96	76	79
168	82	88

Most of the reactions were performed using 2 ml of toluene as the solvent. In some cases the amount of solvent was increased (**S18**, **S19**) or toluene-THF mixture was utilized (**S12**, **S24**) in order to improve the solubility of the starting material. DKRs of all substrates (except **S24**) were performed at room temperature (23 °C) due to simplicity of the operation in a nitrogen-filled glovebox. DKR of **S24** was performed at elevated temperature (60 °C) in a glass bomb charged in a glovebox.

In the attempted DKR of the allylic alcohol **51** enzymatic kinetic resolution only was observed while the racemization catalyst **43a** was inactive towards this substrate.

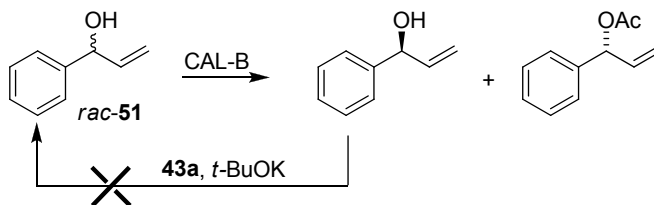


**Figure 27.** Allylic alcohol **51** is not racemized by catalyst **43a**.

### 3.3 Utilization of $Bn_5CpRu(CO)_2Cl$ for large scale DKR

A series of enantiomerically pure *para*-substituted 1-(phenyl)ethanols representing both electron rich (**S7** and **S6**) and electron-deficient *sec*-alcohols (**S3** and **S8**), together with the

parent 1-(phenyl)ethanol (**S1**), were selected and prepared in large scale for use as starting materials for further racemization experiments (Chapter 4.3). In addition, the *ortho*-methyl substituted 1-(phenyl)ethanol **S14** was included in order to investigate the possible influence of steric contributions. In preliminary racemization screening studies, the most electron deficient substrate **S8** was shown to have the slowest racemization rate in the presence of **43a**, being thus most suitable for detailed kinetic investigation. For this reason, the deuterated analogue *d*<sub>1</sub>-**S8** was also prepared for investigating the existence of possible kinetic isotope effects.

As established earlier,<sup>32c</sup> the racemization reaction proceeds much faster in the absence of enzyme as compared to the racemization of the less reactive enantiomer in DKR. A possible explanation is the deactivation of catalyst by acetic acid formed during enzymatic hydrolysis of the acyl donor due to trace water impurities (Chapter 1.2.3). In order to overcome this limitation, relatively high catalyst loading is typically utilized in small scale model reactions (commonly 2-4 mol% of catalyst for 1 mmol loading).<sup>32c</sup> It is well known that large scale organometallic reactions are less sensitive towards oxygen and moisture traces in solvents, reagents, glassware and environment compared to microscale reactions. In this regard, chemoenzymatic DKR is not an exception. As demonstrated earlier by Bäckvall and co-workers,<sup>97</sup> using 122 g of 1-phenylethanol, a 0.05 mol-% loading of the Ph<sub>5</sub>Cp catalyst **17a** with 0.5 mass-% of immobilized CAL-B (Novozym 435) is sufficient to provide (*R*)-**S1** in >99% ee and 97% yield over 20 hr at 70 °C. In this work, 0.05 mol% of catalyst was utilized for 1 mol scale DKR; 0.1 mol-% for reaction with loadings in the range of 0.3-0.5 mol; 0.2 mol% for processes at <0.2 mol scale.

The results from the preparative scale DKRs are collected in Scheme 28 and Table 6

**Scheme 28.** Preparative scale DKR of *sec*-alcohols used for the racemization studies

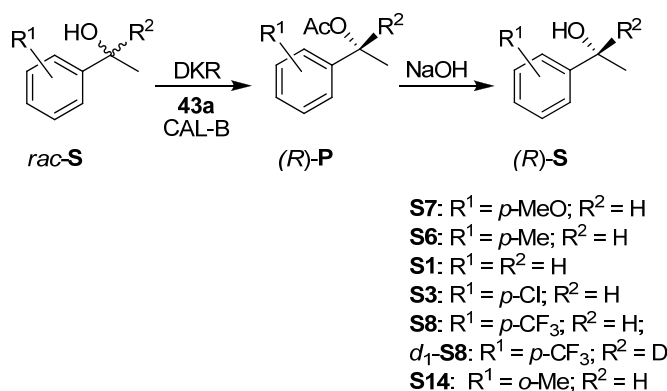


**Table 6.** Reaction conditions and results of the preparative scale DKRs and subsequent alkaline hydrolysis<sup>a</sup>

	Loading				(R)-S	
	<i>rac</i> -S	<b>43a</b>	CAL-B	DKR conditions	Yield <sup>b</sup>	ee
	(mol)	(mol-%)	(g)		(%)	(%)
<b>S1</b>	1	0.05	1	RT (17 d)	93	>99
<b>S3</b>	0.4	0.1	0.4	RT (48h) → 65 °C (65 h)	96	99
<b>S6</b>	0.5	0.1	0.5	65 °C (3 d)	96	>99
<b>S7</b>	1	0.05	1	65 °C (14 d)	94	99
<b>S8</b>	0.12	0.2	0.1	RT (43 h) → 65 °C (67 h)	94	>99
<i>d</i> <sub>1</sub> - <b>S8</b>	0.07	0.2	0.05	65 °C (48 h)	88	>99
<b>S14</b> <sup>c</sup>	0.3	0.1	1	65 °C (19 d)	91	92

(a)  $Na_2CO_3$  0.1 equiv/substrate; isopropenyl acetate 1.2 equiv/substrate; *t*-BuOK (0.25 M solution in THF) 1 equiv/catalyst; toluene/substrate 3-5 v/v. (b) Overall yield over 2 steps. (c) Contains 4% of the corresponding *meta*-isomer (impurity in the commercially available starting ketone).

In some cases, longer reaction times were required to achieve high conversions and high optical purities of the target alcohols. High conversion (98%) and excellent optical purity of the product (*R*)-**P1** (ee >99%) was observed after 10 days. For preparing optically pure (*R*)-**S1**, however, conversions close to 100% are required in the DKR. Stopping of the reaction at lower conversion would retain the (*S*)-enriched alcohol as an impurity which after hydrolysis of (*R*)-**P1** into (*R*)-**S1** significantly decreases the enantiomeric excess. To exemplify, work-up of the reaction at 98% conversion would provide a mixture of (*R*)-**P1** and (*S*)-enriched alcohol **S1** in 49:1 ratio. Furthermore, quantitative separation of alcohol **S1** (bp 204 °C) and acetate **P1** (bp 213 °C) by distillation is difficult due to proximity of their boiling points and by subsequent alkaline hydrolysis at 98% conversion (*R*)-**P1** would be obtained in 96% ee only. By extending the reaction time in order to reach >99% conversion of the starting material, the final product (*R*)-**P1** was, however, obtained in high yield and enantiopurity. In case of *rac*-**S7** completion of the DKR reaction to yield enantiomerically pure (*R*)-**P7** required a reaction time of 2 weeks despite of the fact that 75% conversion of the starting material was observed after 3 days and 95% conversion after 7 days. Following the progress of the reaction by GC revealed that the starting material was, in fact, significantly enriched with the (*S*)-enantiomer, consistent with the rate of racemization of (*S*)-**S7** being the rate limiting step in DKR.

In case of the sterically congested *ortho*-methyl substituted alcohol **S14**, 67% conversion was observed after 1 day of reaction, 82% after 2 days and 91% in 6 days while the starting

material remained practically racemic throughout the reaction. This, again, is consistent with the enzymatic reaction being the rate limiting step. The reaction was quenched after 19 days at 98% conversion providing (*R*)-**P14** in 94% *ee*, contaminated with 2% of the starting material *rac*-**S14**. After subsequent alkaline hydrolysis, the enantiomeric excess of the final product (*R*)-**S14** was only 92% due to the presence of this impurity.

The DKRs of the electron deficient substrates *rac*-**S3** and *rac*-**S8** were initially carried out at ambient temperature. The conversions observed after 2 days (56% and 51%, respectively) were, however, only marginally higher than those in a conventional kinetic resolution indicating that the racemization reaction is the rate limiting step for these substrates. Moderate warming of the reaction mixture led to a significant enhancement of the racemization activity. In the case of **S3** the substrate remained close to racemic throughout the whole reaction indicating that the catalytic activity could possibly be enhanced significantly by adjusting the reaction temperature to sufficiently high level, if desired. It should be noted, however, that organometallic reactions in general are more sensitive at higher temperature setting additional requirements for exclusion of air and moisture, which in chemoenzymatic DKR reactions may prove to be difficult to guarantee. With the deuterated 1-(*para*-trifluoromethylphenyl)ethanol *d*<sub>1</sub>-**S8**, the DKR proceeded smoothly without detectable loss of deuterium label during subsequent transformations.

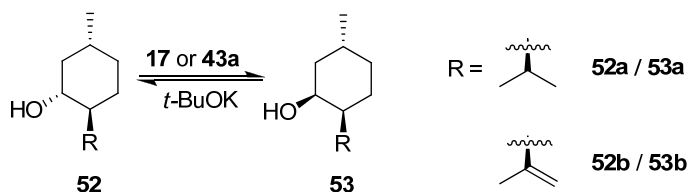
### 3.4 Epimerization of terpenoids

As a further comparison of the two catalysts **17a** and **43a**, both complexes were tested for epimerization of selected chiral alcohols containing multiple stereocenters. In cases where the other stereogenic centers are non-functionalized while one contains a hydroxyl group, the epimerization reactions can essentially be treated as racemizations. Epimerization reactions of sugars catalyzed by complex **17a** have been reported recently.<sup>98</sup> Likewise, heterogeneously catalyzed epimerizations of terpenoids have been studied earlier.<sup>99</sup> The possibility of stereoselective reduction of menthone to any of the desired possible diastereomers has likewise been demonstrated.<sup>100</sup> Principally, inversion of a single stereocenter out of several in a chiral molecule could potentially be utilized for conversion of inexpensive starting materials into more valuable ones provided that the resulting equilibrium mixture contains sufficient amounts of the more expensive and separable diastereoisomer. For example, configurational inversion of the C\*-(H)(OH) stereocenter in the readily available natural products (-)-menthol (**52a**) and (-)-isopulegol (**52b**) would ideally provide a rapid catalytic access to the rare diastereomeric terpenoids (+)-neomenthol (**53a**) and (+)-neoisopulegol (**53b**), respectively (Scheme 29). Upon epimerization of the two terpenes (-)-menthol and (-)-isopulegol with the Bn<sub>5</sub>Cp catalyst **43a**, diastereomeric mixtures of (-)-menthol/(+)-neomenthol and (-)-isopulegol/(+)-neoisopulegol



were indeed obtained in 3:1 and 6:1 ratios, respectively, within a few hours. The diastereomeric ratio remained unchanged for 18 hours. The more expensive, minor diastereomers could be separated and purified by column chromatography in 40-80% yields (based on its concentration in the reaction mixture). Principally, at least, this process could be turned into a dynamic method by combination of the epimerization catalyst with a suitable enzyme or by repeated epimerization/separation cycles of the major diastereoisomer. The  $Ph_5Cp$  complex **17a** was significantly slower as epimerization catalyst providing with both starting materials **52a** and **b** diastereomeric 10:1 mixtures of **52a/53a** and **52b/53b**, respectively, after 24 hours.

**Scheme 29.** Epimerization of (-)-menthol (**52a**) and (-)-isopulegol (**52b**) with catalysts **17a** and **43a**



### 3.5 Summary and conclusions

A new chromatography-free protocol for multi-gram scale preparation of catalyst **43a** was developed. After thorough optimization, **43a** and CAL-B catalyzed DKR of a wide range of structurally varying secondary alcohols was studied using acylation with isopropenyl acetate in toluene. The use of a glovebox allowed convenient and controlled atmosphere for reliable and reproducible reactions and convenient sampling. The secondary alcohols studied were transformed into highly enantiopure (*R*)-acetates in close to quantitative yields. The reaction times needed for full conversions considerably depend on the substrate structure. Thus, electron-rich sterically unhindered substrates underwent fast and smooth transformations. Racemization was the rate limiting step in the case of electron-deficient substrates. Enzymatic acylation was a rate limiting step in the case of sterically hindered substrates. The DKR results in the presence of racemization catalysts **17a** and **43a** are comparable in most cases. The improved performance of **43a** can be explained by utilization of a glovebox allowing dry and air-free conditions.

The applicability of **43a** for large scale (up to 1 mol) DKR of secondary alcohols was demonstrated. Both electron-deficient and electron-rich substrates were transformed to the corresponding acetates in excellent yields. The conversions achieved were close to quantitative allowing the alkaline hydrolysis of the esters prepared to the desired corresponding optically active free alcohols without decrease of enantiopurity.

The possibility to utilize **43a** for preparation of rare terpenoids *via* epimerization of abundant natural products was investigated.

The simple, cost-effective and high-yield preparation of **43a** together with its high performance makes this complex an attractive candidate as leading racemization catalyst for future DKR applications.

## 4 Kinetic and mechanistic studies

### 4.1 Introduction

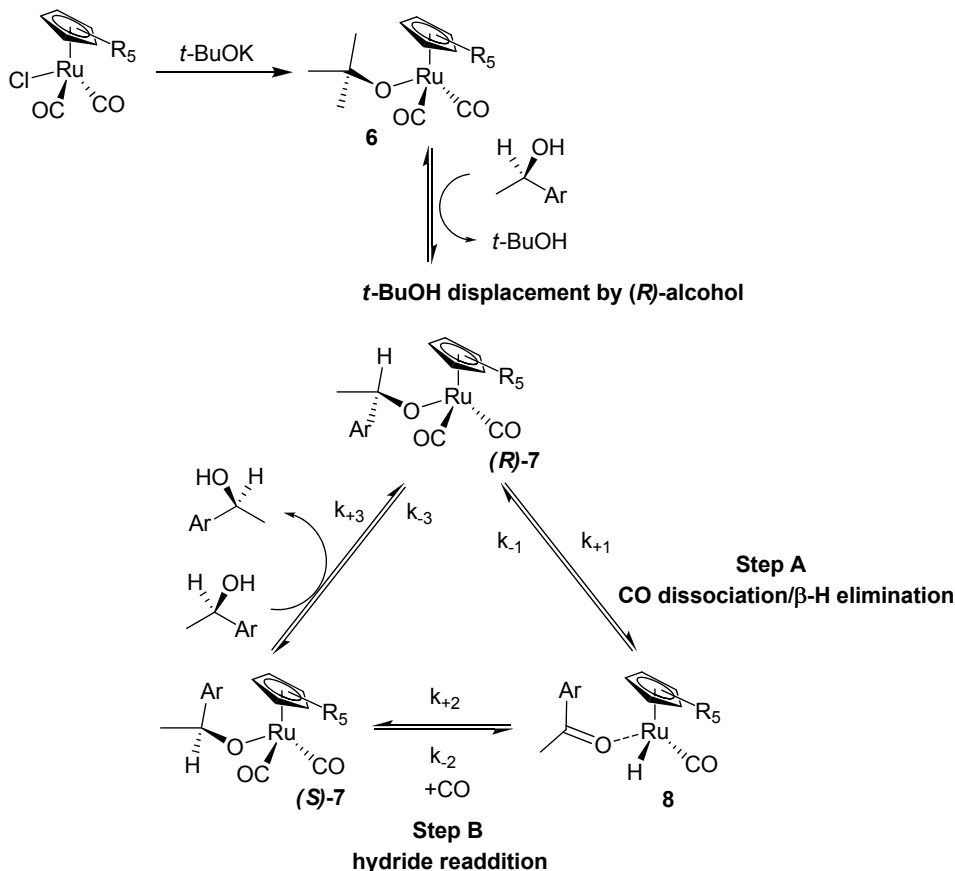
Earlier mechanistical studies by Bäckvall and others have shown that the mechanism of *sec*-alcohol racemization with 18 electron (cyclopentadienyl)ruthenium catalysts is based on (after activation of the catalyst with *t*-BuOK and the subsequent alkoxide exchange) dissociation of one CO ligand to generate a vacant site for  $\beta$ -hydride elimination, subsequently yielding a metal-hydride species with a coordinated ketone (Step **A**) (Scheme 30).<sup>32c, 101</sup> Readdition of the hydride (Step **B**) to the ketone then, after another alkoxide exchange, releases the racemized alcohol.<sup>101</sup> Recent studies on the influence of electronic contribution of the catalyst and substrate structure on the rate of racemization have shown the racemization rate to depend on the electronic properties of the substrate.<sup>102,103</sup> With electron deficient substrates the racemization rate is limited by the hydride abstraction step **A** while the hydride re-addition step **B** is faster. Electron rich substrates, in turn, undergo oxidation with ease while the subsequent reduction step is slowed down by the extensive electron density contribution from the carbonyl group. Consequently, electron deficient catalysts tend to facilitate hydrogen abstraction from electron poor substrates whereas electron rich catalysts become more efficient in hydrogen readdition in combination with electron rich substrates.<sup>102</sup>

While some attempts to describe the racemization kinetics of these systems have been reported earlier,<sup>32c, 40, 75, 101a, 102, 103, 104</sup> accurate determination of the detailed quantitative reaction kinetics remains challenging. From the experimental point of view, the difficulties are mainly associated with the typically small scale of racemization and DKR reactions, and the often questionable reproducibility of organometallic reactions on such minimal reaction scales in the presence of trace amounts of oxygen and/or moisture, particularly in the presence of the resolving enzymes which typically contain water molecules in their reaction spheres. Furthermore, particularly with the most active racemization catalysts, such as **17a** and **43a**, complete racemizations of chiral alcohol starting materials take place within minutes posing challenges for the collection of sufficient number of data points for determination of quantitative reaction kinetics. Accordingly, the earlier published kinetic work on these catalyst systems, and the conclusions based on the same, have often been of semi-quantitative character at the most.

In this work, we have performed a detailed kinetic analysis of the two ruthenium catalysts **17a** and **43a**, based on pentaphenyl and pentabenzyl substituted cyclopentadienyl ligands, respectively, to elucidate their earlier observed differences in racemization of electronically modified *sec*-alcohols (*vide infra*) and for investigating their *true activities*, limits and scope for use in chemoenzymatic dynamic kinetic resolution reactions. As an additional reference catalyst, complex **46**,<sup>75</sup> containing a monobenzyltetraphenyl substituted cyclopentadienyl ligand, and with

racemization behavior closer to the pentaphenylcyclopentadienyl system **14** than **43a**, is included.

**Scheme 30.** Mechanism for racemization of *sec*-alcohols by (cyclopentadienyl)ruthenium catalysts



## 4.2 Comparison of the electronic properties of Bn<sub>5</sub>CpRu(CO)<sub>2</sub>Cl and Ph<sub>5</sub>CpRu(CO)<sub>2</sub>Cl catalysts

In Chapter 3, the precatalysts **17a**, **43a** and **46** were shown to be nearly equally efficient for racemization of the parent (*S*)-1-phenylethanol (*S*)-**S1**, while in DKR of the electron rich *sec*-alcohol 1-(*para*-methoxyphenyl)ethanol **S7**, the Ph<sub>5</sub>Cp catalyst **17a** was less active than its Bn<sub>5</sub>Cp analogue **43a**. Simultaneously, the DKR of the highly electron deficient substrate 1-(*para*-nitrophenyl)ethanol **S10** was fast with **17a** and significantly slower with **43a**.

As evident from Scheme 30, a prerequisite for efficient racemization is the rapid oxidation of the coordinated *sec*-alkoxide to the corresponding ketone and the subsequent readdition of hydrogen for generating the racemic alcohol.<sup>101</sup> An earlier study by Bäckvall and

co-workers showed electron rich catalysts to efficiently racemize electron rich substrates due to more efficient hydrogen readdition.<sup>102</sup> Park and co-workers have reported the faster racemization of (*S*)-**9c** in the presence of electron-rich catalysts.<sup>103</sup>

The Bn<sub>5</sub>Cp ruthenium complex **43a** and its corresponding hydride analogue **43b** are more electron rich than the pentaphenyl- and monobenzyltetraphenylsubstituted complexes **17a**, **17b** and **46**, respectively. The electronic differences become evident by inspection of the IR stretching frequencies of the CO ligands in **17a** and **46** (2049, 2000 cm<sup>-1</sup>) and **43a** (2043, 1992 cm<sup>-1</sup>), respectively, as well as from the selected <sup>1</sup>H and <sup>13</sup>C NMR chemical shifts collected in Table 7. In particular, the 0.55 ppm difference in the Ru-H hydride resonance (-9.39 ppm for **17b** vs. -9.94 ppm for **43b**, respectively) in <sup>1</sup>H NMR is significant, considering the presence of ruthenium hydride intermediate species in the catalytic cycle of the racemization process.

**Table 7.** Selected <sup>1</sup>H and <sup>13</sup>C NMR chemical shifts for complexes **17a**, **17b**, **43a**, **43b** and **46**<sup>a</sup>

Group Nuclei	$\underline{C_5R_5}$ <sup>13</sup> C	$\underline{CO}$ <sup>13</sup> C	Ru- $\underline{H}$ <sup>1</sup> H
<b>17a</b>	107.12	198.04	-
<b>17b</b>	108.94	202.04	9.39
<b>43a</b>	105.78	198.44	-
<b>43b</b>	105.47	202.36	9.94
	102.73		
<b>46</b>	107.11	197.92	-
	117.28		

(a) In C<sub>6</sub>D<sub>6</sub> expressed in ppm.

The electronic differences can further be verified by cyclic voltammetry (Figure 28). The cyclovoltammogram of **43a** significantly differs from those of **17a** and **46**. The reduction peak of **43a** (-1.70 V) occurs at more negative potential than those of **17a** (-1.35 V) and **46** (-1.38 V). Such shift of the Ru(II) – Ru (I) reduction to more negative potential by 0.32-0.35 V indicates that the five benzyl substituents in **43a** increase the electron density on the Ru center as compared to **17a** and **46**. Moreover, complex **43a** demonstrates irreversible CVA reduction, while the reduction of **17a** is quasi-reversible. Complex **46** shows quasi-reversible reduction at high scan rates and irreversible at low scan rates.<sup>87</sup> Geometrically and structurally, as shown by earlier X-ray structure determinations,<sup>32c, 75</sup> complexes **17a**, **43a** and **46** are very similar displaying the expected Ru-C<sub>5</sub> centroid distances 1.893 Å for **17a**, 1.875 for **43a** and 1.884 for **46**.

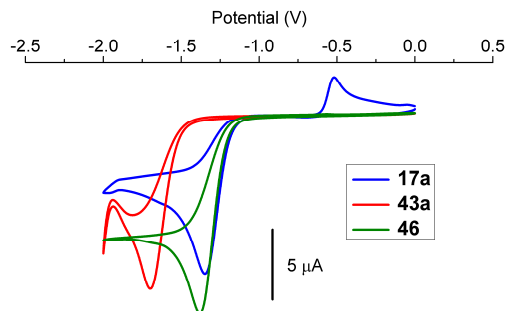


**Figure 28.** Negative parts of the cyclic voltammograms of **17a**, **43a** and **46** (complex concentration 2 mmol/L; DMF, Bu<sub>4</sub>NPF<sub>6</sub> 0.1 mol/L; scan rate 10 mV/sec; auxiliary and working electrodes Pt; reference electrode Ag/AgCl, Fc<sup>+0</sup> conversion at +0.33 V).

### 4.3 Experimental Set-up for the Racemization Studies

Generally, the kinetic data obtainable from DKR reactions is challenging to interpret due to the complicated reaction network consisting of a large number of components. Furthermore, while often employing homogeneous racemization catalysts, chemoenzymatic DKR processes also commonly involve heterogeneous catalysts and reagents, including immobilized enzymes and Na<sub>2</sub>CO<sub>3</sub>, which both may induce diffusion limitations to the rate of reaction. In order to simplify the reaction system, and for obtaining reliable data on the influence of racemization catalyst on the overall DKR performance, the focus was instead shifted into studying the actual racemization reaction. The ruthenium catalyzed racemization step is homogeneous and, therefore, more suitable to be subjected to a detailed kinetic study.

Due to the generally fast reaction rates, investigation of the racemization kinetics is, likewise, a challenging task. Under typical reaction conditions using 2 mol% of homogeneous ruthenium racemization catalyst, such as **17a** or **43a**, and 1 mmol of the *sec*-alcohol substrate, complete racemization is observed within 2 minutes, severely limiting the possible number of data points available for kinetic modeling. Additionally, in order to ensure maximal reproducibility and taking into account the frequent sampling of the reaction mixture required for accurate observation and determination of the reaction kinetics, the racemization studies should ideally be carried out in a nitrogen glove-box. This requirement in turn makes lowering of the reaction temperature as a means for slowing down the rate of racemization to measurable level impractical. On the bench, in a nitrogen or argon Schlenk-line, frequent piercing of septum would increase the permeability towards atmospheric air and moisture potentially decomposing the highly sensitive transition metal catalyst. Furthermore, while possible lowering of the

catalyst/substrate ratio might also be used for slowing down the racemization rate to a measurable level, a substantial decrease of the catalyst loading on an already small scale of the reaction would bring the catalyst concentration to microscale where the predictability and reproducibility of air and moisture sensitive organometallic reactions becomes difficult.<sup>105</sup>

In the initial screening studies for suitable experimental conditions, as a feasible compromising approach, an increase in the loading of the optically active alcohol (*R*)-**S1** to 1 g (8 mmol) while retaining the catalyst loading on 20  $\mu$ mol (0.25 mol%) level was observed to increase the time required for complete racemization to 10-15 min allowing for sufficiently frequent, multiple sampling for obtaining reliable and reproducible kinetic data. Even under such conditions, in a nitrogen glove-box, another critical issue becomes the possible decomposition or changes in enantiomeric excess of the product sample waiting for chiral GC-analysis. In the case of relatively slow DKR experiments, this issue can be solved by withdrawing the sample from the glove-box followed by irreversible quenching with a suitable derivatizing agent which stops the racemization reaction (Scheme 25). For reactions lasting some hours such minute delays induced by time taken for withdrawal of the samples from the glove-box are not crucial. For the rapid 10-15 min racemization reactions, however, a few minutes delay in quenching and derivatization would induce a large experimental error. While highly reactive and corrosive derivatizing agents cannot be introduced into the glove-box as such, this issue was solved by tightly sealed GC-vials containing the derivatizing agent sealed with a septum. This allows the withdrawal of samples directly from the reaction mixture in the glove-box by use of a disposable syringe followed by immediate injection to the GC-vial containing the irreversible derivatization agent, thereby locking the enantiomeric ratio in the sample to the time point of sampling.

#### 4.4 Kinetic Experiments

The racemization reactions for the kinetic experiments were carried out using 8 mmol of the corresponding chiral (*R*)-alcohol **S1**, **S3**, **S6**, **S7**, **S8**, *d*<sub>1</sub>-**S8** and **S14** at 0.25 mol% ruthenium catalyst loading. As shown earlier by Bäckvall and others, the dicarbonylchloro ruthenium precatalyst is first converted to the active species **33** by alkoxylation reaction with *tert*-BuOK<sup>32c</sup> or some other suitable alkoxide.<sup>40,104</sup> In the present work, the precatalysts **17a** and **43a** were first reacted with 1.25 equiv. of *tert*-BuOK and allowed to stir for 5 min before initiating the racemization reactions. All reactions were run in duplicate, unless indicated otherwise. The rate expression for the racemization reaction rate can be written as Equation 5, where [*R*] and [*S*] are the concentrations of the (*R*)- and (*S*)-alcohols, respectively.<sup>106,13</sup>

**Equation 5.** General equation for a racemization rate

$$r = \frac{k_{+1}k_{+2}k_{+3}[R][CO] - k_{-1}k_{-2}k_{-3}[S][CO]}{k_{+1}k_{+2} + (k_{+1}k_{+2} + k_{-1}k_{-2})[CO] + (k_{+2}k_{+1}[CO] + k_{+1}k_{+3} + k_{+1}k_{+3}[CO])[R] + (k_{-2}k_{-3}[CO] + k_{-2}k_{-3} + k_{-1}k_{-3}[CO])[S]}$$

Due to similar racemization mechanisms for both substrate enantiomers in the presence of an achiral catalyst, some simplifications can be made. First, the rate constant for CO abstraction from (*R*)-**54** to form **55** is equal to the rate constant of CO abstraction from (*S*)-**7**, i.e.,  $k_{+2} = k_{-3}$ . Analogously,  $k_{-2} = k_{+3}$ . Both species (*R*)-**7** and (*S*)-**7**, as well as the (*R*)- and (*S*)-alcohols, have similar energies and thus  $k_{+1} = k_{-1}$ . The mass balance analysis for CO generation reveals that:

**Equation 6.** Mass balance equation for CO

$$\frac{d[CO]}{dt} = r_{+1} - r_{-1} - r_{+2} + r_{-2}$$

Equation 6 is, in fact, equal to the steady state approximation for **55**. Therefore,  $d[CO]/dt = 0$  and  $[CO]$  is constant. After simplification of Equation 5, Equation 7 is obtained:

**Equation 7.** Differential form of racemization reaction rate equation

$$r = k'([R] - [S]) = \frac{d[S]}{dt} = -\frac{d[R]}{dt}$$

where  $k'$  is an apparent rate constant:

**Equation 8.** Apparent racemization rate constant

$$k' = \frac{k_{+1}k_{+2}k_{+3}[CO]}{k_{+2}k_{+3} + 2k_{+2}k_{+3}[CO] + C_0(k_{+1}k_{+2} + [CO])(k_{+1}k_{+3} + k_{+1}k_{+2})}$$

$$C_0 = [R] + [S] = \text{const}$$

Solving Equation 7 gives Equation 9 where  $[R]_0$  = the initial concentration and  $[R]_f$  = the final concentration of the (*R*)-enantiomer at equilibrium. Due to identical reactions of both enantiomers with the achiral catalyst,  $[R]_f = [S]_f = 50\%$ . Thus, plot of  $-\ln([R] - [R]_f)$  vs. time yields a straight line with the slope equal to  $2k'$ .



**Equation 9.** Integral form of racemization reaction rate equation

$$\ln \frac{[R]_0 - [R]_f}{[R] - [R]_f} = 2k't$$

The calculated racemization rate constants are summarized in Table 8. An example plot showing the goodness of fit is shown in Figure 29 for racemization of (*R*)-**S7** in the presence of catalyst **43a**. In full accordance with the earlier observations and predictions of Bäckvall and co-workers on the dependence of racemization rate on the electronic properties of both the substrate and the catalyst,<sup>102</sup> the more electron rich Bn<sub>5</sub>Cp catalyst **43a** racemized the electron rich substrates (*R*)-**S7** and (*R*)-**S6** at 15-20 times faster rates compared to the Ph<sub>5</sub>Cp catalyst **17a** (Figures 30 and 31). Earlier, Bäckvall and co-workers observed that extended reaction time was in some cases required for activation of catalyst **17a** with *t*-BuOK.<sup>102</sup> In order to rule out the possible influence of such induction or activation period, additional experiments with 30 min activation of **17a** were performed. Differences in the racemization rate constants were, however, not observed between the racemization experiments on substrate (*R*)-**S7** using the 5 and 30 min activation periods for catalyst **17a**. With the parent unsubstituted 1-(phenyl)ethanol (*R*)-**S1** and the slightly electron deficient (*R*)-**S3**, differences in the racemization rate constants between **17a** and **43a** were less pronounced, with **43a** being four and two times faster than **17a** for substrates (*R*)-**S1** and (*R*)-**S3**, respectively (Figures 32 and 33).

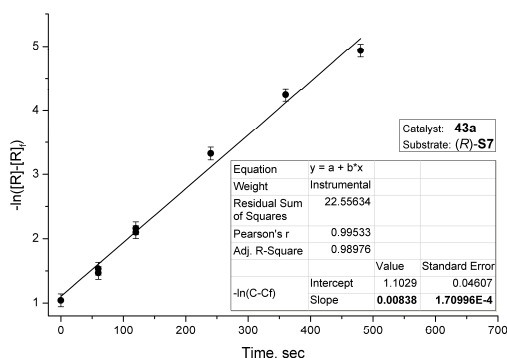


**Figure 29.** Plot for determination of the rate constant for racemization of (*R*)-**S7** in the presence of catalyst **43a**.

With the electron poor substrate (*R*)-**S8**, however, as expected, the more electron deficient (pentaphenyl)cyclopentadienyl catalyst **17a** displayed a five times faster racemization rate compared to **43a** (Figure 34). Interestingly, the rate constant for racemization of (*R*)-**S8** with **17a** is very close to the rate constant for racemization of the electron rich substrate (*R*)-**S7** with

the more electron rich catalyst **43a**. The rate constant for racemization of the deuterated 1-(*para*-trifluoromethylphenyl)-1-*d*-ethanol *d*<sub>1</sub>-(*R*)-**S8** with **43a** was  $1.6\pm0.2$  times smaller than the corresponding rate constant for racemization of the non-deuterated alcohol (*R*)-**S8**. This observation further supports the hypothesis of hydride abstraction being the rate-limiting step in the racemization of electron deficient substrates.<sup>107</sup> With the faster electron deficient catalyst **17a** similar significant isotope effect was not observed in the racemization of *d*<sub>1</sub>-(*R*)-**S8** vs. (*R*)-**S8**, possibly due to the much faster reaction rate which makes rate measurements less accurate.

**Table 8.** Rate constants of the racemization reactions<sup>a,b</sup>

Substrate	Racemization catalyst and rate constants <sup>c</sup>		
	<b>17a</b>	<b>43a</b>	<b>46</b>
( <i>R</i> )- <b>S1</b>	1.30±0.06	5.75±0.14	0.84±0.06
( <i>R</i> )- <b>S3</b>	2.42±0.05	5.00±0.10	1.66±0.06
( <i>R</i> )- <b>S6</b>	0.62±0.06	8.56±0.24	
( <i>R</i> )- <b>S7</b>	0.20±0.06	4.19±0.08	0.20±0.06
( <i>R</i> )- <b>S7</b>	(0.24±0.1) <sup>d</sup>		
( <i>R</i> )- <b>S8</b>	5.40±0.12	1.14±0.06	3.08±0.06
<i>d</i> <sub>1</sub> -( <i>R</i> )- <b>S8</b>	6.85±0.28	0.71±0.05	
( <i>R</i> )- <b>S14</b>	6.73±0.20	3.49±0.07	

(a) Calculated according to Eq. 9. (b) 8 mmol of (*R*)-**S** with 0.25 mol% of catalyst at ambient temperature.

(c)  $10^3 \times k \text{ sec}^{-1}$ . (d) Activation time = 30 min.

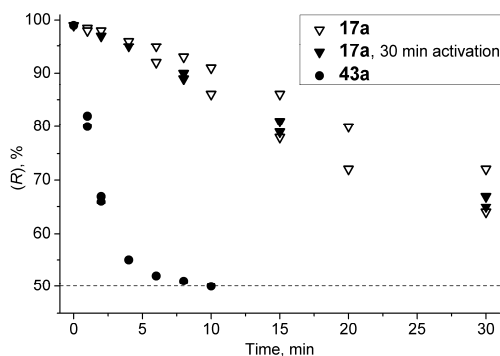


**Figure 30.** Racemization of (*R*)-**S7** with catalysts **17a** and **43a**.

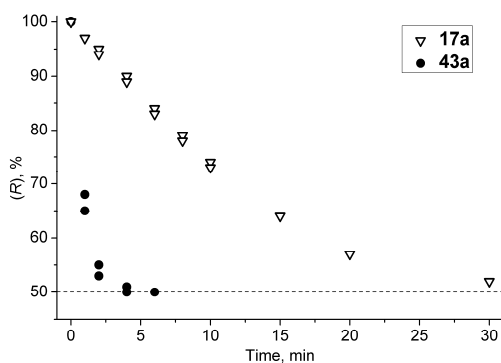


**Figure 31.** Racemization of (*R*)-**S6** with catalysts **17a** and **43a**.

In the case of the *ortho*-methyl substituted alcohol (*R*)-**S14**, the rate of racemization with **43a** was slower than the rate of racemization of the *para*-methyl substituted substrate (*R*)-**S6** with the same catalyst (Figure 35). With the Ph<sub>5</sub>Cp catalyst **17a**, however, the racemization of the *ortho*-methyl substituted phenylethanol (*R*)-**S14** was *faster* than the racemization of the *para*-methyl substituted analogue (*R*)-**S6**. These observations may possibly be explained by shielding of the ruthenium center by the pendant benzyl substituent from interactions with the sterically congested alcohol **S14**.

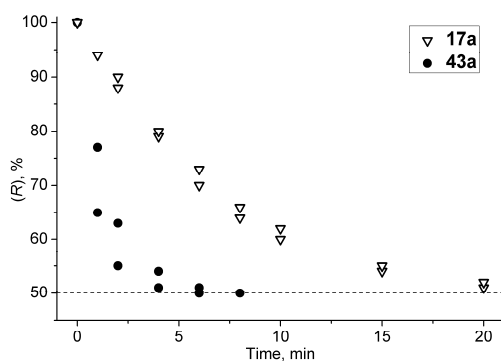


**Figure 32.** Racemization of (*R*)-**S1** with catalysts **17a** and **43a**.

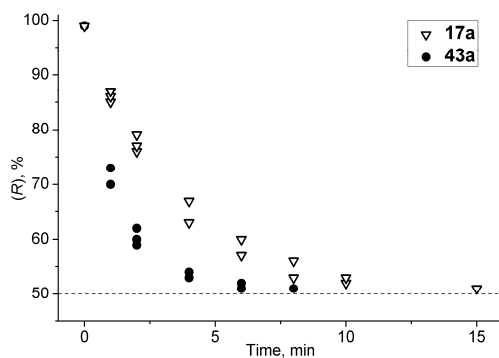


**Figure 33.** Racemization of (*R*)-S3 with catalysts **17a** and **43a**.

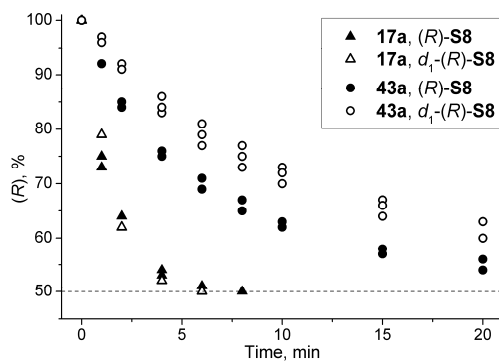


**Figure 34.** Racemization of (*R*)-S8 and *d*<sub>1</sub>-(*R*)-S8 with catalysts **17a** and **43a**.

Finally, for comparison, the (monobenzyltetraphenyl)-cyclopentadienyl ruthenium catalyst **46** was screened for racemization of several substrates (Figures 36 and 37). The structural features of this catalyst, as elucidated by earlier X-ray structure determination, are similar to those of **17a** and **43a** (Chapter 2.3), whereas electronically this complex, with a single benzyl substituent, is closer to the Ph<sub>5</sub>Cp catalyst **17a** as evidenced by CO ligand IR stretching frequencies and the cyclic voltammograms (vide supra, Table 6 and Figure 26). The racemization activity and behavior of **46** was found to be similar to the Ph<sub>5</sub>Cp catalyst **17a**, although slightly lower racemization rates were generally observed.

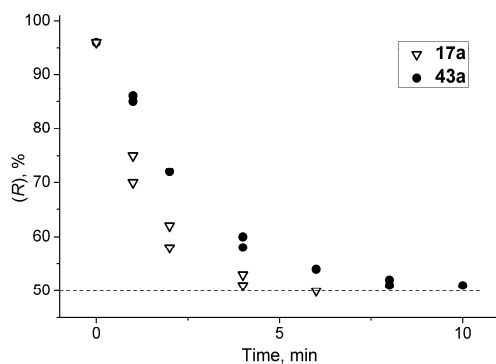


**Figure 35.** Racemization of (*R*)-S14 with catalysts **17a** and **43a**.

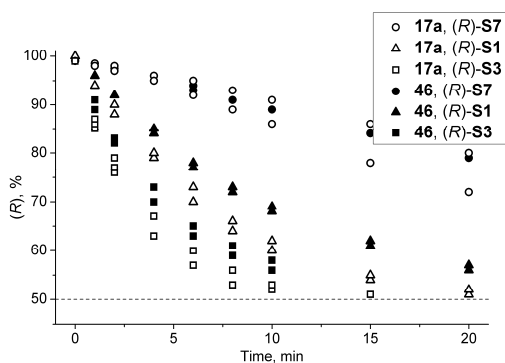


**Figure 36.** Racemization of (*R*)-S1, S3 and S7 with catalysts **17a** and **46**.

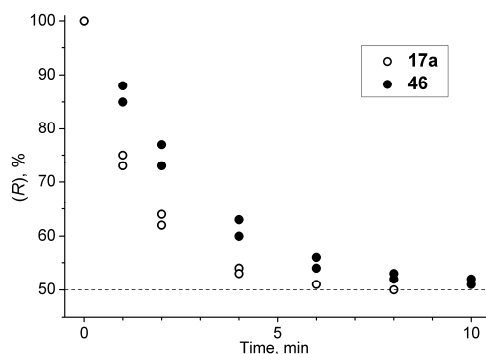


**Figure 37.** Racemization of (*R*)-S8 with catalysts **17a** and **46**.

A Hammett plot of the racemization rates for catalysts **17a** and **43a** is displayed in Figure 38. With the Ph<sub>5</sub>Cp catalyst **17a**, as evident from the linear Hammett plot, the reaction rate increases with the electron-withdrawing character of the *para*-substituent of the 1-phenylethanol substrate, consistent with hydride re-addition being the rate determining step for racemization (see Scheme 30) with constant reaction mechanism for all substrates. The nonlinear, concave

downward plot with catalyst **43a**, however, can be associated with a change in the rate-determining step when proceeding from electron donating to electron withdrawing substituents on the 1-phenylethanol substrate with otherwise constant reaction mechanism.<sup>108</sup> With the electron-poor substrates, the racemization rate is limited by the hydride abstraction (Step **A** in Scheme 30), while with the most electron-rich *para*-methoxy substituted substrate (*R*)-**S7** the hydrogen re-addition (Step **B** in Scheme 30) becomes slow.

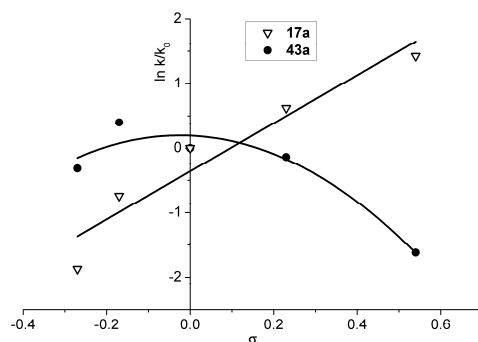
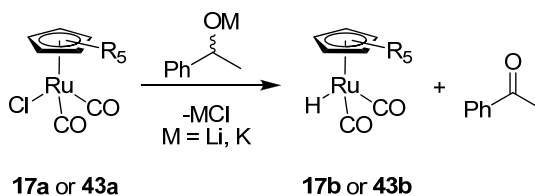


**Figure 38.** Hammett plots of the racemization rates of *sec*-alcohols with catalysts **17a** and **43a**.

#### 4.5 NMR studies on the $\text{Bn}_5\text{CpRu}(\text{CO})_2\text{Cl}$ catalyst activation

Additional NMR experiments were carried out in an attempt to further elucidate the formation of intermediates in the catalytic racemization cycle. As shown earlier by Bäckvall and co-workers,<sup>32c, 101a,c</sup> the chlorodicarbonyl ruthenium precatalyst initially forms, upon activation with *t*-BuOK, a *tert*-butoxide complex which then undergoes ligand exchange with the substrate alcohol to be racemized (Scheme 30). Alternatively, as also described in earlier work,<sup>40</sup> a preformed ruthenium alkoxide of the substrate undergoing racemization can be used directly without the preactivation step. For preparative DKR purposes, however, preactivation with the inexpensive *t*-BuOK has obvious advantages. For mechanistic work and NMR studies, on the other hand, direct utilization of the ruthenium alkoxide of the substrate to be studied simplifies the system by exclusion of the unnecessary *tert*-butoxide – alcohol exchange step and by decreasing the number of components in the reaction mixture.

**Scheme 31.** Formation of Ru-H species from the reactions of catalyst precursors **17a** and **43a** with alkali metal alkoxides of racemic 1-phenylethanol



Here, the reactions between the  $\text{Bn}_5\text{Cp}$  ruthenium catalyst **43a** and alkali metal alkoxides generated from racemic 1-phenylethanol were studied by  $^1\text{H}$  and  $^{13}\text{C}$  NMR. For these experiments, benzene- $d_6$  was used as solvent due to its simple NMR spectrum and high melting point simplifying the freezing of the NMR samples prior to flame sealing of the NMR tubes. The major products observed in these experiments were the corresponding ruthenium hydride and acetophenone (Scheme 31).

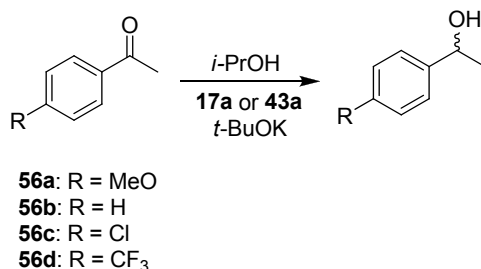
The reaction of **43a** with 1-(phenyl)ethoxylithium proceeded slowly at room temperature and required heating to  $70^\circ\text{C}$ . After three days at room temperature, a 6:1 ratio between the starting material **43a** and ruthenium hydride **43b** was observed. Further heating to  $70^\circ\text{C}$  gave after 12 hours a 1:2 ratio of **43a** and **43b**. Consequently, potassium hydride was next used for preparation of 1-(phenyl)ethoxypotassium which, compared to its lithium analogue, reacted much faster with **43a** resulting in complete transformation to **43b** and acetophenone at room temperature in 2 hours. The conversion of **43a** to **43b** could be followed by  $^1\text{H}$  NMR due to the sharp and intense singlet resonance at 3.46 ppm (**43a**) and 3.62 ppm (**43b**), respectively, from the  $\text{CH}_2$  group of the five equivalent benzyl substituents. In the case of the pentaphenylcyclopentadienyl complex **17a**, corresponding easily identifiable signals are not present in  $^1\text{H}$  NMR. Moreover, with this complex, unidentified side product or decomposition products precipitated from the solution during the reaction with both lithium and potassium alkoxides hampering the collection of any meaningful data. In the literature, the *para*-methylphenyl analogue of the Shvo's catalyst **14** was reported to give characteristic methyl proton resonances in  $^1\text{H}$  NMR.<sup>109</sup> Thus, for possible future mechanistical studies, the tetraphenylbenzylcyclopentadienyl complex **46** could optionally prove to be a suitable alternative and model compound for **17a** due to its similar racemization properties but higher solubility, displaying a sharp resonance from the  $\text{CH}_2$  benzylic protons in the  $^1\text{H}$  NMR spectrum.

At first sight, the observation of the ruthenium hydride species **43b** in the  $^1\text{H}$  NMR spectrum could imply that such hydride would also form as an intermediate in the racemization cycle. However, a model racemization reaction of (*R*)-**S1** using 2 mol-% of **43b** as a catalyst

proceeded very slowly, providing <1% conversion in 3 hours, whereas under identical conditions **43a** catalyzes a complete racemization within minutes. The addition of acetophenone as a possible hydride transfer agent<sup>29</sup> did not either facilitate the racemization. Thus, the ruthenium hydride complex **43b** is, most likely, not an active intermediate or species in the racemization reaction. The appearance of this species in the <sup>1</sup>H NMR spectrum is more likely due to decomposition of the intermediates formed from reactions between the starting lithium or potassium alkoxides and the precatalyst **43a**.

#### 4.6 Transfer hydrogenation experiments

**Scheme 32.** Transfer hydrogenations of acetophenones with catalysts **17a** and **43a**



Finally, for exploring the possibility of obtaining complementary mechanistical and kinetic information from ruthenium catalyzed transfer hydrogenation, which mechanistically should bear some similarities to racemization, four acetophenones **56a-d** were subjected to hydrogenation conditions using complexes **17a** and **43a** as catalysts (Scheme 32). The results have been collected in Table 9. Under standard transfer hydrogenation conditions using refluxing isopropanol both as the solvent and the hydrogen donor,<sup>110</sup> the reduction of acetophenone to racemic 1-phenylethanol with **43a** as the catalyst proceeded smoothly and in high conversion (84%). With the Ph<sub>5</sub>Cp catalyst **17a**, however, apparently due to the poor solubility of the catalyst in the reaction media, a very sluggish reaction took place under heterogeneous reaction conditions resulting in extensive formation of side products. Due to the poor/insolubility of the catalyst, unreacted *t*-BuOK may have induced condensation reactions of the methyl ketone starting material resulting in the formation of various byproducts. By decreasing the amount of polar isopropanol acting as the hydrogen donor, and by changing the solvent to toluene, better controlled reaction conditions were achieved for both catalysts. With the poorly soluble catalyst **17a** the reaction mixture remained cloudy even in toluene but the formation of side products could be suppressed significantly below the detection limit of GC instrument. Under these conditions, similar high conversions were observed for all substrates investigated with both catalysts **17a** and **43a**.



Under the high temperature reaction conditions in transfer hydrogenation, it is not fully obvious whether the catalytically active species generated from **17a** and **43a** are identical or related to those in the corresponding racemization reaction. Therefore, more accurate kinetic measurements were carried out at ambient temperature. In these studies it became obvious that, under the employed reaction conditions, the rate of transfer hydrogenation does not depend on the nature of the *para*-substituent (R = MeO vs. H vs. Cl vs. CF<sub>3</sub>) of the acetophenone substrate but instead on the ruthenium catalyst used. Conversion of the starting ketones to the corresponding alcohols was 30-40% with the Ph<sub>5</sub>Cp catalyst **17a** and 5-10% with the Bn<sub>5</sub>Cp catalyst **43a** in 6 hours at ambient temperature (Figure 39). These results imply that, in the transfer hydrogenation reactions with **17a** and **43a**, slow formation of the ruthenium hydride species as the active intermediate is followed by fast reduction of all ketones studied. It can, therefore, be assumed that the intermolecular transfer hydrogenation proceeds via a different mechanism than the intramolecular racemization reaction with the same catalysts.

**Table 9.** Transfer hydrogenation of acetophenones with catalysts **17a** and **43a**<sup>a</sup>

Substrate	Conversion <sup>b</sup> (%)		Solvent
	<b>17a</b>	<b>43a</b>	
<b>56a</b>	71	64	toluene
<b>56b</b>	-	84	neat <i>i</i> -PrOH
<b>56b</b>	92	84	toluene
<b>56c</b>	95	86	toluene

(a) Reaction conditions: T = 80 °C; 24 hr; catalyst loading = 2 mol-%; [*i*-PrOH] = 10 equiv. except when neat. (b) by GC.

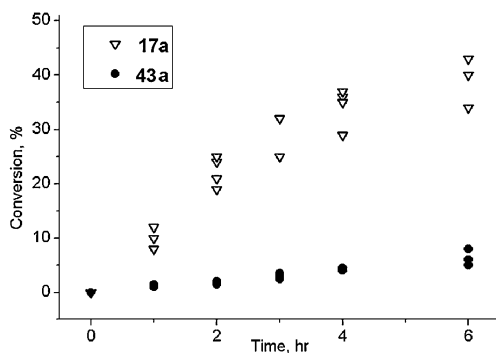


**Figure 39.** Transfer hydrogenations of the substituted acetophenones **56a-d** in the presence **17a** and **43a**.

#### 4.7 Summary and conclusions

Racemization of *sec*-alcohols proceeds via two-step oxidation-reduction mechanism. The difference in electronic properties of the two catalysts compared alters the rate determining step in racemization of secondary alcohols. Thus, in case of the electron-deficient  $\text{Ph}_5\text{Cp}$  catalyst, hydride re-addition appears to be the rate limiting step of racemization while hydride abstraction proceeds easily. Therefore, the Hammett plot demonstrates a clear trend towards a positive slope despite of partially non-linear behavior. In case of the electron-rich  $\text{Bn}_5\text{Cp}$  catalyst, hydrogen abstraction from electron-deficient alcohols is complicated, while hydrogen-readdition is facilitated. By switching from moderately electron-rich substrates to very electron deficient ones, Hammett plot for this catalyst demonstrates negative slope. In case of very electron-rich substrates, the racemization rate also decreases causing the Hammett plot to be concave downwards possibly indicating change in the rate-limiting step. Significant primary isotopic effect in case of this catalyst further supports the hypothesis about rate-limiting role of hydride abstraction-readdition in the racemization reaction.

## 5 DKR of amines

### 5.1 Introduction

In general, racemization of amines is more difficult than the racemization of *sec*-alcohols, typically requiring much harsher conditions. Additional problems are encountered by the typically high temperatures required for racemization of amines being often detrimental for enzyme activity.<sup>111</sup> Earlier strategies have been devised in order to circumvent the limitations for co-existence of the thermolabile enzyme and the amine racemization catalyst, requiring high temperatures for its operation. The enzyme and the catalyst can be separated in space, as exemplified by the MEDKR system where the DKR is carried out in an apparatus containing a "hot" racemization vessel and a "cold" enzyme vessel connected by tubing.<sup>112</sup> Circulation of the reaction mixture through the vessels was achieved by HPLC pump and leakage of enzyme into the "hot" racemization vessel was prevented by an ultra-filtration unit. In this work an initial approach towards an alternative reaction and reactor setup for chemoenzymatic DKR of amines based on a simple, modified Soxhlet extraction system was developed.<sup>113</sup> In this setup, the racemization catalyst operates in solution or suspension in the reaction flask under heating at reflux at high temperature, whereas the enzyme is placed in the extractor socket under continuous cooling. Prospects and limitations of the approach are discussed.

### 5.2 The approach to the DKR of amines utilizing a Soxhlet apparatus

A schematic illustration of the DKR Soxhlet reactor system is shown in Figure 40. The reaction flask (**I**) is filled with solvent, racemization catalyst, amine and acyl donor. The enzyme, packed into porous polyethylene envelopes, is placed in the extractor chamber (**II**). Ideally, the solvent and the acyl donor may be selected in such away that their boiling points are close to the boiling point of the racemic amine to be resolved allowing for circulation and condensation of all compounds via the reflux condenser and the extraction socket. Potential examples of such combinations are diglyme (bp 165 °C and *iso*-propylmethoxyacetate (bp 160 °C) for amines with boiling points below 180-190 °C, triglyme (bp 210 °C) and ethyl caprylate (bp 208 °C) for amines with boiling points below 230 °C, and tetraglyme (bp 275 °C) and ethyl laurate (bp 269 °C) for amines with boiling points below 300 °C. A wide range of low-priced "glymes" and fatty acid esters for fine tuning of the system are commercially available. Upon heating of the reaction flask to reflux, all volatile compounds (solvent, acyl donor and the amine) will evaporate and pass through a side arm (**III**) of the extractor, cooling down to suitable temperature while condensing in the reflux condenser (**IV**), and will then collect in the chamber (**II**) of the extractor where the enzymatic resolution reaction takes place. After that the chamber is filled, the reaction mixture returns to the racemization flask (**I**) through a siphon side-arm (**V**).

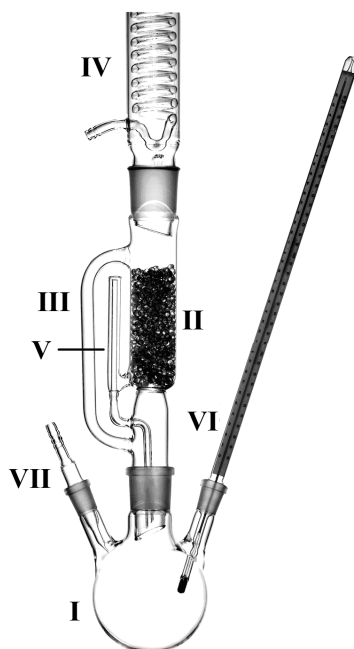


**Figure 40.** Schematic illustration of the Soxhlet reactor setup.

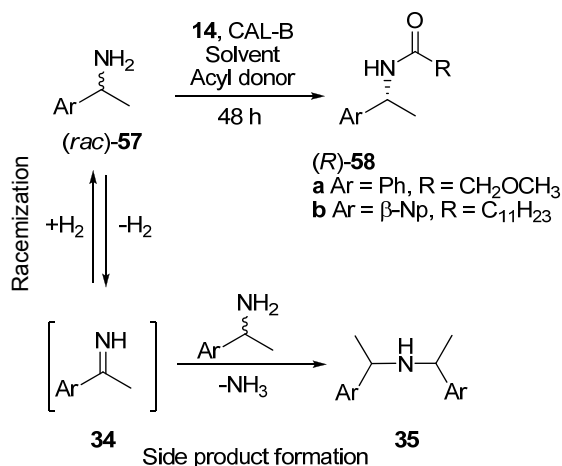
Removing of an alcohol (ethanol or *i*-propanol) formed during the enzymatic acylation reaction by evaporation shifts the equilibrium towards the desired product.<sup>114</sup> Mixing of the extraction chamber content takes place mainly by liquid flow back to the racemization flask. In order to decrease the inner volume of the extraction chamber (II) of the Soxhlet extractor and the duration of the extraction cycle, the chamber can be filled with glass beads. This also, subsequently, decreases the total volume of solvent required for the reaction.

Since most of the relevant target amines to be resolved have boiling points above 150 °C, the refluxing is ideally performed under reduced pressure. In principle, the extent of reduced pressure can be selected in such a way that the boiling point of the reaction mixture is sufficiently high for the metal catalyzed racemization of amines to proceed, i.e., close to 100 °C. During the condensation, the volatile components will cool down to approximately 50-60 °C temperature range which, in contrast to the reflux temperature in the reaction flask, is viable for CAL-B enzyme. In the case of thermolabile enzymes, the condensation temperature can be lowered by applying external cooling to the extractor vessel. After completion of the DKR, the solvent and excess of acyl donor can be removed by vacuum distillation and reused for a subsequent reaction with the same amine.

For monitoring of the temperature in the racemization flask, an inner thermometer (**VI**) can be applied. The temperature in the extraction chamber (**II**) can be determined by placing a thermometer into the glass beads. In such case, the reflux condenser (**IV**) should have an appropriate construction allowing the insertion of thermometer into the center of the condenser. Uniform boiling can be facilitated by capillar (**VII**). Temperature of the oil bath or heating mantel used for heating of the flask (**I**) does not influence the boiling temperature but will define the rate of evaporation. In order to ensure that the local temperature in the enzyme envelope will not exceed the upper limit for enzyme stability and function during the reactions, disposable thermo-sensors can be incorporated to the enzyme package, for example sealed capillars filled with crystalline solid with predetermined melting point such as tosylchloride (mp 69 °C) or benzophenone (mp 50°C). After completion of the reaction, the thermosensors can easily be removed for inspection.

### 5.3 Utilization of the Soxhlet apparatus for a model DKR

For investigating the feasibility of the Soxhlet system, chemoenzymatic DKR of 1-phenylethylamine was investigated in the presence of CAL-B and the Shvo's catalyst **14** (Scheme 33, Table 9). First, regular KRs using 20 mmol of *rac*-1-phenylethylamine in the Soxhlet reactor were performed providing optimized loadings for acyl donor, enzyme and the solvent. By use of 200 mg of enzyme, 36 mmol of acyl donor and 70 ml of diglyme under reflux at 100 °C and reduced pressure (130 mbar) for 18h, close to 50% conversion in the KR was observed after cooling down of the reaction mixture and analysis by chiral GC. Next, for DKR under similar conditions, the reaction loading was adjusted to 10 mmol and 1 mol-% of Shvo's catalyst **14** was added. In DKR, The reduced pressure applied and the air-sensitivity of the catalyst makes monitoring of the reaction by sampling difficult. For this reason, the test reactions were run for 48 hours and only the final samples after cooling were analyzed showing in most cases conversions exceeding 90%. From these reactions, the (*R*)-product was isolated either by crystallization or column chromatography in 65-70% yield and 99% ee. For preliminary investigations towards extension of the approach, also KR and DKR of the less volatile 1-(naphthyl)ethylamine (bp ~280 °C) was screened using tetraglyme as the solvent and ethyl laurate as the acyl donor. In this case the KR proceeded fairly slowly (10% conversion in 9 hr) due to lower activity of the acyl donor. DKR, in turn, was performed by refluxing of the reaction mixture at 120 °C/0.5 mbar for 48 hr with increased catalyst loading (2 mol-%) providing moderate isolated yield of the target (*R*)-amide only due to excessive formation of side products.

**Scheme 33.** DKR of 1-phenylethylamine and 1-( $\beta$ -naphthyl)ethylamine in the Soxhlet reactor system**Table 10.** Conditions of the DKR of **57a,b** in the Soxhlet reactor system

Conditions	<b>57a</b>	<b>57b</b>
Solvent	Diglyme	Tetraglyme
Acyl donor	<i>i</i> -PrCO <sub>2</sub> CH <sub>2</sub> OMe	EtCO <sub>2</sub> C <sub>11</sub> H <sub>23</sub>
Pressure, mbar	130	0.5
Temperature, °C	105	120
Isolated yield, %	70	37
Side product formed, %	~10 <sup>a</sup>	~35 <sup>b</sup>

(a) By GC. (b) By <sup>1</sup>H NMR.

#### 5.4 Suppression of side product formation

DKR of amines is often complicated by formation of side products.<sup>30b, 50b, 55c</sup> Racemization of secondary amines commonly proceeds via an imine intermediate, which upon reaction with a second amine molecule irreversibly results in the formation of dimers (Scheme 34). Here, reduced pressure facilitates the oxidative dehydrogenation of amine to imine and suppresses the reverse reaction. The subsequent increase in the concentration of the imine intermediate facilitates side product formation. Comparison of the DKRs of 1-phenylethylamine **57a** at 130 mbar and 1-naphthylethylamine **57b** below 1 mbar demonstrates the strong dependence of side product formation from the applied pressure in the Soxhlet reaction vessel. In the case of **57a**, 10% of side product were formed as determined by GC analysis. In the case of **57b**, the amount of side product formed increased significantly and reached the level of 30-40% as determined by NMR. In principle, different hydrogen donors can be utilized for reduction of the imine intermediate generated and, therefore, for suppression of the side product formation.

For example, 2,4-dimethyl-3-pentanol **59** as a hydrogen donor has been reported to suppress side product formation in one-pot DKR of amines.<sup>114</sup> This compound easily forms a ketone while releasing hydrogen upon Ru-catalyzed transfer hydrogenation. The branched structure of **59** in turn prevents its enzymatic acylation. Due to its relatively low boiling point (140 °C), however, this alcohol is not compatible with the Soxhlet reactor setup when higher boiling components are used. Thus other reducing agents for suppression of dimerization under the Soxhlet conditions were screened. The model racemization reaction for reducing agent screening under reduced pressure is shown in Scheme 34 with the results presented in Table 11.

**Scheme 34.** Model reaction studied for suppression of side product formation

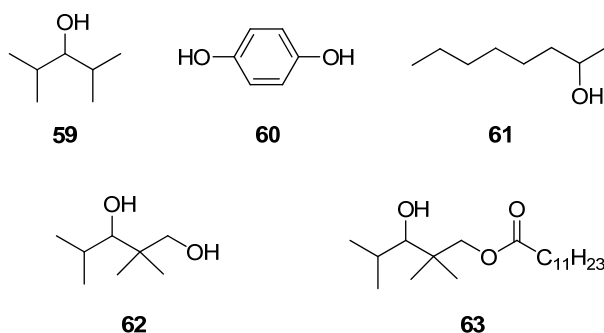
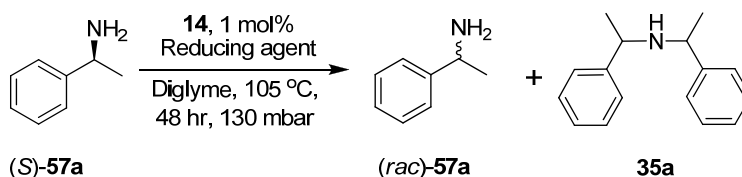


**Figure 41.** Reducing agents utilized for the suppression of the side product formation.

**Table 11.** Screening of reducing agents for suppression of side product formation

Run	Reducing agent <sup>a</sup>	Side product formed
1	-	9%
2	- <sup>b</sup>	~1%
3	<b>60</b>	15%
4	<b>61</b>	~1%
5	<b>62</b>	~3%
6	<b>62</b> <sup>c</sup>	~3%
7	<b>63</b>	~3%
8	H <sub>2</sub> bubbling	~1%

(a) 0.5 eq if otherwise not stated. (b) at 1 bar. (c) 1 eq

As evident from Entry 1, racemization under reduced pressure in the absence of reducing agents results in significant dimerization. When the racemization reaction was performed at atmospheric pressure (Entry 2), only minor amounts of the side product were detected. This observation is consistent with Le Chatelier's principle with inverse dependence of side product formation on the pressure applied. The use of hydroquinone **60**, a widely utilized reducing agent (Entry 3), did not suppress side product formation to any desired extent. A possible explanation may be related to the relatively high acidity of the OH group in hydroquinone ( $\text{pK}_a^1=10$ ), resulting in decomposition of the ruthenium hydride catalyst intermediate and the subsequent liberation of hydrogen gas. Promising results were obtained by use of 2-octanol **61** (Entry 4). This compound has a boiling point of 180 °C and can only be utilized with low boiling amines in the Soxhlet system. In the case of higher boiling substrates, **61** will be carried together with the other vapors to the enzyme chamber resulting in enzymatic acylation and a loss of reducing properties. The economically viable and commercially readily available 2,2,4-trimethyl-1,3-pentanediol **62**, likewise, demonstrated acceptable efficiency (Entry 5). Increase in the loading of this reducing agent did not improve the result (Entry 6). The high boiling point of compound **62** (232 °C) enables its use and compatibility with a broad range of amines. A model reaction on enzymatic acylation of this compound showed acylation mainly at the primary alcohol group with only minor amounts of secondary alcohol group acylation observed. The isolated acyl product **63** from the enzymatic test reaction was evaluated for side product suppression (Entry 7), showing similar behavior and efficiency compared to the non-acylated parent diol. Since the oxidation to ketone only involves the secondary alcohol moiety, the primary alcohol function



does not influence the results of side product suppression. The introduction of gaseous hydrogen into the reaction mixture via capillar (Entry 8) also efficiently suppresses side product formation being, however, complicated due to the high diffusion rate through the rubber tubing.

In accordance with earlier reports,<sup>50</sup> heterogeneous Pd/C demonstrates excellent racemization activity towards **57a** under atmospheric pressure without any detectable formation of side products. Unfortunately, when Pd/C was here employed instead of the Shvo's catalyst in the Soxhlet reactor setup, dimerization became the dominant reaction under reduced pressure. The interaction which binds hydrogen to palladium metal is weak compared to the covalent hydride bond in the Shvo's catalyst. Consequently, loss of hydrogen under reduced pressure followed by dimerization is likely to become a major reaction pathway in the case of heterogeneous catalysts.

Scheme 35. Dimerization of the 4-phenyl-2-aminobutane amine **64**



Finally, it could be assumed that the imine intermediate formed during the racemization reaction will be further stabilized by conjugation of the C=NH double bond with the aromatic ring. To investigate this, we also tested 4-phenyl-2-aminobutane **64**, an amine without aromatic ring in the  $\alpha$ -position to the nitrogen atom. To our disappointment, significant side product formation was observed in this case as well, possibly facilitated by the decrease in steric hindrance (Scheme 35).

## 5.5 Summary and conclusions

To summarize, a flexible system for chemoenzymatic DKR of amines based on space separated racemization and enzymatic vessels in a Soxhlet-type reactor setup was developed. Mass transfer of the reaction mixture is performed by repeating cycles of evaporation, condensation and siphon flow. This approach allows the usage of membrane pump instead of HPLC pump for liquid circulation. Different solvents and acyl donors with a broad range of boiling points are widely available from commercial sources and should allow the further fine tuning of the system. Currently, the main limiting factor with the developed system is the vacuum enhanced loss of hydrogen which facilitates side product formation, complicates the DKR process and decreases the yield of the desired product to the level of conventional kinetic

resolution. Preliminary results demonstrate that such side product formation can be suppressed by additional hydrogen donors in the system, requiring, however, further improvement and optimization. Other modifications of the system can, likewise, be envisioned for future investigation. For example, when using the Shvo's catalyst for racemization, temperatures above 80 °C are required for activation of the dimeric catalyst precursor to form the catalytically active monomer(s).<sup>115</sup> In principle, a "catalyst saving mode" could be applied in the beginning of the reaction by adjusting the pressure inside the system to allow for refluxing below the activation temperature of the racemization catalyst. Under such conditions only conventional kinetic resolution should take place. After this initial period, the pressure can be increased, simultaneously increasing the boiling point and inducing activation of the racemization catalyst and starting the DKR reaction.

## 6 Concluding discussion

### 6.1 Summary

In this thesis work, thirteen new half-sandwich ruthenium and palladium complexes have been prepared and eight of them have been characterized by X-crystallography. The complexes obtained were evaluated as catalysts for racemization of optically active secondary alcohols. A leading catalyst candidate was identified, characterized and applied in the chemoenzymatic DKR of over thirty substrates. A chromatography-free procedure was developed for preparation of this catalyst in ten gram scale. Molar scale DKR procedures followed by alkaline hydrolysis were utilized for preparation of large quantities of optically active alcohols utilizing separation by distillations only. The possibility to utilize the developed catalyst for epimerization of abundant natural compounds into rare products was demonstrated. A new protocol for accurate measurement of racemization kinetics was developed. Detailed kinetic and mechanistic studies of the racemization catalyzed by the developed catalyst were performed. An alternative approach to DKR of amines based on space separated vessels was addressed. Moreover, extensive comparisons between the earlier reported and widely used racemization catalyst  $\text{Ph}_5\text{CpRu}(\text{CO})_2\text{Cl}$  and the newly developed  $\text{Bn}_5\text{CpRu}(\text{CO})_2\text{Cl}$  catalyst were performed.

### 6.2 Conclusions

Catalytic activities of the ruthenium-based systems for racemization of secondary alcohols shows a clear dependence on the substitution pattern of the substrate and the catalyst. Only fully substituted cyclopentadienyl complexes demonstrated acceptable racemization rates. The half-sandwich ruthenium complex  $\text{Bn}_5\text{CpRu}(\text{CO})_2\text{Cl}$  is a new lead catalyst for DKR of secondary alcohols due to its ease of preparation and high catalytic activity. High solubility of the ligand precursor facilitates purification of the catalyst by crystallization. High solubility of the catalyst makes it versatile for operation at the limits of solubility, also in polar solvents. This catalyst is applicable for DKR of a large variety of electron-rich and moderately electron-deficient secondary alcohols including potentially useful building blocks for medicinal chemistry. Extensive kinetic studies reveal that the differences in the electronic properties between racemization catalysts influence the rate determining step in the racemization of secondary alcohols. The  $\text{Bn}_5\text{CpRu}(\text{CO})_2\text{Cl}$  catalyst developed in this work is the preferred catalyst for a very broad range of alcohols, except for highly electron-deficient substrates. This observation together with a significant primary isotopic effect observed during racemization of secondary alcohols with this catalyst further supports the hypothesis about rate-limiting role of hydride abstraction-readdition in the racemization mechanism.

### 6.3 Future perspectives

The simple, cost-effective and high-yield preparation of  $\text{Bn}_5\text{CpRu}(\text{CO})_2\text{Cl}$  together with its high performance makes this complex an attractive candidate as racemization catalyst for future DKR applications. Applicability to large scale DKRs demonstrates the potential even for industrial applications. Epimerization of readily available natural products, if further developed and possibly combined with a resolving enzyme, may prove to be a potential route towards rare diastereoisomers of these compounds.

A deeper understanding of the racemization mechanism and the underlying electronic and steric relationships will allow the further improvement and optimization of the DKR protocol and the racemisation catalyst.

Further optimization of the DKR of amines utilizing Soxhlet apparatus and preliminary screened in the present work may provide an attractive and practical route for preparation of chiral amines.

Optically active alcohols and especially amines play a very important role in modern medicinal chemistry. Development of large scale DKR procedures combining biotechnologies with the atom economy approach may provide a wide range of small molecules as building blocks for research and production in pharmaceutical industry.

- <sup>1</sup> (a) Francotte, E.; Lindner, W. (Ed.) *Chirality in drug research*, Wiley: Weinheim, **2006**. For reviews see: (b) Gal, J. *Chirality* **2011**, *23*, 1–16. (c) Drayer D. E. *Clin. Research & Reg. Affairs* **2001**, *18*, 181–203.
- <sup>2</sup> Shallenberger, R. S. *Pure Appl. Chem.* **1997**, *69*, 659–666.
- <sup>3</sup> Easson, L. H.; Stedman, E. *Biochem. J.* **1933**, 1256–1266.
- <sup>4</sup> (a) Knowles, W. S. *Angew. Chem. Int. Ed.* **2002**, *41*, 1998–2007. (b) Knowles, W. S.; Noyori, R. *Acc. Chem. Res.* **2007**, *40*, 1238–1239.
- <sup>5</sup> Bentley, R. *Chem. Rev.* **2006**, *106*, 4099–4112.
- <sup>6</sup> Henry, M. E.; Schmidt, M. E.; Hennen, J.; Villafuerte, R. A.; Butman, M. L.; Tran, P.; Kerner, L. T.; Cohen B.; Renshaw, P. F. *Neuropsychopharmacology* **2005**, *30*, 1576–1583.
- <sup>7</sup> (a) Bymaster, F. P.; Beedle, E. E.; Findlay, J.; Gallagher, P. T.; Krushinski, J. H.; Mitchell, S.; Robertson, D. W.; Thompson, D. C.; Wallace, L.; Wonga, D. T. *Bioorg. Med. Chem. Lett.* **2003**, *13*, 4477–4480. (b) Liu, X.; Du, Y. *Eur. J. Med. Chem.* **2010**, *45*, 4043–4049.
- <sup>8</sup> (a) Lurie, I. S.; Bozenko J. S. Jr.; Li, L.; Miller, E. E.; Greenfield, S. J. *Microgram J.* **2011**, *8*, 24–28. (b) Mendelson, J.; Uemura, N.; Harris, D.; Nath, R. P.; Fernandez, E.; Jacob, P.; Everhart E. T.; Jones, R. T. *Clin. Pharmacol. Ther.* **2006**, *80*, 403–420. (c) Mendelson, J. E.; McGlothlin, D.; Harris, D. S.; Foster, E.; Everhart, T.; Jacob, P.; Jones, R. T. *BMC Clin. Pharmacol.* **2008**, *8*:4.
- <sup>9</sup> FDA, Guidances (Drugs) Development of New Stereoisomeric Drugs, 5/1/1992, accessed 26.06.2012 at <http://www.fda.gov/drugs/GuidanceComplianceRegulatoryInformation/Guidances/ucm122883.htm>
- <sup>10</sup> Blaser, H. U. *Chem. Rev.* **1992**, *92*, 935–952.
- <sup>11</sup> (a) Christmann, M.; Bräse S. (Ed.) *Asymmetric Synthesis – The Essentials*, Wiley: Weinheim, **2007**. (b) Ojima, I. (Ed.) *Catalytic Asymmetric Synthesis*, Wiley: **2010**.
- <sup>12</sup> (a) Collet, A.; Brienne M.-J.; Jacques, J. *Chem. Rev.* **1980**, *80*, 215–230. (b) Kellogg, M.; Nieuwenhuijzen, J. W.; Pouwer, K.; Vries, T. R.; Broxterman, Q. B.; Grimbergen, R. F. P.; Kaptein, B.; La Crois, R. M.; de Wever, E.; Zwaagstra, K.; van der Laan, A. C. *Synthesis* **2003**, *10*, 1626–1638. (c) Breuer, M.; Ditrich, K.; Habicher, T.; Hauer, B.; Keßeler, M.; Stürmer, R.; Zelinski, T. *Angew. Chem. Int. Ed.* **2004**, *43*, 788–824.
- <sup>13</sup> Reinhold, D. F.; Utne, T.; Abramson, N. L. US 4716246 A, **1987**.
- <sup>14</sup> Kinbara, K.; Sakai, K.; Hashimoto, Y.; Nohira, H.; Saigo, K. *Tetrahedron: Asymmetry* **1996**, *7*, 1539–1542.
- <sup>15</sup> Francotte, E. *J. Chromatogr. A* **1994**, *666*, 565–601.
- <sup>16</sup> (a) Chen, C. S.; Fujimoto, Y.; Girdaukas, G.; Sih, C. J. *J. Am. Chem. Soc.* **1982**, *104*, 7294–7299. (b) Chen, C. S.; Wu, S. H.; Girdaukas, G.; Sih C. J. *J. Am. Chem. Soc.* **1987**, *109*, 2812–2817.
- <sup>17</sup> Kamal, A.; Azhar, M. A.; Krishnaji, T.; Malik, M. S.; Azeza S. *Coord. Chem. Rev.* **2008**, *252*, 569–592.
- <sup>18</sup> (a) Kirk, O.; Christensen, M. W. *Org. Process Res. Dev.* **2002**, *6*, 446–451. (b) Gotor-Fernández, V.; Busto, E.; Gotor, V. *Adv. Synth. Catal.* **2006**, *348*, 797–812.
- <sup>19</sup> Kazlauskas, R. J.; Weissfloch, A. N. E.; Rappaport, A. T.; Cuccia, L. A. *J. Org. Chem.* **1991**, *56*, 2656–2665.
- <sup>20</sup> (a) Hæffner, F.; Norin, T.; Hult, K. *Biophys. J.* **1998**, *74*, 1251–1262. (b) Jaeger, K.-E.; Dijkstra, B. W.; Reetz, M. *T. Annu. Rev. Microbiol.* **1999**, *53*, 315–351.
- <sup>21</sup> Liu, H.-L.; Anthonsen, T. *Chirality* **2002**, *14*, 25–27.
- <sup>22</sup> Noyori, R.; Ikeda, T.; Ohkuma, T.; Widhalm, M.; Kitamura, M.; Takaya, H.; Akutagawa, S.; Sayo, N.; Saito, T. *J. Am. Chem. Soc.* **1989**, *111*, 9134–9135.
- <sup>23</sup> Inagaki, M.; Hiratake, J.; Nishioka, T.; Oda J. *J. Am. Chem. Soc.* **1991**, *113*, 9360–9361.

- <sup>24</sup> Allen, J. V.; Williams, J. M. J. *Tetrahedron Letters* **1996**, 37, 1859-1862.
- <sup>25</sup> Dinh, P. M.; Howarth, J. A.; Hudnott, A. R.; Williams, M. J. *Tetrahedron Lett.* **1996**, 37, 7623-7626.
- <sup>26</sup> Reetz, M. T.; Schimossek, K. *Chimia* **1996**, 50, 668-669.
- <sup>27</sup> Larsson, A. L. E.; Persson, B. A.; Bäckvall, J.-E. *Angew. Chem. Int. Ed.* **1997**, 36, 1211-1212.
- <sup>28</sup> Conley, B. L.; Pennington-Boggio, M. K.; Boz, E.; Williams, T. J. *Chem. Rev.* **2010**, 110, 2294-2312.
- <sup>29</sup> Persson, B. A.; Larsson, A. L. E.; Le Ray, M.; Bäckvall, J.-E. *J. Am. Chem. Soc.* **1999**, 121, 1645-1650.
- <sup>30</sup> For reviews, see: (a) Martín-Matute, B.; Bäckvall, J.-E. *Curr. Opin. Chem. Biol.* **2007**, 11, 226-232. (b) Ahn, Y.; Ko, S.-B.; Kim, M.-J.; Park, J. *Coord. Chem. Rev.* **2008**, 252, 647-658. (c) Lee, J. H.; Han, K.; Kim, M.-J.; Park, J. *Eur. J. Org. Chem.* **2010**, 999-1015. (d) Turner, N. J. *Curr. Opin. Chem. Biol.* **2010**, 14, 115-121. (e) Kim, Y.; Park, J.; Kim, M.-J.; *Chem. Cat. Chem.* **2011**, 3, 271-277.
- <sup>31</sup> (a) Choi, J. H.; Kim, Y. H.; Nam, S. H.; Shin, S. T.; Kim, M.-J.; Park, J. *Angew. Chem. Int. Ed.* **2002**, 41, 2373-2376. (b) Choi, J. H.; Choi, Y. K.; Kim, Y. H.; Park, E. S.; Kim, E. J.; Kim, M.-J.; Park, J. *J. Org. Chem.* **2004**, 69, 1972-1977.
- <sup>32</sup> (a) Csjermyik, G.; Bogár, K.; Bäckvall, J.-E. *Tetrahedron Letters* **2004**, 45, 6799-6802. (b) Martín-Matute, B.; Edin, M.; Bogár, K.; Bäckvall, J.-E. *Angew. Chem. Int. Ed.* **2004**, 43, 6535-6539. (c) Martín-Matute, B.; Edin, M.; Bogár, K.; Kaynak, F. B.; Bäckvall, J.-E. *J. Am. Chem. Soc.* **2005**, 127, 8817-8825.
- <sup>33</sup> (a) Kim, N.; Ko, S.-B.; Kwon, M. S.; Kim, M.-J.; Park, J. *Org. Lett.* **2005**, 7, 4523-4526. (b) Kim, M.-J.; Choi, Y. K.; Kim, S.; Kim, D.; Han, K.; Ko, S.-B.; Park, J. *Org. Lett.* **2008**, 10, 1295-1298.
- <sup>34</sup> (a) Lee, D.; Huh, E. A.; Kim, M.-J.; Jung, H. M.; Koh, J. H.; Park, J. *Org. Lett.* **2000**, 2, 2377-2379. (b) Roengphithya, C.; Patterson, D. A.; Gibbins, E. J.; Taylor, P. C.; Livingston, A. G. *Ind. Eng. Chem. Res.* **2006**, 45, 7101-7109.
- <sup>35</sup> Dijkstra, A.; Elzinga, J. M.; Li, Yu-Xin.; Arends, I. W. C. E.; Sheldon, R. A. *Tetrahedron: Asymmetry* **2002**, 12, 879-884.
- <sup>36</sup> (a) van As, B. A. C.; van Buijtenen, J.; Heise, A.; Broxterman, Q. B.; Verzijl, G. K. M.; Palmans, A. R. A.; Meijer, E. W. *J. Am. Chem. Soc.* **2005**, 127, 9964-9965. (b) Hilker, I.; Rabani, G.; Verzijl, G. K. M.; Palmans, A. R. A.; Heise, A. *Angew. Chem. Int. Ed.* **2006**, 45, 2130-2132.
- <sup>37</sup> Broxterman, Q. B.; Verzijl, G. K. M. PCT Int. Appl. **2003**, WO 2003043575 A2.
- <sup>38</sup> Stürmer, R. *Angew. Chem. Int. Ed.* **1997**, 36, 1173-1174.
- <sup>39</sup> Koh, J. H.; Jung, H. M.; Kim, M.-J.; Park, J. *Tetrahedron Lett.* **1999**, 40, 6281-6284.
- <sup>40</sup> Xi, Q.; Zhang, W.; Zhang, X. *Synlett* **2006**, 6, 0945-0947.
- <sup>41</sup> Ko, S.-B.; Baburaj, B.; Kim, M.-J.; Park, J. *J. Org. Chem.* **2007**, 72, 6860-6864.
- <sup>42</sup> Marr, A. C.; Pollock, C. L.; Saunders, G. C. *Organometallics* **2007**, 26, 3283-3285.
- <sup>43</sup> Gauthier, S.; Solari, E.; Dutta, B.; Scopelliti, R.; Severin, K. *Chem. Commun.* **2007**, 1837-1839.
- <sup>44</sup> Haak, R. M.; Berthiol, F.; Jerphagnon, T.; Gayet, A. J. A.; Tarabiono, C.; Postema, C. P.; Ritleng, V.; Pfeffer, M.; Janssen, D. B.; Minnaard, A. J.; Feringa, B. L.; de Vries, J. G. *J. Am. Chem. Soc.* **2008**, 130, 13508-13509.
- <sup>45</sup> Chen, Q.; Yuan, C. *Chem. Commun.* **2008**, 5333-5335.
- <sup>46</sup> Nun, P.; Fortman, G. C.; Slawin, A. M. Z.; Nolan, S. P. *Organometallics* **2011**, 30, 6347-6350.
- <sup>47</sup> K. Faber, *Chem. Eur. J.* **2001**, 7, 5004-5010.
- <sup>48</sup> (a) Veum, L.; Hanefeld, U. *Tetrahedron: Asymmetry* **2004**, 15, 3707-3709. (b) Veum, L.; Kanerva, L. T.; Halling, P. J.; Maschmeyer, T.; Hanefeld, U. *Adv. Synth. Catal.* **2005**, 347, 1015-1021.
- <sup>49</sup> For review see Seeman, J. I. *Chem. Rev.* **1983**, 83, 83-134.

- <sup>50</sup> (a) Parvulescu, A.; De Vos, D.; Jacobs, P. *Chem. Commun.* **2005**, 5307-5309. (b) Parvulescu, A. N.; Jacobs, P. A.; De Vos, D. E. *Chem. Eur. J.* **2007**, *13*, 2034-2043. (c) Parvulescu, A. N.; Jacobs, P. A.; De Vos, D. E. *Appl. Catal. A: General* **2009**, *368*, 9-16.
- <sup>51</sup> Andrade, L. H.; Silva, A. V.; Pedrozo, E. C. *Tetrahedron Lett.* **2009**, *50*, 4331-4334.
- <sup>52</sup> Kim, M.-J.; Kim, W.-H.; Han, K.; Choi, Y. K.; Park, J. *Org. Lett.* **2007**, *9*, 1157-1159.
- <sup>53</sup> Parvulescu, A. N.; Jacobs, P. A.; De Vos, D. E. *Adv. Synth. Catal.* **2008**, *350*, 113-121.
- <sup>54</sup> Pámies, O.; Éll, A. H.; Samec, J. S. M.; Hermanns, N.; Bäckvall, J.-E. *Tetrahedron Lett.* **2002**, *43*, 4699-4702.
- <sup>55</sup> (a) Paetzold, J.; Bäckvall, J.-E. *J. Am. Chem. Soc.* **2005**, *127*, 17620-17621. (b) Hoben, C. E.; Kanupp, L.; Bäckvall, J.-E. *Tetrahedron Lett.* **2008**, *49*, 977-979. (c) Thalén, L. K.; Zhao, D.; Sortais, J.-B.; Paetzold, J.; Hoben, C.; Bäckvall, J.-E. *Chem. Eur. J.* **2009**, *15*, 3403-3410.
- <sup>56</sup> Veld, M. A. J.; Hult, K.; Palmans, A. R. A.; Meijer, E. W. *Eur. J. Org. Chem.* **2007**, 5416-5421.
- <sup>57</sup> (a) Stirling, M.; Blacker, J.; Page, M. I. *Tetrahedron Lett.* **2007**, *48*, 1247-1250. (b) Blacker, A. J.; Stirling, M. J.; Page, M. I. *Org. Proc. Res. Develop.* **2007**, *11*, 642-648.
- <sup>58</sup> Jerphagnon, T.; Gayet, A. J. A.; Berthiol, F.; Ritleng, V.; Mršić, N.; Meetsma, A.; Pfeffer, M.; Minnaard, A. J.; Feringa, B. L.; de Vries, J. G. *Chem. Eur. J.* **2009**, *15*, 12780-12790.
- <sup>59</sup> Blidi, L. E.; Nechab, M.; Vanthuyne, N.; Gastaldi, S.; Bertrand, M. P.; Gil, G. *J. Org. Chem.* **2009**, *74*, 2901-2903.
- <sup>60</sup> Mangas-Sánchez, J.; Rodríguez-Mata, M.; Busto, E.; Gotor-Fernández, V.; Gotor, V. *J. Org. Chem.* **2009**, *74*, 5304-5310.
- <sup>61</sup> (a) Schneider, N.; Prosenc, M.-H.; Brintzinger, H.-H. *J. Organomet. Chem.* **1997**, *545-546*, 291. (b) Schneider, N.; Huttenloch, M. E.; Stehling, U.; Kirsten, R.; Schaper, F.; Brintzinger, H. H. *Organometallics* **1997**, *16*, 3413-3420. (c) Schneider, N.; Schaper, F.; Schmidt, K.; Kirsten, R.; Geyer, A.; Brintzinger, H. H. *Organometallics* **2000**, *19*, 3597-3604. (d) Luttikhedde, H. J. G.; Leino, R.; Wilén, C.-E.; Näsman, J. H. *Polym. Prepr. (Am. Chem. Soc., Div. Polym. Chem.)* **1998**, *39(1)*, 229-230. (e) Rigby, S. S.; Decken, A.; Bain, A. D.; McGlinchey, M. J. *J. Organomet. Chem.* **2001**, *637-639*, 372-381. (f) Sun, J.; Berg, D. J.; Twamley, B. *Organometallics* **2008**, *27*, 683-690.
- <sup>62</sup> (a) Repo, T.; Jany, G.; Hakala, K.; Klinga, M.; Polamo, M.; Leskelä, M.; Rieger, B. *J. Organomet. Chem.* **1997**, *549*, 177-186. (b) Aitola, E.; Hakala, K.; Byman-Fagerholm, H.; Leskelä, M.; Repo, T. *J. Polym. Sci., Part A: Polym. Chem.* **2008**, *46*, 373-382.
- <sup>63</sup> Sato, M.; Maruyama, G.; Tanemura, A. *J. Organomet. Chem.* **2002**, *655*, 23-30.
- <sup>64</sup> Hoshi, T.; Nakazawa, T.; Saitoh, I.; Mori, A.; Suzuki, T.; Sakai, J.-i.; Hagiwara, H. *Org. Lett.* **2008**, *10*, 2063-2066.
- <sup>65</sup> (a) Komatsu, K.; Fujiura, R.; Okamoto, K. *Chem. Lett.* **1988**, 265-268. (b) Eliasson, B.; Nouri-Sorkhabi, M. H.; Trogen, L.; Sethson, I.; Edlund, U.; Sygula, A.; Rabinovitz, M. *J. Org. Chem.* **1989**, *54*, 171-176.
- <sup>66</sup> See for example, (a) Leino, R.; Luttikhedde, H.; Wilén, C.-E.; Sillanpää, R.; Näsman, J. H. *Organometallics* **1996**, *15*, 2450-2453. (b) Leino, R.; Luttikhedde, H. J. G.; Lehtonen, A.; Sillanpää, R.; Penninkangas, A.; Strandén, J.; Mattinen, J.; Näsman, J. H. *J. Organomet. Chem.* **1998**, *558*, 171-179. (c) Leino, R.; Luttikhedde, H. J. G.; Långstedt, L.; Penninkangas, A. *Tetrahedron Lett.* **2002**, *43*, 4149-4151.
- <sup>67</sup> Kreicberga, J.; Neilands, O.; Kampars, V. *Zhurn. Org. Khim.* **1975**, *11*, 1941-1945.
- <sup>68</sup> Dennis, G. D.; Edward-Davis, D.; Field, L. D.; Masters, A. F.; Maschmeyer, T.; Ward, A. J.; Buys, I. E.; Turner, P. *Austr. J. Chem.* **2006**, *59*, 135-146.

- <sup>69</sup> (a) Sassmannshausen, J.; Powell, A. K.; Anson, C. E.; Wocadlo, S.; Bochmann, M. *J. Organomet. Chem.* **1999**, *592*, 84-94. (b) Deckers, P. J. W.; Hessen, B.; Teuben, J. H. *Angew. Chem. Int. Ed.* **2001**, *40*, 2516-2519. (c) Deckers, P. J. W.; Hessen, B.; Teuben, J. H. *Organometallics* **2002**, *21*, 5122-5135.
- <sup>70</sup> Antunes, M. A.; Alves, L. G.; Namorado, S.; Ascenso, J. R.; Veiros, L. F.; Martins, A. M. *Organometallics* **2012**, ASAP, DOI: 10.1021/om300070m
- <sup>71</sup> Mavrynsky, D.; Sillanpää, R.; Leino, R. *Organometallics* **2009**, *28*, 598-605.
- <sup>72</sup> a) Bullock, R. M.; Fagan, P. J.; Hauptman, E. M. (DuPont), PCT Int. Appl. **2001**, WO 01/98241 A2. b) Ghosh, P.; Fagan, P. J.; Marshall, W. J.; Hauptman, E.; Bullock, R. M. *Inorg. Chem.* **2009**, *48*, 6490-6500.
- <sup>73</sup> (a) Dyker, G.; Heiermann, J.; Miura, M.; Inoh, J.-I.; Pivsa-Art, S.; Satoh, T.; Nomura, M. *Chem. Eur. J.* **2000**, *6*, 3426-3433. (b) Thépot, J.-Y.; Lapinte, C. *J. Organomet. Chem.* **2001**, *627*, 179-188. (c) Xi, Z.; *Top. Catal.* **2005**, *35*, 63-71. (d) Enders, M.; Baker, R. W. *Curr. Org. Chem.* **2006**, *10*, 937-953.
- <sup>74</sup> (a) Hirsch, S. S.; Bailey, W. J. *J. Org. Chem.* **1978**, *43*, 4090-4094. (b) Chambers, J. W.; Baskar, A. J.; Bott, S. G.; Atwood, J. L.; Rausch, M. D. *Organometallics* **1986**, *5*, 1635-1641. (c) Tsai, W.-M.; Rausch, M. D.; Rogers, R. D. *Organometallics* **1996**, *15*, 2591-2594.
- <sup>75</sup> Mavrynsky, D.; Päiviö, M.; Lundell, K.; Sillanpää, R.; Kanerva, L. T.; Leino, R. *Eur. J. Org. Chem.* **2009**, 1317-1320.
- <sup>76</sup> (a) Schmid, G.; Thewalt, U.; Troyanov, S. I.; Mach, K. *J. Organomet. Chem.* **1993**, *453*, 185-191. (b) Schmid, G.; Thewalt, U.; Polasek, M.; Mach, K.; Sedmera, P.; *J. Organomet. Chem.* **1994**, *482*, 231-241. (c) Schmid, G.; Thewalt, U.; Sedmera, P.; Hanuš, V.; Mach, K. *Collect. Czech. Chem. Commun.* **1998**, *63*, 636-645.
- <sup>77</sup> Rausch, M. D.; Tsai, W.-M.; Chambers, J. W.; Rogers, R. D.; Alt, H. G. *Organometallics* **1989**, *8*, 816-821.
- <sup>78</sup> Delville-Desbois, M.-H.; Mross, S.; Astruc, D.; Linares, J.; Varret, F.; Rabaã, H.; Le Beuze, A.; Saillard, J.-Y.; Culp, R. D.; Atwood, D. A.; Cowley, A. H. *J. Am. Chem. Soc.* **1996**, *118*, 4133-4147.
- <sup>79</sup> (a) Song, L.-C.; Zhang, L.-Y.; Hu, Q.-M.; Huang, X.-Y. *Inorg. Chim. Acta* **1995**, *230*, 127-131. (b) Martins, A. M.; Romão, C. C.; Abrantes, M.; Azevedo, M. C.; Cui, J.; Dias, A. R.; Duarte, M. T.; Lemos, M. A.; Lourenço, T.; Poli, R. *Organometallics* **2005**, *24*, 2582-2589. (c) Antunes, M. A.; Namorando, S.; de Avezo, C. G.; Lemos, M. A.; Duarte, M. T.; Ascenso, J. R.; Martins, A. M. *J. Organomet. Chem.* **2010**, *695*, 1328-1336.
- <sup>80</sup> Mavrynsky, D.; Kanerva, L. T.; Sillanpää, R.; Leino, R. *Pure Appl. Chem.* **2011**, *83*, 479-487.
- <sup>81</sup> Blank, F.; Vieth, J. K.; Ruiz, J.; Rodríguez, V.; Janiak, C. *J. Organomet. Chem.* **2011**, *696*, 473-487.
- <sup>82</sup> (a) Ready, T. E.; Chien, J. C. W.; Rausch, M. D. *J. Organomet. Chem.* **1996**, *519*, 21-28. (b) Jany, G.; Gustafsson, M.; Repo, T.; Aitola, E.; Dobado, J. A.; Klinga, M.; Leskelä, M. *J. Organomet. Chem.* **1998**, *553*, 173-178. (c) Grimmer, N. E.; Coville, N. J.; de Koning, C. B.; Smith, J. M.; Cook, L. M. *J. Organomet. Chem.* **2000**, *616*, 112-127.
- <sup>83</sup> Mavrynsky, D.; Rahkila, J. T. W.; Leino, R. et al., to be published
- <sup>84</sup> Kraus, H.-J.; Werner, H.; Krüger, C. *Z. Naturforsch. B* **1983**, *38*, 733-737.
- <sup>85</sup> Watanabe, S.; Kurosawa, H. *Organometallics* **1998**, *17*, 479-482.
- <sup>86</sup> Namorado, S.; Antunes, M. A.; Veiros, L. F.; Ascenso, J. R.; Duarte, M. T.; Martins, A. M. *Organometallics* **2008**, *27*, 4589-4599.
- <sup>87</sup> Mavrynsky, D.; Murzin, D. Yu.; Leino, R., submitted to *Chem. Cat. Chem.*
- <sup>88</sup> Päiviö, M.; Mavrynsky, D.; Leino, R.; Kanerva, L. T. *Eur. J. Org. Chem.* **2011**, 1452-1457.
- <sup>89</sup> Rocha, L. C.; Rosset, I. G.; Luiz, R. F.; Raminelli, C.; Porto, A. L. M. *Tetrahedron: Asymmetry* **2010**, *21*, 926-929.



- <sup>90</sup> The manipulation of air-sensitive compounds, Shriver D. F.; Drezdson, M. A. Wiley 1986, p 11.
- <sup>91</sup> Derome, A. E. Modern NMR techniques for chemistry research. Pergamon 1987, p172.
- <sup>92</sup> Wernerova, M.; Hudlicky, T. *Synlett* **2010**, 18, 2701-2707.
- <sup>93</sup> Claridge, T. D. W.; Davies, S. G.; Polywka, M. E. C.; Roberts, P. M.; Russell, A. J.; Savory, E. D.; Smith, A. D. *Org. Lett.* **2008**, 10, 5433–5436.
- <sup>94</sup> Cucullu, M. E.; Nolan, S. P.; Belderrain, T. R.; Grubbs R. H. *Organometallics* **1999**, 18, 1299–1304.
- <sup>95</sup> Generally lower reproducibilities of the DKR reactions were observed when **17** was compared with **43a**. A possible explanation can be clogging of the immobilized enzyme surface with a precipitated catalyst or products of its decomposition caused by low solubility of the polyarylsubstituted species.
- <sup>96</sup> Ghanem, A.; Schurig, V. *Monatsh. Chem.*, **2003**, 134, 1151–1157.
- <sup>97</sup> Bogár, K.; Martín-Matute, B.; Bäckvall, J.-E. *Beilstein J. Org. Chem.* **2007**, 3, No. 50, no pp. given.
- <sup>98</sup> Ramstadius, C.; Träff, A. M.; Krumlinde, P.; Bäckvall, J.-E.; Cumpstey, I. *Eur. J. Org. Chem.* **2011**, 4455-4459.
- <sup>99</sup> Etzold, B.; Jess, A.; Nobis M. *Catal. Today* **2009**, 140, 30-36.
- <sup>100</sup> Haut S. A. *J. Agric. Food Chem.* **1985**, 33, 278-280.
- <sup>101</sup> (a) Martín-Matute, B.; Åberg, J. B.; Edin, M.; Bäckvall, J. -E. *Chem. Eur. J.* **2007**, 13, 6063–6072. (b) Nyhlén, J.; Privalov, T.; Bäckvall, J.-E. *Chem. Eur. J.* **2009**, 15, 5220-5229. (c) Åberg, J. B.; Nyhlén, J.; Martín-Matute, B.; Privalov, T.; Bäckvall, J.-E. *J. Am. Chem. Soc.* **2009**, 131, 9500-9501. (d) Bosson, J.; Nolan, S. P. *J. Org. Chem.* **2010**, 75, 2039-2043. (e) Warner, M. C.; Verho, O.; Bäckvall, J.-E. *J. Am. Chem. Soc.* **2011**, 133, 2820-2823.
- <sup>102</sup> Verho, O.; Johnston, E. V.; Karlsson, E.; Bäckvall, J.-E. *Chem. Eur. J.* **2011**, 17, 11216-11222.
- <sup>103</sup> Lee, J. H.; Kim, N.; Kim, M.-J.; Park J. *ChemCatChem* **2011**, 3, 354-359.
- <sup>104</sup> (a) Eckert, M.; Brethon, A.; Li, Y.-X.; Sheldon, R. A.; Arends, I. W. C. E. *Adv. Synth. Catal.* **2007**, 349, 2603-2609. (b) Merabet-Khelassi, M.; Vriamont, N.; Aribi-Zouieueche, L.; Riant, O. *Tetrahedron: Asymm.* **2011**, 22, 1790-1796.
- <sup>105</sup> A catalyst loading of 2 mol% on 1 mmol scale corresponds to 20  $\mu$ mol (10-15 mg) of the organometallic compound and a further decrease of the catalyst amount would be questionable in terms of reproducibility. Possibilities to increase the amount of substrate are likewise limited due to the relatively high price of enantiomerically pure *sec*-alcohols required for the racemization studies.
- <sup>106</sup> D. Murzin, T. Salmi Catalytic Kinetics, Elsevier Science & Technology Books 2005
- <sup>107</sup> Simmons, E. M.; Hartwig, J. F. *Angew. Chem. Int. Ed.* **2012**, 51, 3066-3072.
- <sup>108</sup> (a) Schrek, J. O. *J. Chem. Ed.* **1971**, 48, 103-107. For other recent examples of nonlinear Hammett-effects in organometallic catalysis, see: (b) Firstrup, P.; Le Quement, S.; Tanner, D.; Norrby, P.-O. *Organometallics* **2004**, 23, 6160-6165. (c) Furuya, T.; Benitez, D.; Tkatchouk, E.; Strom, A. E.; Tang, P.; Goddard, III, W. A.; Ritter, T. *J. Am. Chem. Soc.* **2010**, 132, 3793-3807.
- <sup>109</sup> Casey, P. C.; Beetner, S. E.; Johnson, J. B. *J. Am. Chem. Soc.* **2008**, 130, 2285-2295.
- <sup>110</sup> Yamada, I.; Noyori, R. *Org. Lett.* **2000**, 2, 3425-3427.
- <sup>111</sup> Halling, P. in: Enzyme Catalysis in Organic Synthesis, Vol. 1, eds. K. Drauz, H. Waldmann (Wiley-VCH, Weinheim, 2002) p. 274
- <sup>112</sup> (a) C. Roengpithya, D. A. Patterson, P. C. Taylor, A. G. Livingston, *Desalination* **2006**, 199, 195-197. (b) C. Roengpithya, D. A. Patterson, A. G. Livingston, P. C. Taylor, J. L. Irwin, M. R. Parrett, *Chem. Commun.* **2007**, 3462-3463.
- <sup>113</sup> Mavrynsky, D.; Leino, R., manuscript.

- <sup>114</sup> Veld, M. A. J.; Hult, K.; Palmans, A. R. A.; Meijer, E. W. *Eur. J. Org. Chem.* **2007**, 5416-5421.
- <sup>115</sup> Thorson, M. K.; Klinkel, K. L.; Wang, J.; Williams, T. J. *Eur. J. Inorg. Chem.* **2009** 295-302.





ISBN 978-952-12-2813-1  
Painosalama Oy – Turku/Åbo, Finland 2012